

Intraspecific predator interference promotes biodiversity in ecosystems

Ju Kang^{1†}, Shijie Zhang^{2†}, Xin Wang^{1*}

1. *School of Physics, Sun Yat-sen University, Guangzhou 510275, China.*

2. *School of Mathematics, Sun Yat-sen University, Guangzhou 510275, China.*

[†]These authors contributed equally to this work

*Correspondence: wangxin36@mail.sysu.edu.cn

Abstract

Explaining biodiversity is a fundamental issue in ecology. A long-standing puzzle lies in the paradox of the plankton: many species of plankton feeding on a limited type of resource coexist, apparently flouting Competitive Exclusion Principle (CEP), which holds that the species number of predators (consumers) cannot exceed that of the resources at steady state. Here we present a mechanistic model, and show that the intraspecific interference among the consumers enables strikingly a plethora of consumer species to coexist at constant population densities with only one or a handful types of resources, which naturally breaks the CEP and may resolve the paradox of the plankton. We further reveal that the facilitated biodiversity is resistant to stochasticity, either with stochastic simulations or the individual-based modelling. Our model developed here is broadly applicable, which quantitatively illustrates classical experiments that invalidating the CEP, and can be used to explain biodiversity in natural ecosystems.

Introduction

The most prominent feature of life on Earth is its remarkable species diversity: Countless macro- and micro-species fill every corner on land and in the water [1-7]. In tropical forests, thousands of plant species and vertebrate species coexist [5]. Within only a gram of soil, the number of microbial species is estimated to be 2,000-18,000. Explaining the astonishing biodiversity is a major focus in ecology [1]. A great challenge stems from the well-known Competitive Exclusion Principle (CEP): two species competing for a single type of resources cannot coexist at constant population densities [8-11], or generically, the species number of consumers cannot exceed that of resources at steady state [12-13]. On the contrary, in the paradox of plankton, a handful types of resources support hundreds or more coexisting species of phytoplankton [14]. Then, how can planktons somehow liberate the constraint of the CEP?

The mathematical proof of the CEP was proposed by MacArthur and Levin in a classical paper of the 1960s [14] (see SI. Sec. 1 and ref[15]). Over the past six decades,

various mechanisms have been put forward to overcome the limit set by the CEP and explain biodiversity. Some suggest that the system never approaches steady state where the CEP applies, due to temporal variations or spatial heterogeneity [16-18], or species' self-organized dynamics [19-20]. Others consider factors such as toxin [21-22], cross-feeding [23-25], kill the winner [26-27], pack hunting [15], collective behavior [28], metabolic trade-offs [29-31], co-evolution [32], and other complex species interactions [33-42].

Although many mechanisms mentioned above are likely broadly relevant, special attention needs to be paid to resolve the paradox of plankton, where the system is roughly well-mixed. First and foremost, there should exist a non-zero volume of parameter space where the number of consumer species in enduring coexistence significantly exceeds that of the resources. Mechanisms that can break the constraint of the CEP do not guarantee of this character. Another crucial aspect is that the facilitated biodiversity should still be maintained in a stochastic framework, as stochasticity is ubiquitous in natural processes. Recent studies find that mechanisms supporting biodiversity in a deterministic framework may lead to species extinction when stochasticity is incorporated [32] [43-44].

Two classical experimental studies [45] [46] reported that, in their respective laboratory systems, two species of insects enduringly coexist for roughly years or more with only one type of resources. With close inspections, we deduce that the coexistence might be caused by predator interference, i.e., temporary pairwise encounters between consumer individuals such as staring contest and fighting, which leads to a waste of time. Here we present a mechanistic model of predator interference, excelling the classical Beddington-DeAngelis phenomenological model (B-D model) [33-34] with a detailed consideration of the pairwise encounters. In our model with predator interference, an expected wide range of consumer species can coexist with only one or a handful types of resources. Inspiringly, the coexistence state is resistant to stochasticity and hence can be realized in natural ecosystems. Our model naturally illustrates classical experiments that invalidating the CEP and contributes to resolving the paradox of the plankton.

Results

A generic model of pairwise encounters

Predator interference is commonly described by the well-known B-D model [33-34], which in essence is phenomenological. However, in mechanistic basis, the functional response of the B-D model can be formally derived from the consumption process between a consumer species and a resource species without involving any form of predator interference [15] [47] (see SI Sec. 2 for details). To resolve this issue, we consider a generic mechanistic model of pairwise encounters. Specifically, M consumer species C_1, \dots, C_M competing for N resource species R_1, \dots, R_N (Figure 1a). The consumers are biotic, while the resources can be either biotic or abiotic. For simplicity,

we assume that all species are motile and each moves at a certain speed, namely, v_{C_i} for consumer species C_i ($i=1, \dots, M$) and v_{R_l} for resource species R_l ($l=1, \dots, N$). For abiotic resources, they cannot propel themselves, yet may passively drift due to environmental factors. Each consumer is free to feast on one or multiple types of resources, while consumers do not directly interact with one another other than pairwise encounters.

Then, we proceed to explicitly consider the population structure of the consumers and resources: some are wandering around freely, taking Brownian motions; others are encountering with one another, forming ephemeral entangled pairs. Specifically, when an individual consumer C_i and a resource R_l get close in space within a distance of $r_{il}^{(C)}$ (Figure 1a), the consumer can chase the resource and form a chasing pair, denoted as $C_i^{(P)} \vee R_l^{(P)}$ (Figure 1b), where the superscript ‘‘P’’ represents pair. The resource can either escape with rate d_{il} or be caught and consumed by the consumer with rate k_{il} . Meanwhile, when an individual consumer C_i encounters another consumer C_j ($j=1, \dots, M$) of the same ($i=j$) or a different ($i \neq j$) species within a distance of $r_{ij}^{(I)}$ (Figure 1a), they can stare to, fight against or play with each other and thus form an interference pair, denoted as $C_i^{(P)} \vee C_j^{(P)}$ (Figure 1b). The paired state is evanescent, two consumers separate from each other with rate d'_{ij} . For simplicity, we assume that all $r_{il}^{(C)}$ and $r_{ij}^{(I)}$ are identical respectively, i.e., $\forall i, j, l, r_{il}^{(C)} \approx r^{(C)}$ and $r_{ij}^{(I)} \approx r^{(I)}$.

In a well-mixed system, the encounter rates among the species can be calculated with the mean-field approximations. For example, in a squared system in a length of L , the encounter rate between species C_i and R_l is $a_{il} = 2r^{(C)}L^2\sqrt{v_{C_i}^2 + v_{R_l}^2}$, while that between species C_i and C_j is $a'_{ij} = 2r^{(I)}L^2\sqrt{v_{C_i}^2 + v_{C_j}^2}$ (see SI Sec. 6 and Figure S21 for details). Then, we can explicitly describe the population dynamics of the system. For clarity, we classify the scenarios into cases involving different types of pairwise encounters. Specifically, for a system involving only chasing pair:

$$\begin{cases} \dot{x}_{il} = a_{il}C_i^{(F)}R_l^{(F)} - (d_{il} + k_{il})x_{il}, \\ \dot{C}_i = \sum_{l=1}^M w_{il}k_{il}x_{il} - D_iC_i, \\ \dot{R}_l = g_l(\{R_l\}, \{x_i\}, \{C_i\}), \quad i=1, \dots, M, \quad l=1, \dots, N. \end{cases} \quad (1)$$

Here, the superscript ‘‘F’’ represents the populations that are freely wandering, while $x_{il} \equiv C_i^{(P)} \vee R_l^{(P)}$ stands for the chasing pair. g_l is an unspecific function, while D_i and w_{il} are two constants, where D_i denotes the mortality rate of consumer C_i , and w_{il} means the mass conversion ratio [15] from resource R_l to consumer C_i . With the integration of intraspecific predator interference, we combine Equation 1 and the following equation:

$$\dot{y}_i = a'_i [C_i^{(F)}]^2 - d'_i y_i, \quad i=1, \dots, M, \quad (2)$$

where $a'_i = a'_{ii}$, $d'_i = d'_{ii}$, and $y_i \equiv C_i^{(P)} \vee C_i^{(P)}$ represents the intraspecific interference pair. For a system involving chasing pair and interspecific interference, we combine Equation 1 and that of the following:

$$\dot{z}_{ij} = a'_{ij}C_i^{(F)}C_j^{(F)} - d'_{ij}z_{ij}, \quad i, j=1, \dots, M, \quad i \neq j, \quad (3)$$

with $z_{ij} \equiv C_i^{(P)} \vee C_j^{(P)}$ symbolizing the interspecific interference pair. In the case that chasing pair and both intra- and inter-specific interference are all relevant, we combine Equations 1-3 and the populations of consumers and resources are given by $C_i = C_i^{(F)} + \sum_l x_{il} + 2y_i + \sum_{j \neq i} z_{ij}$ and $R_l = R_l^{(F)} + \sum_i x_{il}$, respectively.

Generically, the consumption and interference processes are much quicker compared to the birth and death processes [15], thus in the derivation of the functional response, $\mathcal{F}_{il}(\{R_l\}, \{C_i\}) \equiv k_{il}x_{il}/C_i$ by the definition, the consumption and interference

processes are supposed to be in fast equilibrium (i.e., $\dot{x}_{il} = 0$, $\dot{y}_i = 0$, and $\dot{z}_{ij} = 0$ wherever applies). For scenarios involving all different types of pairwise encounters, we implement rigorous derivations from a mechanistic perspective, and identify that the functional response in the B-D model is a valid approximation only for a special case with $d_{il} = 0$ ($i=1, \dots, M$, $l=1, \dots, N$) and $R_l \gg \sum_{i=1}^M C_i$ ($l=1, \dots, N$) (Figures

S3-S5). Referring to SI Sec. 2 for the rigorous forms and derivation details.

In Equation 1, the explicit form of function g_l is unspecified. To facilitate further analysis, we assume that the population dynamics of the resources follow the same construction rule as that in the MacArthur's consumer-resource model [48] [49]. Then,

$$g_l(\{R_l\}, \{x_i\}, \{C_i\}) = \begin{cases} R_0^{(l)} R_l \left(1 - R_l / K_0^{(l)}\right) - \sum_{i=1}^M k_{il} x_{il}, & \text{for biotic resources.} \\ R_a^{(l)} \left(1 - R_l / K_0^{(l)}\right) - \sum_{i=1}^M k_{il} x_{il}, & \text{for abiotic resources.} \end{cases} \quad (4)$$

In the absence of consumers, biotic resources follow logistic population growth. Therefore, $R_0^{(l)}$ and $K_0^{(l)}$ represent the intrinsic growth rate and the carrying capacity of consumer species R_l , respectively. For abiotic resources, $R_a^{(l)}$ stands for the external resource supply rate of R_l , while $K_0^{(l)}$ signifies resource R_l 's abundance at steady state without consumers.

Intraspecific interference facilitates species coexistence and breaks the CEP

To clarify the specific mechanism that can facilitate species coexistence, we systematically investigate the scenarios involving different forms of pairwise encounters in a simple case of $M=2$, $N=1$, i.e., two consumer species C_i ($i=1, 2$) competing for one resource species R_l ($l=1$). To simplify the notations, we omit the “ l ” in the sub-/super-scripts since $N=1$. For clarity, we assign each consumer species of unique competitiveness by the setting that the mortality rate D_i is the only parameter with each different value between the two-consumer species, and define $\Delta \equiv (D_1 - D_2) / D_2$ as the competitive difference.

First, we conduct the analysis in a deterministic framework with ordinary differential equations (ODEs). In the scenario involving only chasing pair, consistent with our previous study, consumer species can never coexist at steady state except for special parameter settings (sets of measure zero) [15]. In practice, if all species coexist, the steady-state equations of the consumer species ($\dot{C}_i = 0$) yield

$$f_i(R^{(F)}) \equiv R^{(F)} / (R^{(F)} + K_i) = D_i \quad (i=1, 2), \quad \text{with } K_i = (d_i + k_i) / a_i, \quad \text{which corresponds}$$

to two parallel surfaces in the (C_1, C_2, R) coordinate (Figure 1f, see also Figure S1 a-b), making steadily coexistence mission impossible (Figures 1c and S1c-d, see also S1a-

b and ref [15] for details).

On the contrary, in the scenario involving chasing pair and interspecific interference, if all species coexist, then the steady-state equations of the species correspond to three non-parallel surfaces $\Omega'_i(R, C_1, C_2) = D_i$ ($i=1, 2$), $G'(R, C_1, C_2) = 0$ (Figures 1g, S17 a-b, see SI Sec. 4 for details), which can intersect at a common point (fixed point). However, this fixed point is unstable (see Figure S17 e-f and SI Sec. 4 for details), and thus consumer species are still unable to steadily coexist. With abiotic resources, one of the consumer species is doomed to extinct (Figure 1d). Conversely, in the case of biotic resource, both consumer species may enduringly coexist with time series dynamics, namely, with periodic oscillation (Figure S16e, g) or quasi-periodic oscillation (Figure 2 a-b, S16f, h, and i-j, ODEs results). Interestingly, the region for oscillating coexistence in the parameter space presents a patch pattern (Figure 2c).

Then we turn to the scenario involving chasing pair and intraspecific interference. Likewise, the requirement for species steady coexistence is that three non-parallel surfaces $\Omega_i(R, C_1, C_2) = D_i$ ($i=1, 2$), $G(R, C_1, C_2) = 0$ (Figures 1h, S7 a-b, see SI Sec. 3.1 for details) cross at a common point. Obviously, this can naturally happen and inspiringly, the fixed point can be stable. Then, the two-consumer species can steadily coexist with only one type of resources, which actually breaks the CEP (Figures 1e, S6c). In fact, there exist one or multiple types of enduring coexistence patterns depending on the life form of the resources. With abiotic resources, steady coexistence is the only type and the coexistence state is globally attractive (Figure 2d, g). When the resources are biotic, the steady coexistence state is either globally attractive (Figure 2e) or unstable, where the species dynamics may end in a limit cycle (Figure 2f, h and i, S6d-e). In particular, regardless of the life form of the resources, there exists a non-zero volume of parameter space where the two-consumer species stably coexist at constant population densities (Figure 2g-i), which illustrates that the mechanism of intraspecific interference can break the CEP without involving special parameter settings.

We further consider the scenario involving chasing pair and both intra- and inter-specific interference (Figure S18-20). Much as expected, the species coexistence behavior is very similar to that without interspecific interference (Figure S16).

Intraspecific interference promotes biodiversity in the presence of stochasticity

Mathematically, an ideal steady state precludes the association of stochasticity. However, as stochasticity is ubiquitous in nature, to facilitate biodiversity in a real system, stochasticity naturally involves. Coexistence states that are vulnerable to stochasticity can hardly be realized in an ecosystem. Nevertheless, recent studies show that stochasticity is prone to jeopardize species coexistence [32] [43] [44]. Influential mechanisms such as “kill the winner” fail when stochasticity is incorporated [32].

Consistent with this, we identify that two notable cases of oscillating coexistence [19-20] turn into species extinction as stochasticity is introduced (Figure S2), where we simulate the model systems with stochastic simulation algorithm (SSA) [50] and adopt the same parameters as that in the original references [19-20].

Then, we proceed to investigate the impact of stochasticity on the enduring coexistence behavior of our model using SSA. Specifically, in the scenario involving chasing pair and interspecific interference, the two-consumer species fail to coexist along with stochasticity (Figures 2a, S16, SSA results). Conversely, in the scenario involving chasing pair and intraspecific interference, species can enduringly coexist in the SSA simulations. To be more precise, they can either fluctuate around a globally attractive steady state (Figure 2j, m) or present sustainable stochastic oscillations in the vicinity of a stable limit cycle (Figure 2k-l). In the scenario with additional interspecific interference, unsurprisingly, all species can still enduringly coexist along with stochasticity (Figure S20).

To further mimic the time evolution in a real ecosystem, we resort to individual-based modeling (IBM) [51-52], a virtually stochastic simulation method, which widely used in ecology. The system is homogenous, with a squared landscape of length L and periodic boundary conditions (see SI. Sec. 6 for details). Likewise, we still consider the case of $M=2, N=1$. In the scenario involving chasing pair and intraspecific interference, snapshots of the system in the time evolution are shown in Figure 2o. By collecting species abundances in the time series, it is evident that the two-consumer species can enduringly coexist with only one type of resources (Figures 2n). Comparing the IBM time series results with that of the ODEs, both with the same set of parameters, they are roughly similar overall, yet still of noticeable differences in the average behavior (Figures 2n), especially comparing to the case between the SSA and ODEs time series (Figure 2j-k). This may partly attribute to the mean-field approximations in the parameter settings. Above all, with the SSA and IBM simulation studies, it is evident that intraspecific interference can promote species coexistence regardless of stochasticity.

A handful of resource species can support an unexpected wide range of consumer species

With a thorough study in the case of $M=2, N=1$, mechanistically, we are still unsure if the species number of consumers can significantly exceed that of the resources, although apparently this has been demonstrated in the paradox of the plankton. To solve this puzzle, we consider the generic case that M consumers species competing for N resource species within the scenario involving chasing pair and intraspecific interference. Then, the population dynamics can be described by equations combining Equations 1-2. For clarity, as with the case above, we set each consumer species of a unique competitiveness through a distinctive D_i .

Inspiringly, we identify (with ODEs) that a plethora of consumer species can coexist at steady state with only one type of resources ($M \gg 1, N = 1$), and in particular, the facilitated biodiversity can still be maintained in stochastic simulations (with SSA) with identical settings of the model parameters. The enduring coexistence behavior are exemplified in Figures 3 and S9-S12, involving resource species that are biotic or abiotic, and simulations with or without stochasticity. The number of consumer species in enduring coexistence is 5, 20 and 100 (Figures 3), and actually this number can even much larger. To mimic real ecosystems, we further analyze the cases with more than one type of resources, such that systems with $M \gg N, N = 3$. Just like the case of $M \gg 1, N = 1$, an extensive range of consumer species enduringly coexist regardless of stochasticity (Figures 3, S9, S13-S14).

In fact, when the population of each resource species significantly exceeds the total population of consumers (i.e., $R_l \gg \sum_{i=1}^M C_i$, with $l = 1, \dots, N$), in the case of a single

type of resources ($N = 1$), or if the resource species are all biotic, the steady state population of each consumer and resource species can be calculated analytically (see SI Sec. 3.2 for details). In Figures 1e, 3a-b, S7c-d and S9c-d, we see that the analytical results are highly consistent with the numerical results and can even accurately predict the coexistence region in the parameter space (Figure S7e-f).

Comparison with experimental studies that reject the CEP

To investigate whether the predicted biodiversity in our model involving intraspecific interference has ever been realized in ecosystems, we resort to experimental studies. In fact, the paradox of plankton is highly relevant. As demonstrated in Figures 3 and S9-S14, a handful types of resources support a plethora of consumer species, which qualitatively agree well with the coexistence behavior of the plankton. The pity is that up to now there are still no such time series data in a real ecosystem. Contrastingly, there are many existing experimental studies of microbial systems, yet since cross-feeding (which promotes biodiversity) is prevalent among microbial species, special attention must be paid to disentangle the respective contributions.

In practice, two classical experiments in laboratory systems are highly relevant, both using insects as the consumer species. Specifically, in the 1960s, Francisco Ayala, an evolutionary biologist, reported that two species of flies, *Drosophila serrata* and *Drosophila pseudoobscura*, coexist for more than 40 weeks (duration of the experiment) when competing for the same abiotic resources in a bottle with serial transfer (resource supply) [45]. Likewise, even earlier in the 1950s, Thomas Park, an animal ecologist,

observed that two species of beetles, *Tribolium confusum* and *Tribolium castaneum*, coexist for more than two years (duration of the experiment) when competing for the same type of food (flour) within a laboratory. Evidently, these two experiments are not compatible with the CEP, while factor such as temporal variations, spatial heterogeneity, cross-feeding, pack hunting, etc. are clearly not involved in such systems. Interestingly, intraspecific fighting is prevalent among insects [53], and actually there are many reports for *Drosophila* [54-55]. Inspired by this, we naturally apply our model with chasing pair and intraspecific interference to simulate the two systems. The simulated time series are shown together with the experimental data in Figure 4 (see also Figure S8), which overall shows good consistency, and the moderate fluctuations in time series can be mainly account by stochasticity (simulated with SSA). This demonstrates that our model can quantitatively illustrate the two classical experiments invalidating the CEP.

Discussion

The paradox of the plankton is a long-standing puzzle in ecology. Over the past six decades, many mechanisms have been proposed to overcome the limit set by the CEP, however, it is still unclear how can a plethora of plankton species in aquatic environment enduringly coexist with only a handful types of resources. To address this problem, we investigate a generic mechanistic model with detailed consideration of pairwise encounters, especially the formation of chasing pair and intra-/inter-specific (predator) interference pair. With extensive numerical simulations and mathematical analysis, we identify that in a system with intraspecific interference and chasing pair, a handful types of resources can support a plethora of consumer species regardless of stochasticity. In the ODEs simulation, all species may coexist at constant population densities with a non-zero volume of parameter space, which apparently breaks the CEP. Along with stochasticity, species can still enduringly coexist, offering a feasible solution to the paradox of the plankton. Applying the analysis to a system with two types of consumers and one type of resources, our model naturally illustrates two classical experimental studies that rejecting the CEP.

Intuitively, the fact that intraspecific interference may facilitate species coexistence can be understood from the underlying feedback mechanism. Specifically, as the population density of consumer species C_i increases, a larger portion of species C_i are then getting involved in an intraspecific interference pair which temporarily absent from hunting (Figure S15), which is due to the impact of pairwise encounters. Consequently, the fraction of species C_i within a chasing pair decreases (Figure S15), which virtually forms a negative feedback in the functional response. This negative feedback results in an overall balance among the consumer species, and thus promotes biodiversity.

Previously, predator interference was commonly described by the celebrated B-D model, which introduced consumer dependency in the functional response using hand-waving derivations. Thus, in essence, the B-D model is phenomenological. With further simplification (depends on parameter settings), this model can present a ratio-dependent predation form [56-57], which also widely applied in theoretical ecology. In mechanistic studies, the functional response in the B-D model can be derived from the scenario involving only chasing pair or its equivalence without predator interference [15] [47], which confounds the mechanistic basis of the B-D model. With a generic mechanistic model, we resolve the discrepancy by first deriving the rigorous forms of the functional responses in various scenarios, and we further get the approximate forms depending on parameter settings. Although they are overall different from that of the B-D model, yet the differences are not obvious when $d_{il} = 0$ ($i = 1, \dots, M$, $l = 1, \dots, N$)

and $R_l \gg \sum_{i=1}^M C_i$ ($l = 1, \dots, N$) (Figures S3-S5, see SI Sec. 2 for details). Still, we

emphasize that special attention is required when applying the approximate forms of functional response to explain biodiversity, as a little careless may lead to an erroneous picture of species coexistence.

Finally, our modelling framework is broadly applicable to many systems with pairwise interactions, with the potential to yield insights in areas such as statistical physics, biochemistry, immunology, oceanology and ecology. For practical use in ecology, we still need to mention that the facilitated biodiversity in our model is parameter dependent, although it does not depend on special parameters. To elucidate species coexistence in a real system, special attention needs to be paid to disentangle the contributions of other mechanisms such as cross-feeding and spatial heterogeneity. Our study contributes to explaining how biodiversity may naturally emerge and maintain in an ecosystem, yet it is still a great challenge to understand in a quantitative framework how do tremendous species coexist and evolve in various changing ecosystems in the wild.

Figures

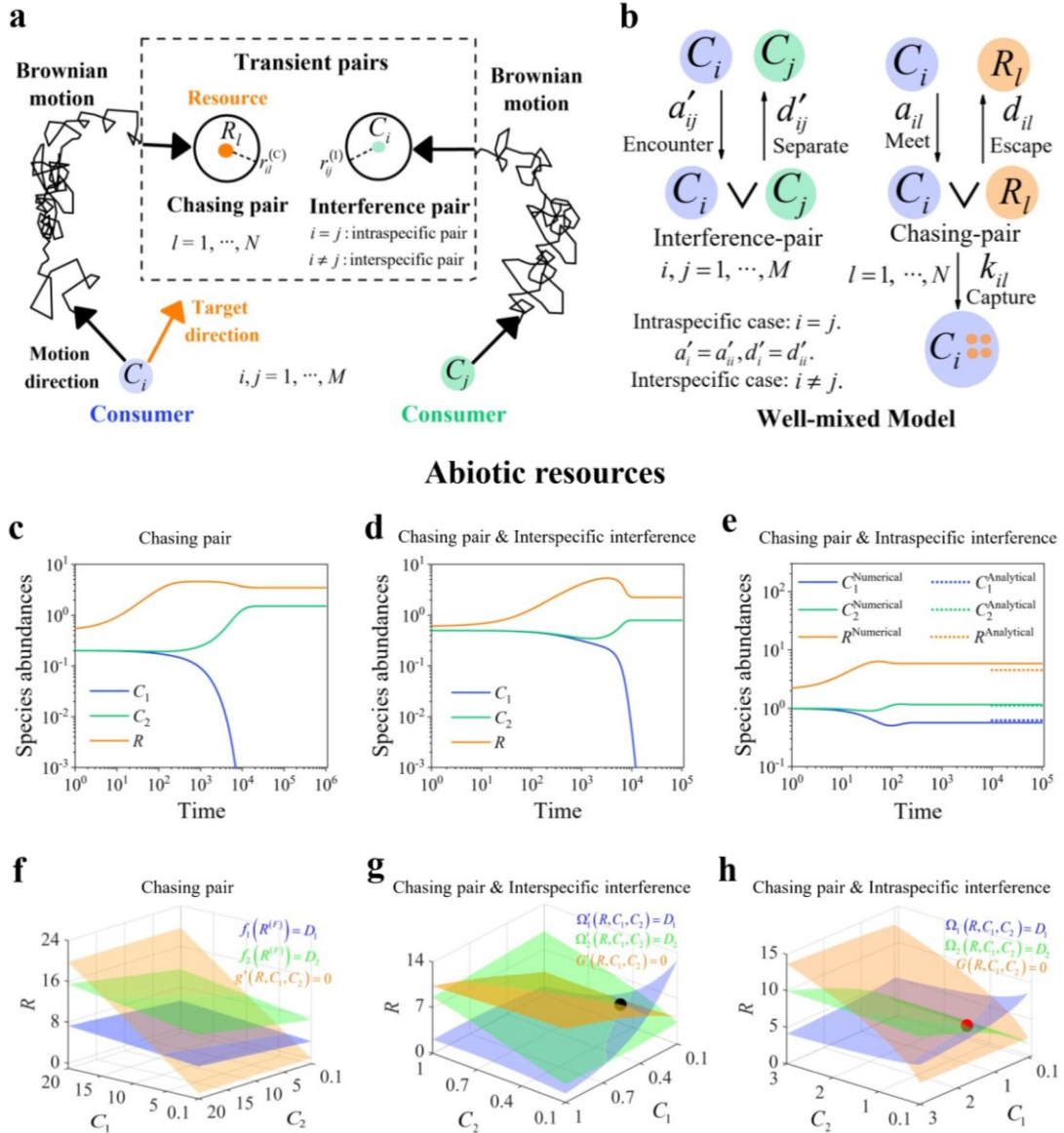
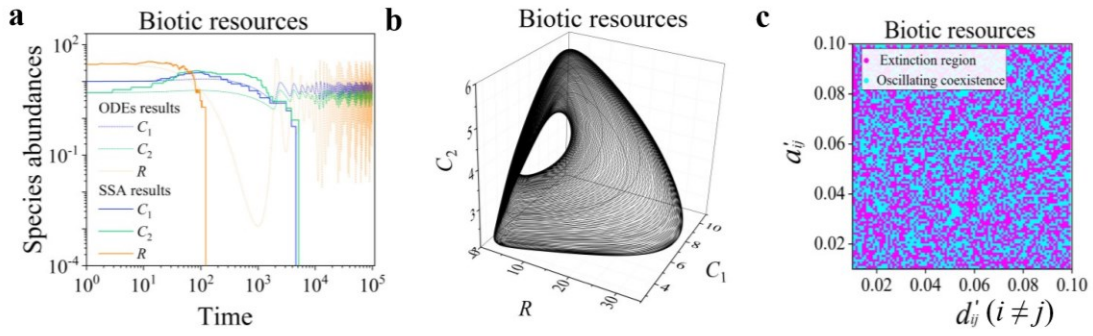


Figure 1 | A model of pairwise encounters may naturally break Competitive Exclusion Principle (CEP). (a-b) A generic model of M consumer species competing for N resource species with pairwise encounters. (a) Consumer moves randomly in space. It can form a chasing pair with a resource when their distance is less than $r^{(C)}$, and form an interference pair with another consumer when their distance is less than $r^{(I)}$. (b) The well-mixed model of (a). (c-h) A simple case of two consumer species ($M=2$) feeding on one abiotic resource species ($N=1$). (c-e) Time courses of the species abundances in different scenarios. (f-h) Positive solutions to the steady-state equations: $\dot{R}_l = 0$ (orange surface), $\dot{C}_1 = 0$ (blue surface), $\dot{C}_2 = 0$ (green surface). (c, f) In the scenario involving only chasing pair, the green surface and blue surface in (f) are

parallel to each other, and thus the consumer species cannot coexist at steady state (see **(c)** for time courses). **(d, g)** In the scenario involving chasing pair and interspecific interference, the three surfaces in **(g)** are not parallel to each other and hence share a common point (shown in black). Yet this fixed point is unstable, and thus the consumer species still cannot coexist at steady state (see **(d)** for time courses). **(e, h)** In the scenario involving chasing pair and intraspecific interference, all surfaces in **(h)** are unparallel to each other and therefore intersect at one point (shown in red). This fixed point is stable and hence the consumer species may coexist at steady state (see **(e)** for time courses). The dotted lines in **(e)** are the analytical steady-state solutions (labeled with superscript “Analytical”) calculated in Equations S3.11 and S3.15. See Table S1 for simulation details.

Chasing pair & Interspecific interference



Chasing pair & Intraspecific interference

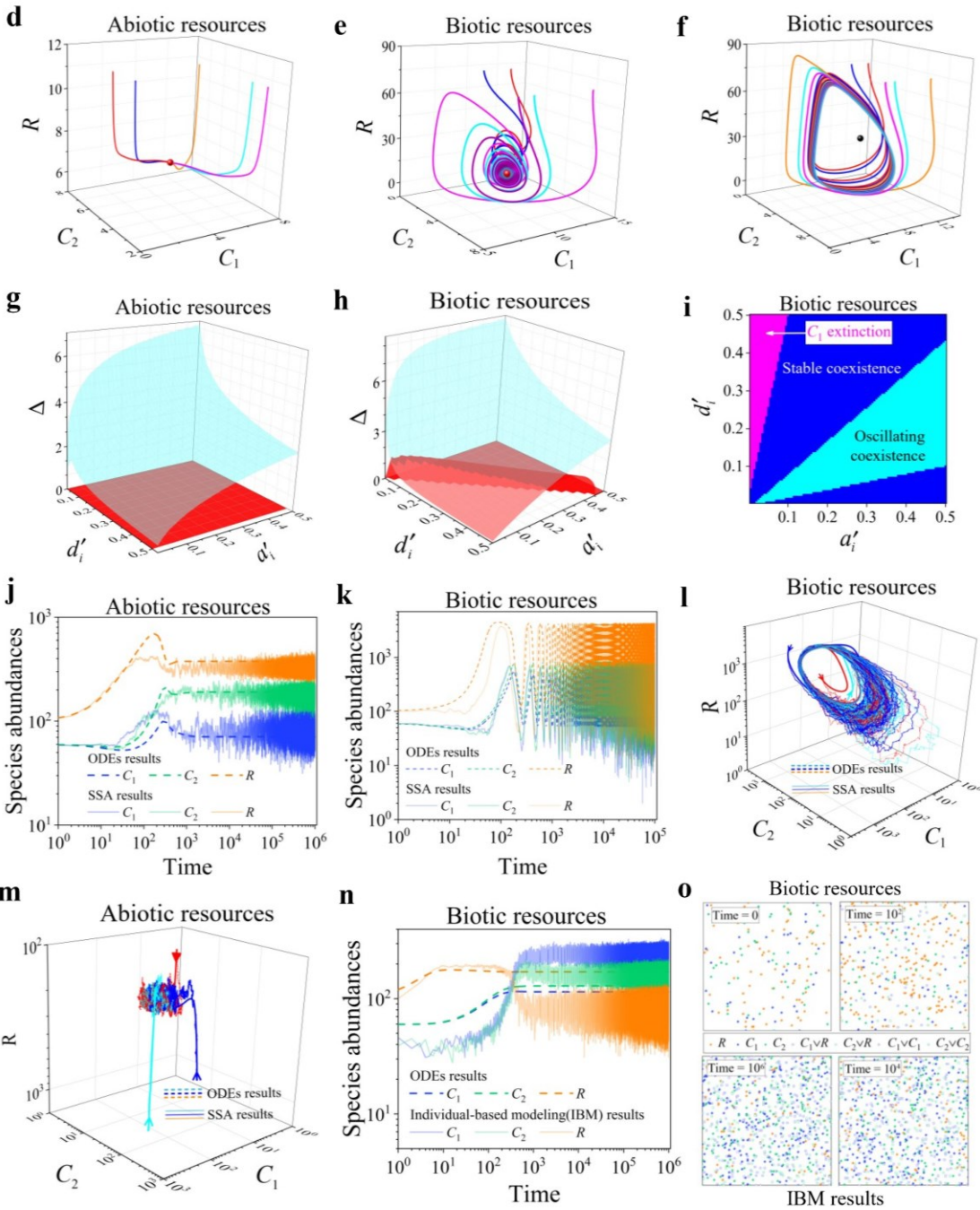


Figure 2 | Intraspecific interference facilitates species coexistence disregarding of stochasticity. Here we consider the case of $M=2$, $N=1$. **(a-c)** Scenario of biotic resources involving chasing pair and interspecific interference. **(d-o)** Scenario involving chasing pair and intraspecific interference. **(a, j and k)** Time courses of the species abundances simulated with ordinary differential equations (ODEs, dashed lines), or stochastic simulation algorithm (SSA, solid lines). **(a)** Species may coexist unsteadily in the ODEs simulations, yet the coexistence is vulnerable to stochasticity. **(b)** Trajectory of a quasiperiodic orbit in the state space (see solid lines in **(a)** for time courses). **(c)** Phase diagram of species' deterministic coexistence. Blue areas mark species coexistence with self-organized dynamics, while pink areas mark competitive exclusion. **(d-f)** Different types of deterministic coexistence trajectories in the state space. **(d-e)** The fixed points (shown in red) corresponding to species coexistence are globally attractive. **(f)** With unstable fixed point (shown in black), all trajectories attract to a limit cycle. **(g-h)** 3D Phase diagram of species' deterministic coexistence. D_i ($i=1,2$) is the only parameter with each different value between the two consumer species, and $\Delta \equiv (D_1 - D_2)/D_2$ measures the competitive difference between the two species. The parametric region below the blue surface yet above the red surface represents species stable coexistence, while that below the red surface and above $\Delta=0$ represents unstable fixed points. **(i)** The transection corresponding to the $\Delta=1$ plane in **(h)**. **(l-m)** Different types of stochastic coexistence trajectories in the state space. **(l)** The stochastic limit-cycle is stable, species oscillating coexist (see **(k)** for time courses). **(m)** The stochastic coexistence state is stable and globally attractive (see **(j)** for time courses). **(n)** Time courses of the species abundances simulated with individual based modelling (IBM). Species may enduringly coexist. **(o)** Snapshots of the IBM simulations. See Table S1 for simulation details.

Chasing pair & Intraspecific interference

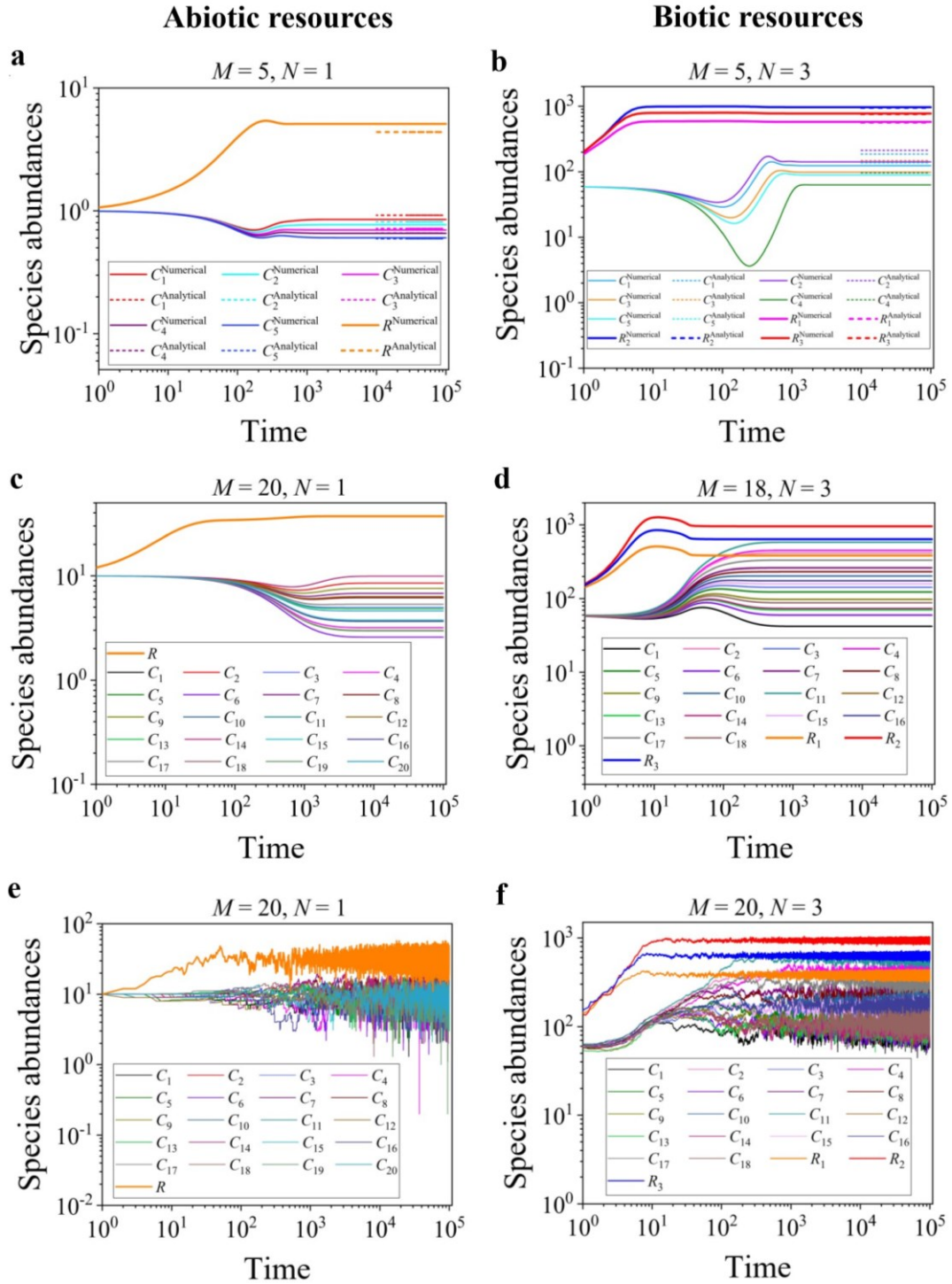


Figure 3 | With intraspecific interference, a handful of resource species (N) can support an unexpected wide range of consumers species ($M \gg N$) regardless of stochasticity. Here, D_i ($i = 1, \dots, M$) is the only parameter of each different value among the consumer species, thus each consumer species owns a unique competitiveness. **(a-d)** Time courses of the species abundances simulated with ODEs. The dashed lines in **(a-b)** are the analytical steady-state solutions calculated in

Equations S3.23-S3.28. **(e-f)** Time courses of the species abundances simulated with SSA (corresponds to **(c-d)**). With intraspecific interference, the coexisting number of consumer species can greatly exceed that of the resources. See Table S1 for simulation details. See also Fig. S9-S14.

Chasing pair & Intraspecific interference

Abiotic resources, $M = 2$, $N = 1$

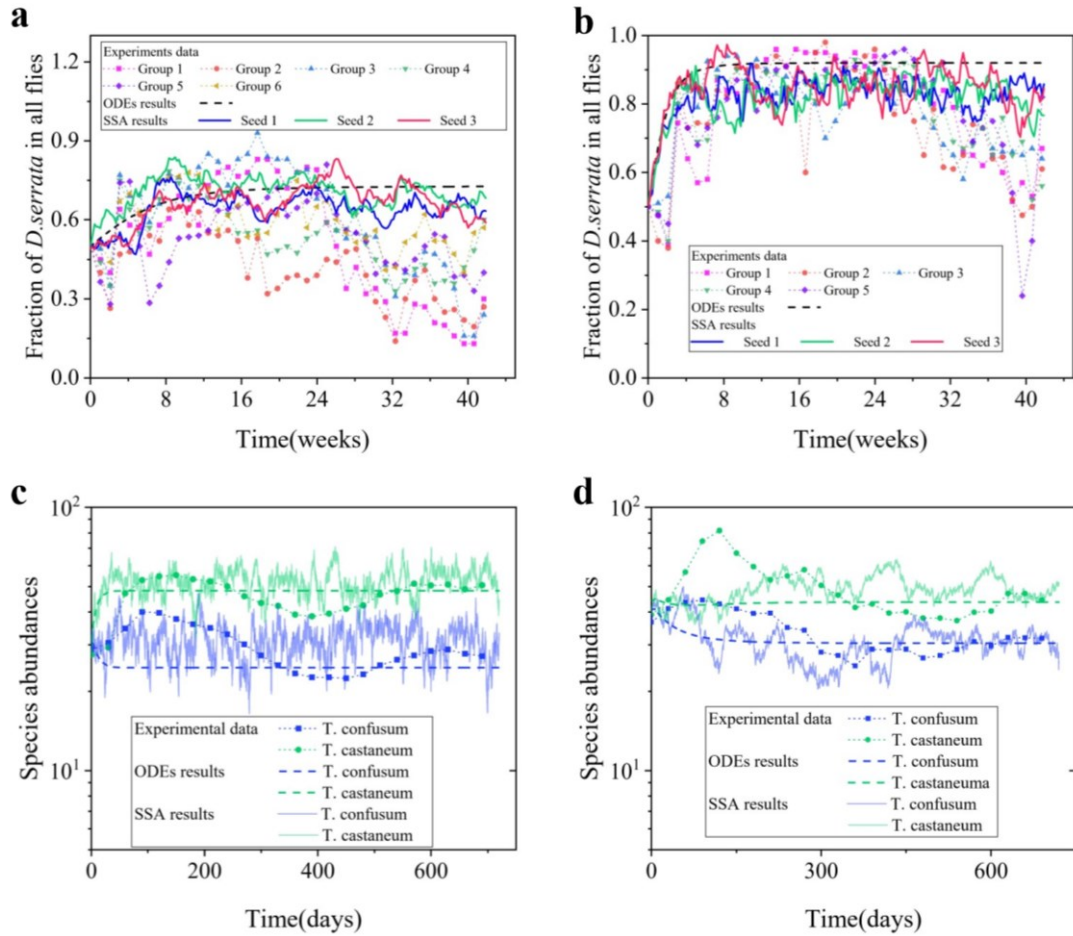


Figure 4 | A model of intraspecific interference explains two classical experimental studies that invalidating the CEP. Here, the solid dots, triangles and boxes represent the time serials experimental data, which are connected by the dotted lines for the sake of visibility. The dashed lines and solid lines stand for the ODEs and SSA simulation results, respectively. In all cases, two consumer species ($M=2$) enduringly coexist with only one type of resources ($N=1$). **(a-b)** In Ayala's experiment [45], two *Drosophila* species (consumers), *D. serrata* and *D. pseudoobscura*, compete for the same type of abiotic resources in a laboratory bottle. **(c-d)** In Park's experiment [46], two *Tribolium* species, *T. confusum* and *T. castaneum*, compete for the same food (flour). See Table S1 for simulation details.

Acknowledgments

We thank Roy Kishony, Eric D. Kelsic and Fan Zhong for helpful discussions. This work was supported by National Natural Science Foundation of China (Grant No.12004443), Guangzhou Municipal Innovation Fund (Grant No.202102020284) and the Hundred Talents Program of Sun Yat-sen University.

Author contributions

X.W. conceived and designed the project, developed the model, and mainly carried out the analytical calculations. J.K. carried out the numerical calculation, performed the ODE simulations, participated in the analytical calculations and stochastic simulations. S.J.Z mainly carried out the stochastic simulations. J.K. and S.J.Z analyzed the experimental data. X.W. and J.K. wrote the paper.

Competing interests

The authors declare no competing interests.

References

- [1] Pennisi, E., What determines species diversity? *Science*, 309(5731): 90-90 (2005).
- [2] Rull, V., Speciation timing and neotropical biodiversity: the Tertiary-Quaternary debate in the light of molecular phylogenetic evidence. *Molecular Ecology*, 17(11): 2722-2729 (2008).
- [3] Jaramillo, C., M. J. Rueda, G. Mora, Cenozoic plant diversity in the neotropics. *Science*, 311(5769): 1893-1896 (2006).
- [4] Albert, J. S., et al., Aquatic biodiversity in the Amazon: habitat specialization and geographic isolation promote species richness. *Animals (Basel)*, 1(2): 205-241 (2011).
- [5] Pennington, R. T., M. Hughes, P. W., Moonlight, The origins of tropical rainforest hyperdiversity. *Trends Plant Sci.*, 20(11): 693-695 (2015).
- [6] ter Steege, H, et al., Hyperdominance in the Amazonian tree flora. *Science*, 342(6156): 325-335 (2013).
- [7] Feng, X., et al., How deregulation, drought and increasing fire impact Amazonian biodiversity. *Nature*, 597(7877): 516-521 (2021).
- [8] Gause, G., *The Struggle for Existence*. The Williams & Wilkins company (1934).
- [9] Armstrong, R. A., McGehee, R. Competitive exclusion. *American Naturalist*, 115(2): 151-170 (1980).
- [10] Hardin, G., The competitive exclusion principle. *Science*, 131: 1292-1297 (1960).
- [11] Gilpin, M. E., Justice, K. E., Reinterpretation of the invalidation of the principle of competitive exclusion. *Nature*, 236(5345): 273-274 (1972).
- [12] MacArthur, R., Levins, R., Competition, habitat selection, and character displacement in a patchy environment. *Proceedings of the National Academy of Sciences of the United States of America*, 51(6): 1207-1210 (1964).
- [13] Levin, S. A., Community equilibria and stability, and an extension of the

- competitive exclusion principle. *The American Naturalist*, 104(939): 413-423 (1970).
- [14] Hutchinson, G. E., The paradox of the plankton. *The American Naturalist*, XCV(882): 137-145 (1961).
- [15] Wang, X., Y. Y. Liu, Overcome competitive exclusion in ecosystems. *iScience*, 23(4): 101009 (2020).
- [16] Chesson, Peter, Mechanisms of maintenance of species diversity. *Annual Review of Ecology and Systematics*, 31(1): 343-366 (2000).
- [17] Maciel, G. A., F. Lutscher, Movement behaviour determines competitive outcome and spread rates in strongly heterogeneous landscapes. *Theoretical Ecology*, 11(3): 351-365 (2018).
- [18] Gupta, et al., Effective Resource Competition Model for Species Coexistence. *Phys. Rev. Lett.*, 127 (20): 208101 (2021).
- [19] Koch, A. L., Competitive coexistence of two predators utilizing the same prey under constant environmental conditions. *Journal of Theoretical Biology*, 44(2): 387-395 (1974).
- [20] Huisman, J., Weissing, F. J., Biodiversity of plankton by species oscillations and chaos. *Nature*, 402(6760): 407-410 (1999).
- [21] Majeed, H., et al., Competitive interactions in *Escherichia coli* populations: the role of bacteriocins. *ISME J*, 5(1): 71-81 (2011).
- [22] Czárán, T. L., Hoekstra, R. F., Pagie, L., Chemical warfare between microbes promotes biodiversity. *Proceedings of the National Academy of Sciences*, 99(2): 786-790 (2002).
- [23] Turner, P. E., Souza, V., Lenski, R. E., Tests of ecological mechanisms promoting the stable coexistence of two bacterial genotypes. *Ecology*, 77(7): 2119-2129 (1996).
- [24] Goyal, A., S. Maslov, Diversity, Stability, and reproducibility in stochastically assembled microbial ecosystems. *Phys. Rev. Lett.*, 120(15): 158102 (2018).
- [25] Goldford, J. E., et al., Emergent simplicity in microbial community assembly. *Science*, 361(6401): 469-474 (2018).
- [26] Thingstad, T. F., Risto Lignell, Elements of a theory for the mechanisms controlling abundance, diversity, and biogeochemical role of lytic bacterial viruses in aquatic systems. *Limnology and Oceanography*, 45(6): 1320-1328 (2000).
- [27] Thingstad, T. F., Risto Lignell, Theoretical models for the control of bacterial growth rate, abundance, diversity and carbon demand. *Aquatic microbial ecology*, 13(1): 19-27 (1997).
- [28] Dalziel, B. D., et al. Collective behaviour can stabilize ecosystems. *Nature Ecology & Evolution*, 5: 1435–1440 (2021).
- [29] Posfai, A., T. Taillefumier, Wingreen, N. S., Metabolic trade-offs promote diversity in a model ecosystem. *Phys. Rev. Lett.*, 118(2): 028103 (2017).
- [30] Cadotte, M. W., et al. On testing the competition-colonization trade-off in a multispecies assemblage. *The American Naturalist*, 168(5): 704-709 (2006).
- [31] Weiner, B. G., Posfai, A., Wingreen, N. S., Spatial ecology of territorial populations. *Proceedings of the National Academy of Sciences*, 116(36): 17874-

- 17879 (2019).
- [32] Xue, C., N. Goldenfeld, Coevolution maintains diversity in the stochastic "Kill the Winner" model. *Phys. Rev. Lett.*, 119(26): 268101 (2017).
 - [33] Beddington, J. R., Mutual interference between parasites or predators and its effect on searching efficiency. *The Journal of Animal Ecology*, 44(1): 331-340 (1975).
 - [34] DeAngelis, D. L., Goldstein, R. A., O'Neill, R. V., A model for trophic interaction. *Ecology*, 56(4): 881-892 (1975).
 - [35] Tyutyunov, Y., L. Titova, R. Arditi, Predator interference emerging from trophotaxis in predator–prey systems: An individual-based approach. *Ecological Complexity*, 5(1): 48-58 (2008).
 - [36] Chakraborty, S., et al., Revealing the role of predator interference in a predator–prey system with disease in prey population. *Ecological Complexity*, 21: 100-111 (2015).
 - [37] Grether, G. F., et al., Predicting evolutionary responses to interspecific interference in the wild. *Ecol. Lett.*, 23(2): 221-230 (2020).
 - [38] Butler, S., J. P. O'Dwyer, Stability criteria for complex microbial communities. *Nat. Commun.*, 9(1): 2970 (2018).
 - [39] Yeakel, J. D., et al., Diverse interactions and ecosystem engineering can stabilize community assembly. *Nat. Commun.*, 11(1): 3307 (2020).
 - [40] Grilli, J., et al., Higher-order interactions stabilize dynamics in competitive network models. *Nature*, 548(7666): 210-213 (2017).
 - [41] Levine, J. M., et al., Beyond pairwise mechanisms of species coexistence in complex communities. *Nature*, 546(7656): 56-64 (2017).
 - [42] Ratzke, C., Julien Barrere, Jeff Gore, Strength of species interactions determines biodiversity and stability in microbial communities. *Nature ecology & evolution*, 4(3): 376–383 (2020).
 - [43] Capitan, J. A., S. Cuenda, D. Alonso, Stochastic competitive exclusion leads to a cascade of species extinctions. *J. Theor. Biol.*, 419: 137-151 (2017).
 - [44] Pfeiffer T., et al., Cooperation and Competition in the Evolution of ATP-Producing Pathways. *Science*, 292(5516): 504-507 (2001).
 - [45] Ayala, F. J., Experimental invalidation of the principle of competitive exclusion. *Nature*, 224(5224): 1076-1079 (1969).
 - [46] T. Park, Experimental studies of interspecies competition II: temperature, humidity, and competition in two species of *Tribolium*. *Physiological Zoology*, 27(3): 177-238 (1954).
 - [47] Huisman, G., Rob J. De Boer, A formal derivation of the “Beddington” functional response. *Journal of Theoretical Biology*, 185(3), 389-400 (1997).
 - [48] MacArthur, R., Species packing and competitive equilibrium for many species. *Theoretical Population Biology*, 1(1): 1-11 (1970).
 - [49] Chesson, P., MacArthur's consumer-resource model. *Theoretical Population Biology*, 37(1): 26-38 (1990).
 - [50] Gillespie, D. T., Stochastic simulation of chemical kinetics. *Annu. Rev. Phys. Chem.*, 58: 35-55 (2007).
 - [51] Grimm V., et al. *Individual-based Modeling and Ecology*. Princeton University

- Press (2013).
- [52] Vetsigian, K., Diverse modes of eco-evolutionary dynamics in communities of antibiotic-producing microorganisms. *Nature Ecology & Evolution*, 1: 0189 (2017).
 - [53] Boomsma, J. J., Baer, B., Heinze, J., The evolution of male traits in social insects. *Annual Review of Entomology*, 50: 395-420 (2005).
 - [54] Dankert, H., et al., Automated monitoring and analysis of social behavior in *Drosophila*. *Nature Methods*, 6(4): 297-303 (2009).
 - [55] Chen, S., et al., Fighting fruit flies: a model system for the study of aggression. *Proceedings of the National Academy of Sciences*, 99(8): 5664-5668 (2002).
 - [56] Abrams, P. A., Ginzburg, L. R., The nature of predation: prey dependent, ratio dependent or neither? *Trends Ecol. Evol.*, 15: 337-341 (2000).
 - [57] Arditi, R., Ginzburg, L. R., Coupling in predator-prey dynamics: ratio-dependence. *Journal of Theoretical Biology*, 139: 311-326 (1989).

Supplemental Information

Intraspecific predator interference promotes biodiversity in ecosystems

| | |
|---|----|
| S1 Competitive Exclusion Principle (CEP) | 1 |
| S1.1 The content of the CEP | 1 |
| S1.2 The classical proof of the CEP..... | 1 |
| S2 Comparison of the functional response with Beddington-DeAngelis' model in scenarios involving different types of pairwise encounters | 2 |
| S2.1 Beddington's model | 2 |
| S2.2 Scenario involving only chasing pair..... | 2 |
| S2.2 Scenario involving chasing pair and intraspecific interference | 5 |
| S2.3 Scenario involving chasing pair and interspecific interference | 8 |
| S3 Scenario involving chasing pair and intraspecific interference | 11 |
| S3.1 Two consumers species competing for one resource species..... | 11 |
| S3.1.1 Analytical solutions of species abundances at steady state..... | 12 |
| S3.1.2 Stability analysis and a Hopf bifurcation | 15 |
| S3.2 M consumers species competing for N resources species | 15 |
| S3.2.1 Analytical solutions of species abundances at steady state..... | 16 |
| S4 Scenario involving chasing pair and interspecific interference | 19 |
| S4.1 Analytical results of the fixed-point solutions | 20 |
| S4.2 Stability analysis of the coexistence behavior | 21 |
| S5 Scenario involving chasing-pairs and both intra- and inter-specificinterference..... | 22 |
| 5.1 Analytical solutions of species abundances at steady state | 22 |
| S5.2 Stability analysis of the coexisting state | 23 |
| S6 Methods | 24 |
| 6.1 Derivation of the encounter rates with mean-field approximations | 24 |
| 6.2 Stochastic simulations and Individual-based modeling | 25 |
| Supplemental Figures..... | 28 |
| Supplemental Tables..... | 52 |

S1 Competitive Exclusion Principle (CEP)

S1.1 The content of the CEP

The notion of the competitive exclusion dates back to Charles Darwin's theory of evolution, survival of the fittest. The earliest form of the CEP [8] [10], also referred as the Gause's law, states that two species competing for the same limited resources cannot coexist at constant population densities. In the 1960s, MacArthur and Levin extended this principle to a generic case with an arbitrary number of resources [12-13]. The principle states that, in a well-mixed system of M types of consumers feeding on N types of resources, the number of consumer species in coexistence cannot exceeds that of the resources at steady state, i.e., $M \leq N$. (See the SI in Ref. [15] for more details.)

S1.2 The classical proof of the CEP

In a classical paper [12-13], MacArthur and Levin proposed a mathematical proof the CEP. We rephrase the idea of the proof in a simple case of $M=2$ and $N=1$, i.e., two consumer species C_1 and C_2 competing for one resource species R . In fact, it is easy to generalize this proof to higher dimensions with several types of consumers and resources. Then, the population dynamics of the species can be described as follows:

$$\begin{cases} \dot{C}_i = C_i (f_i(R) - D_i), & i=1,2; \\ \dot{R} = g(R, C_1, C_2). \end{cases} \quad (\text{S1.1})$$

Here C_i and R represent the population abundances of consumers and resources, while the functional forms of $f_i(R)$, $g_i(R, C_1, C_2)$ are unspecific. D_i stands for the mortality rate of the species C_i . If all consumer species can coexist at steady state, then $f_i(R)/D_i = 1$ ($i=1,2$). In a 2-D representation, this requires that three lines, $y = f_i(R)/D_i$ ($i=1,2$) and $y = 1$, share a common point, which is commonly impossible unless the model parameters satisfy special constraint (sets of Lebesgue measure zero). In a 3-D representation, the two planes, which correspond to $f_i(R)/D_i = 1$ ($i=1,2$), are parallel to each other, and hence do not share a common point (See also Fig. S1a -b. See Ref. [15] for details).

S2 Comparison of the functional response with Beddington-DeAngelis' model in scenarios involving different types of pairwise encounters

S2.1 Beddington's model

In the 1970s, Beddington [33] proposed a mathematical model to describe the influence of predator interference on the functional response, where he applied handwaving derivations in a simple system with one type of consumers and one type of resources. In the same year, DeAngelis [34] considered a related question and put forward a similar model. Essentially, both models are phenomenological, and they were called Beddington-DeAngelis model (B-D model) in the subsequent studies. In practice, the B-D model can be extended into scenarios involving different types of pairwise encounters with Beddington's modelling method. In this section, we systematically compare the functional response in our mechanistic model with that of the B-D model in all the relevant scenarios.

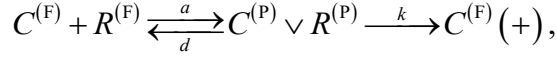
Recalling Beddington's analysis [33], he considered a simple case of one consumer species C and one resource species R ($M = 1, N = 1$). In a well-mixed environment, an individual consumer meets a resource with rate a , while encounters another consumer with rate a' . There are two other phenomenological parameters in this model, namely, the handling time t_h and the wasting time t_w , which actually can be both determined by specifying the scenario and with further statistical physics modeling analysis. In fact, Beddington analyzed the searching efficiency $\Xi_{\text{B-D}}$ rather than the functional response $\mathcal{F}_{\text{B-D}}$, while both can be reciprocally derived with $\Xi_{\text{B-D}} \equiv \mathcal{F}_{\text{B-D}}/R$. Here R stands for the population abundance of the resources, and the specific form of $\Xi_{\text{B-D}}$ is [33]:

$$\Xi_{\text{B-D}}(R, C) = \frac{a}{1 + at_h R + a't_w C'}, \quad (\text{S2.1})$$

where $C' = C - 1$, with C stands for the population abundance of the consumes. Generally, $C \gg 1$, and thus $C' \approx C$.

S2.2 Scenario involving only chasing pair

Here we consider the scenario involving only chasing pair for the simple case of one type of consumers and one type of resources ($M = 1, N = 1$). When an individual consumer is chasing a resource, they form a chasing pair.



where the superscript ‘‘F’’ stands for populations that are freely wandering, and ‘‘(+’’ signifies gaining biomass (we count $C^{(F)}(+)$ as $C^{(F)}$). $C^{(P)} \vee R^{(P)}$ represents chasing pair (where ‘‘P’’ signifies pair), denoted as x . a , d and k stand for encounter rate, escape rate and capture rate, respectively. Hence, the total number of consumers and resources are $C \equiv C^{(F)} + x$ and $R \equiv R^{(F)} + x$. Then, the population dynamics of the consumers and resources follows:

$$\begin{cases} \dot{x} = aR^{(F)}C^{(F)} - (k+d)x, \\ \dot{C} = w k x - DC, \\ \dot{R} = g(R, x, C), \end{cases} \quad (S2.2)$$

where the functional form of $g(R, x, C)$ is unspecific, D and w represent the mortality rate of the consumer species and biomass conversion ratio, respectively. Since the consumption process is much faster than the birth/death process, thus, in deriving the functional response, the consumption process is supposed to be in fast equilibrium (i.e., $\dot{x} = 0$). Then, we can solve for x with:

$$x^2 - (R + C + K)x + RC = 0, \quad (S2.3)$$

where $K = \frac{k+d}{a}$, and then,

$$x = \frac{2RC}{(R+C+K)} \frac{1}{\left(1 + \sqrt{1 - \frac{4RC}{(R+C+K)^2}}\right)}. \quad (S2.4)$$

By definition, the functional response and search efficiency are:

$$\mathcal{F}_{CP}(R, C) = \frac{kx}{C}, \quad (S2.5a)$$

$$\Xi_{CP}(R, C) = \frac{kx}{RC}. \quad (S2.5b)$$

Hence, we obtain the functional response and search efficiency in this chasing-pair scenario:

$$\mathcal{F}_{CP}(R, C)_1 = k \frac{(R+C+K)}{2C} \left(1 - \sqrt{1 - \frac{4RC}{(R+C+K)^2}}\right), \quad (S2.6a)$$

$$\Xi_{CP}(R, C)_1 = k \frac{(R+C+K)}{2RC} \left(1 - \sqrt{1 - \frac{4RC}{(R+C+K)^2}}\right). \quad (S2.6b)$$

Since $\frac{4RC}{(R+C+K)^2} < 4 \frac{C}{R} \ll 1$, by applying first order approximations in Eq. S2.6, we

obtain $\sqrt{1 - \frac{4RC}{(R+C+K)^2}} \approx 1 - \frac{2RC}{(R+C+K)^2}$. Then the functional response and search efficiency are:

$$\mathcal{F}_{\text{CP}}(R, C)_2 = k \frac{R}{R+C+K}, \quad (\text{S2.7a})$$

$$\Xi_{\text{CP}}(R, C)_2 = \frac{k}{R+C+K}. \quad (\text{S2.7b})$$

Evidently, there is entirely no predator interference within the chasing-pair scenario, yet the functional response form is identical to the B-D model involving intraspecific interference (see Eq. S2.1).

Meanwhile, by applying first order approximations in the denominator of Eq. (S2.4),

we have $x \approx \frac{RC}{(R+C+K) - \frac{RC}{(R+C+K)}}$. Hence,

$$\mathcal{F}_{\text{CP}}(R, C)_3 = k \frac{R}{(R+C+K) - \frac{RC}{(R+C+K)}}, \quad (\text{S2.8a})$$

$$\Xi_{\text{CP}}(R, C)_3 = \frac{k}{(R+C+K) - \frac{RC}{(R+C+K)}}. \quad (\text{S2.8b})$$

In the case that $R \gg C$, then $R \gg C > x = R - R^{(F)}$. By applying $R^{(F)} \approx R$ in Eq.

S2.2, we obtain $x \approx \frac{RC}{R+K}$. Then,

$$\mathcal{F}_{\text{CP}}(R, C)_4 = k \frac{R}{R+K}, \quad (\text{S2.9a})$$

$$\Xi_{\text{CP}}(R, C)_4 = \frac{k}{R+K}. \quad (\text{S2.9b})$$

To compare these functional responses with that of the B-D model, we determine the parameters t_h and t_w in the B-D model by calculating their average value in a

stochastic framework. Then $\langle t_h \rangle = \frac{1}{k}$ and $\langle t_w \rangle = \frac{1}{d'}$ (in the chasing-pair scenario, $a' = 0$), and thus,

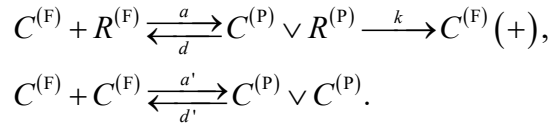
$$\Xi_{\text{B-D}}(R, C) = \frac{a}{1 + Ra/k} = \frac{k}{k/a + R}, \quad (\text{S2.10a})$$

$$\mathcal{F}_{\text{B-D}}(R, C) = \frac{kR}{k/a + R}. \quad (\text{S2.10b})$$

In the special case of $d = 0$ and $R \gg C$, $\Xi_{\text{B-D}}(R, C) = \Xi_{\text{CP}}(R, C)_4$, the B-D model is consistent with our mechanistic model. However, the discrepancy can be large out of this region (e.g., $d \gg 0$) (Figure S3).

S2.2 Scenario involving chasing pair and intraspecific interference

Here we consider the scenario with additional involvement of intraspecific interference in the simple case of $M=1$ and $N=1$:



where $C^{(\text{P})} \vee C^{(\text{P})}$ stands for the intraspecific predator interference pair, denoted as y . a' and d' represent the encounter rate and separation rate of the interference pair, respectively. Then, the total population of consumers and resources are $C \equiv C^{(\text{F})} + x + 2y$ and $R \equiv R^{(\text{F})} + x$. Hence the population dynamics of the consumers and resources can be described as follows:

$$\begin{cases} \dot{x} = aR^{(\text{F})}C^{(\text{F})} - (k+d)x, \\ \dot{y} = a'[C^{(\text{F})}]^2 - d'y, \\ \dot{C} = w k x - D C, \\ \dot{R} = g(R, x, C). \end{cases} \quad (\text{S2.11})$$

The consumption process and interference process are supposed to be in fast equilibrium (i.e., $\dot{x} = 0, \dot{y} = 0$), then we can solve for x with:

$$x^3 + \phi_2 x^2 + \phi_1 x + \phi_0 = 0, \quad (\text{S2.12})$$

where $\phi_0 \equiv -CR^2$, $\phi_1 = 2CR + KR + R^2$, $\phi_2 = 2\beta K^2 - K - C - 2R$, with $\beta = a'/d'$. The discriminant of Eq. S2.12 (denoted as Λ) is

$$\Lambda = -4\psi^3 - 27\varphi^2, \quad (\text{S2.13})$$

with $\psi = \phi_1 - (\phi_2)^2/3$ and $\varphi = \phi_0 - \phi_1\phi_2/3 + 2(\phi_2)^3/27$. When $\Lambda < 0$, there are one real solution x_{S1} and two complex solutions x_{S2} , x_{S3} , which are

$$x_{S1} = \theta_1 + \theta_2 - \phi_2/3, x_{S2} = \omega\theta_1 + \omega^2\theta_2 - \phi_2/3, x_{S3} = \omega^2\theta_1 + \omega\theta_2 - \phi_2/3, \quad (\text{S2.14})$$

where $\omega = -1/2 + i\sqrt{3}/2$ (i stands for the imaginary unit), $\theta_1 = \left(-\varphi/2 + \sqrt{-\Lambda/108}\right)^{1/3}$, and $\theta_2 = \left(-\varphi/2 - \sqrt{-\Lambda/108}\right)^{1/3}$. On the other hand, when $\Lambda > 0$, there are three real solutions, x_{S1} , x_{S2} , and x_{S3} , which are

$$x_{S1} = \psi' \cos \varphi' - \phi_2/3, x_{S2} = \psi' \cos\left(\varphi' + \frac{2\pi}{3}\right) - \phi_2/3, x_{S3} = \psi' \cos\left(\varphi' + \frac{4\pi}{3}\right) - \phi_2/3, \quad (\text{S2.15})$$

where $\psi' = (-4\psi/3)^{1/2}$, and $\varphi' = \arccos\left(-(-\psi/3)^{-3/2} \varphi/2\right)/3$. Note that $x \in [0, \min(R, C)]$, then we obtain the feasible solution of x (exact solution), and thus, the functional response and search efficiency are

$$\mathcal{F}_A(R, C)_1 = \frac{kx}{C}, \quad (\text{S2.16a})$$

$$\Xi_A(R, C)_1 = \frac{kx}{RC}. \quad (\text{S2.16b})$$

In the case that $R \gg C$, then $R \gg C > x$, and thus $R^{(F)} \approx R$. The consumption process is supposed to be in fast equilibrium (i.e., $\dot{x} = 0$, $\dot{y} = 0$), then we obtain

$$x \approx \frac{RC}{\sqrt{\left[\frac{1}{2}(K+R)\right]^2 + 2C\beta K^2 + \frac{1}{2}(K+R)}}, \quad (\text{S2.17})$$

and thus,

$$\mathcal{F}_A(R, C)_2 = k \frac{R}{\sqrt{\left[\frac{1}{2}(K+R)\right]^2 + 2C\beta K^2 + \frac{1}{2}(K+R)}}, \quad (\text{S2.18a})$$

$$\Xi_A(R, C)_2 = k \frac{1}{\sqrt{\left[\frac{1}{2}(K+R)\right]^2 + 2C\beta K^2 + \frac{1}{2}(K+R)}}. \quad (\text{S2.18b})$$

When $\beta \ll \frac{1}{8C}$ or $8\beta C/(1+R/K)^2 \ll 1$, by applying first order approximations to the denominator of Eq. S2.17, we have:

$$x \approx \frac{RC}{(K+R) + \frac{2K}{(1+R/K)}\beta C}, \quad (\text{S2.19})$$

and then,

$$\Xi_A(R, C)_3 = k \frac{1}{(K+R) + \frac{2K}{(1+R/K)} \beta C}, \quad (\text{S2.20a})$$

$$\mathcal{F}_A(R, C)_3 = k \frac{R}{(K+R) + \frac{2K}{(1+R/K)} \beta C}. \quad (\text{S2.20b})$$

In the case that $8\beta C / (1+R/K)^2 \gg 1$, with first order approximations, we obtain

$$x \approx \frac{RC}{K\sqrt{2C\beta} + \frac{(K+R)^2}{8K\sqrt{2C\beta}} + \frac{1}{2}(K+R)}, \quad (\text{S2.21})$$

and thus,

$$\Xi_A(R, C)_4 = k \frac{1}{K\sqrt{2C\beta} + \frac{(K+R)^2}{8K\sqrt{2C\beta}} + \frac{1}{2}(K+R)}, \quad (\text{S2.22a})$$

$$\mathcal{F}_A(R, C)_4 = k \frac{R}{K\sqrt{2C\beta} + \frac{(K+R)^2}{8K\sqrt{2C\beta}} + \frac{1}{2}(K+R)}. \quad (\text{S2.22b})$$

Meanwhile, the B-D model can only match to the case with $d = 0$. By calculating the average values of t_h and t_w in a stochastic framework, and then $\langle t_h \rangle = \frac{1}{k}$,

$\langle t_w \rangle = \frac{1}{d'}$. Thus,

$$\Xi_A^{\text{B-D}}(R, C) = \frac{a}{1 + \frac{a}{k}R + \frac{a'}{d'}C} = \frac{a}{1 + R/K|_{d=0} + \beta C}, \quad (\text{S2.23a})$$

$$\mathcal{F}_A^{\text{B-D}}(R, C) = \frac{aR}{1 + R/K|_{d=0} + \beta C}. \quad (\text{S2.23b})$$

In fact, the searching efficiency (and thus the functional response) of the B-D model do not match with either the rigorous form $\Xi_A(R, C)_1$, the quasi rigorous form $\Xi_A(R, C)_2$, or the more simplified forms $\Xi_A(R, C)_3$ and $\Xi_A(R, C)_4$. However, the discrepancy is small when $d \approx 0$ and $R \gg C$ (Figure S4). Intuitively, when $\beta \ll \frac{1}{8C}$

and $d=0$, then $\Xi_A(R, C)_3 = \frac{a}{1 + \frac{a}{k}R + \frac{2}{(1+R/K)}\beta C_i}$. Consequently, if

$R/K_i = x/C_i^{(F)} < 1$, then $\frac{2}{(1+R/K_i)} \in [1, 2]$. In this case, the difference between Ξ_A^{B-D}

and $\Xi_A(R, C)_3$ is small. Actually, the above analysis also applies to cases with more than one types of consumer species (i.e., for cases with $M > 1$).

S2.3 Scenario involving chasing pair and interspecific interference

Next, we consider the scenario involving chasing pair and interspecific interference in the case of $M=2$ and $N=1$:

$$\begin{aligned} C_i^{(F)} + R^{(F)} &\xrightleftharpoons[d_i]{a_i} C_i^{(P)} \vee R^{(P)} \xrightarrow{k_i} C_i^{(F)} (+), i = 1, 2, \\ C_1^{(F)} + C_2^{(F)} &\xrightleftharpoons[d'_{12}]{a'_{12}} C_1^{(P)} \vee C_2^{(P)}, \end{aligned}$$

where $C_1^{(P)} \vee C_2^{(P)}$ stands for the interspecific interference pair, denoted as z . a'_{12} and d'_{12} represent the encounter rate and separation rate of the interference pair, respectively. Then, the total population of consumers and resources are $C_i \equiv C_i^{(F)} + x_i + z$ and $R \equiv R^{(F)} + x_1 + x_2$. The population dynamics of the consumers and resources follows:

$$\begin{cases} \dot{x}_i = a_i R^{(F)} C_i^{(F)} - (d_i + k_i) x_i, & i = 1, 2, \\ \dot{z} = a'_{12} C_1^{(F)} C_2^{(F)} - d'_{12} z, \\ \dot{C}_i = w_i k_i x_i - D_i C_i, \\ \dot{R} = g(R, x_1, x_2, C_1, C_2), \end{cases} \quad (\text{S2.24})$$

where the functional form of $g(R, x_1, x_2, C_1, C_2)$ is unspecific, while D_i and w_i represents the mortality rates of the two consumers species and biomass conversion ratios. Still, the consumption/interference process is supposed to be in fast equilibrium, i.e., $\dot{x} = 0, \dot{z} = 0$. In the case that $R \gg C_1 + C_2 > x_1 + x_2$, by applying $R^{(F)} \approx R$, we obtain

$$x_1 \approx \frac{2C_1(R/K_2 + 1)R/K_1}{\sqrt{\gamma(C_2 - C_1) + \left(\frac{R}{K_1} + 1\right)\left(\frac{R}{K_2} + 1\right)^2 + 4\gamma C_1\left(\frac{R}{K_2} + 1\right)\left(1 + \frac{R}{K_1}\right) + \gamma(C_2 - C_1) + \left(\frac{R}{K_1} + 1\right)\left(\frac{R}{K_2} + 1\right)}} \quad (\text{S2.25a})$$

$$x_2 \approx \frac{2C_2(1+R/K_1)R/K_2}{\gamma(C_1-C_2)+\left(\frac{R}{K_1}+1\right)\left(\frac{R}{K_2}+1\right)+\sqrt{\left[\gamma(C_1-C_2)+\left(\frac{R}{K_1}+1\right)\left(\frac{R}{K_2}+1\right)\right]^2+4\gamma C_2\left(\frac{R}{K_2}+1\right)\left(1+\frac{R}{K_1}\right)}}, \quad (\text{S2.25b})$$

and then, the searching efficiencies and functional responses are:

$$\Xi_1(R, C_1, C_2)_1 = \frac{2k_1(R/K_2+1)/K_1}{\sqrt{\left[\gamma(C_2-C_1)+\left(\frac{R}{K_1}+1\right)\left(\frac{R}{K_2}+1\right)\right]^2+4\gamma C_1\left(\frac{R}{K_2}+1\right)\left(1+\frac{R}{K_1}\right)+\gamma(C_2-C_1)+\left(\frac{R}{K_1}+1\right)\left(\frac{R}{K_2}+1\right)}}, \quad (\text{S2.26a})$$

$$\Xi_2(R, C_1, C_2)_1 = \frac{2k_2(1+R/K_1)/K_2}{\gamma(C_1-C_2)+\left(\frac{R}{K_1}+1\right)\left(\frac{R}{K_2}+1\right)+\sqrt{\left[\gamma(C_1-C_2)+\left(\frac{R}{K_1}+1\right)\left(\frac{R}{K_2}+1\right)\right]^2+4\gamma C_2\left(\frac{R}{K_2}+1\right)\left(1+\frac{R}{K_1}\right)}}, \quad (\text{S2.26b})$$

$$\mathcal{F}_1(R, C_1, C_2)_1 = \frac{2k_1(R/K_2+1)R/K_1}{\sqrt{\left[\gamma(C_2-C_1)+\left(\frac{R}{K_1}+1\right)\left(\frac{R}{K_2}+1\right)\right]^2+4\gamma C_1\left(\frac{R}{K_2}+1\right)\left(1+\frac{R}{K_1}\right)+\gamma(C_2-C_1)+\left(\frac{R}{K_1}+1\right)\left(\frac{R}{K_2}+1\right)}}, \quad (\text{S2.26c})$$

$$\mathcal{F}_2(R, C_1, C_2)_1 = \frac{2k_2(1+R/K_1)R/K_2}{\gamma(C_1-C_2)+\left(\frac{R}{K_1}+1\right)\left(\frac{R}{K_2}+1\right)+\sqrt{\left[\gamma(C_1-C_2)+\left(\frac{R}{K_1}+1\right)\left(\frac{R}{K_2}+1\right)\right]^2+4\gamma C_2\left(\frac{R}{K_2}+1\right)\left(1+\frac{R}{K_1}\right)}}, \quad (\text{S2.26d})$$

Since $\frac{4\gamma^2 C_1 C_2}{\left[\gamma C_1 + \gamma C_2 + \left(\frac{R}{K_1} + 1\right)\left(\frac{R}{K_2} + 1\right)\right]^2} < 1$, by applying first order approximation to

the denominator of Eq. S2.25, we obtain:

$$x_1 \approx \frac{C_1 R}{(R+K_1) + \frac{\gamma K_1 K_2 C_2}{(R+K_2)} - \frac{\gamma^2 K_1 K_2 C_1 C_2}{\left[\gamma(C_2+C_1) + \left(\frac{R}{K_1}+1\right)\left(\frac{R}{K_2}+1\right)\right](R+K_2)}}, \quad (\text{S2.27a})$$

$$x_2 \approx \frac{C_2 R}{(R+K_2) + \frac{\gamma K_1 K_2 C_1}{(K_1+R)} - \frac{\gamma^2 K_1 K_2 C_1 C_2}{\left[\gamma(C_1+C_2) + \left(\frac{R}{K_1}+1\right)\left(\frac{R}{K_2}+1\right)\right](K_1+R)}}, \quad (\text{S2.27b})$$

and the searching efficiencies and functional responses are

$$\Xi_1(R, C_1, C_2)_2 = \frac{k_1}{(R+K_1) + \frac{\gamma K_1 K_2 C_2}{(R+K_2)} - \frac{\gamma^2 K_1 K_2 C_1 C_2}{\left[\gamma(C_2+C_1) + \left(\frac{R}{K_1}+1\right)\left(\frac{R}{K_2}+1\right)\right](R+K_2)}}, \quad (\text{S2.28a})$$

$$\Xi_2(R, C_1, C_2)_2 = \frac{k_2}{(R+K_2) + \frac{\gamma K_1 K_2 C_1}{(K_1+R)} - \frac{\gamma^2 K_1 K_2 C_1 C_2}{\left[\gamma(C_1+C_2) + \left(\frac{R}{K_1}+1\right)\left(\frac{R}{K_2}+1\right)\right](K_1+R)}}, \quad (\text{S2.28b})$$

$$\mathcal{F}_1(R, C_1, C_2)_2 = \frac{k_1 R}{(R+K_1) + \frac{\gamma K_1 K_2 C_2}{(R+K_2)} - \frac{\gamma^2 K_1 K_2 C_1 C_2}{\left[\gamma(C_2 + C_1) + \left(\frac{R}{K_1} + 1\right) \left(\frac{R}{K_2} + 1\right) \right] (R+K_2)}}, \quad (\text{S2.28c})$$

$$\mathcal{F}_2(R, C_1, C_2)_2 = \frac{k_2 R}{(R+K_2) + \frac{\gamma K_1 K_2 C_1}{(K_1+R)} - \frac{\gamma^2 K_1 K_2 C_1 C_2}{\left[\gamma(C_1 + C_2) + \left(\frac{R}{K_1} + 1\right) \left(\frac{R}{K_2} + 1\right) \right] (K_1+R)}}. \quad (\text{S2.28d})$$

Likewise, the B-D model can only match to cases with $d = 0$. By calculating the average

values in a stochastic framework, we obtain $\langle t_h^i \rangle = \frac{1}{k_i}$, $\langle t_w^i \rangle = \frac{1}{d'_{12}}$. Thus,

$$\Xi_1^{\text{B-D}}(R, C_1, C_2) = \frac{a_1}{1 + \frac{a_1}{k_1} R + \frac{a'_{12}}{d'_{12}} C_2} = \frac{a_1}{1 + R/K_1|_{d=0} + \gamma C_2}, \quad (\text{S2.29a})$$

$$\Xi_2^{\text{B-D}}(R, C_1, C_2) = \frac{a_2}{1 + \frac{a_2}{k_2} R + \frac{a'_{12}}{d'_{12}} C_1} = \frac{a_2}{1 + R/K_2|_{d=0} + \gamma C_1}. \quad (\text{S2.29b})$$

Consequently,

$$\mathcal{F}_1^{\text{B-D}}(R, C_1, C_2) = \frac{a_1 R}{1 + R/K_1|_{d=0} + \gamma C_2}, \quad (\text{S2.30a})$$

$$\mathcal{F}_2^{\text{B-D}}(R, C_1, C_2) = \frac{a_2 R}{1 + R/K_2|_{d=0} + \gamma C_1}. \quad (\text{S2.30b})$$

Evidently, the searching efficiency in the B-D model do not match with either the quasi rigorous form $\Xi_i(R, C_1, C_2)_1$, or the simplified form $\Xi_i(R, C_1, C_2)_2$. However, the discrepancy can be small when $d \approx 0$ and $R \gg C$ (Figure S5). Intuitively, when $\gamma \ll \min(C_1^{-1}, C_2^{-1})$, we have

$$\Xi_1(R, C_1, C_2)_2 \approx \frac{a_1}{\left(\frac{a_1}{k_1} R + 1\right) + \frac{\gamma C_2}{(R/K_2 + 1)}}, \quad (\text{S2.31a})$$

$$\Xi_2(R, C_1, C_2)_2 \approx \frac{a_2}{\left(\frac{a_2}{k_2} R + 1\right) + \frac{\gamma C_1}{(R/K_1 + 1)}}. \quad (\text{S2.31b})$$

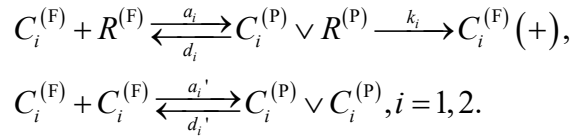
Consequently, if $R/K_i = x/C_i^{(F)} < 1$, and then $\frac{1}{(1 + R/K_i)} \in [0.5, 1]$, Thus, in this case,

the difference between Ξ_A^{B-D} and $\Xi_i(R, C_1, C_2)_2$ is small.

S3 Scenario involving chasing pair and intraspecific interference

S3.1 Two consumers species competing for one resource species

We consider the scenario involving chasing pair and intraspecific interference in the simple case of $M = 2$ and $N = 1$ (Fig. S6a, b):



Here, the variables and parameters are just extended from the case of $M = 1$ and $N = 1$ (see SI Sec. S2.2). The total number of consumers and resources are

$C_i = C_i^{(F)} + x_i + 2y_i$ and $R = R^{(F)} + \sum_{i=1}^2 x_i$. Hence, the population dynamics of the

consumers and resources can be described as follows:

$$\begin{cases} \dot{x}_i = a_i R^{(F)} C_i^{(F)} - (d_i + k_i) x_i, i = 1, 2, \\ \dot{y}_i = a_i' [C_i^{(F)}]^2 - d_i' y_i, \\ \dot{C}_i = w_i k_i x_i - D_i C_i, \\ \dot{R} = g(R, x_1, x_2, C_1, C_2). \end{cases} \quad (S3.1)$$

where the functional form of $g(R, x_1, x_2, C_1, C_2)$ is unspecified. For simplicity, we define $K_i \equiv (d_i + k_i)/a_i$, $\alpha_i \equiv D_i/(w_i k_i)$, and $\beta_i \equiv a_i'/d_i'$ ($i = 1, 2$). At steady state, from

$\dot{x}_i = 0$, $\dot{y}_i = 0$ ($i = 1, 2$), we have

$$\begin{cases} x_i = R^{(F)} C_i^{(F)} / K_i, i = 1, 2, \\ y_i = \beta_i [C_i^{(F)}]^2, \end{cases} \quad (S3.2)$$

and note that $C_i = C_i^{(F)} + x_i + 2y_i$ and $R = R^{(F)} + \sum_{i=1}^2 x_i$, then,

$$R^{(F)} = R / \left(1 + C_1^{(F)} / K_1 + C_2^{(F)} / K_2 \right), \quad (S3.3a)$$

$$C_i = C_i^{(F)} + R^{(F)} C_i^{(F)} / K_i + 2\beta_i [C_i^{(F)}]^2, \quad i = 1, 2. \quad (S3.3b)$$

By substituting Eq. S3.3a into Eq. S3.3b, we have

$$\left\{ \begin{array}{l} C_2^{(F)} = \frac{K_2}{K_1} \left[\frac{RC_1^{(F)}}{C_1 - C_1^{(F)} - 2\beta_1 [C_1^{(F)}]^2} - K_1 - C_1^{(F)} \right], \end{array} \right. \quad (\text{S3.4a})$$

$$\left(C_2 - C_2^{(F)} - 2\beta_2 [C_2^{(F)}]^2 \right) (1 + C_1^{(F)}/K_1 + C_2^{(F)}/K_2) = RC_2^{(F)}/K_2. \quad (\text{S3.4b})$$

To illustrate the dependencies among the variables, for this moment, we regard C_1 , C_2 and R as parameters rather than variables. Then, by further substituting Eq. S3.4a into Eq. S3.4b, we get an equation where $C_1^{(F)}$ is the single variable. Thus, we can present $C_1^{(F)}$ with C_1 , C_2 and R , i.e., $C_1^{(F)} = \Phi(C_1, C_2, R)$. By further combining with Eqs. S3.2, S3.3a and S3.4a, we can express $C_2^{(F)}$, $R^{(F)}$, x_i and y_i using C_1 , C_2 and R . Specifically, for x_i , we have:

$$x_i = u_i(R, C_1, C_2), \quad i = 1, 2. \quad (\text{S3.5})$$

If all species can coexist, by defining $\Omega_i(R, C_1, C_2) \equiv \frac{w_i k_i}{C_i} u_i(R, C_1, C_2)$, then, the

steady-state equations of $\dot{C}_i = 0$ ($i = 1, 2$) and $\dot{R} = 0$ are:

$$\left\{ \begin{array}{l} \Omega_1(R, C_1, C_2) - D_1 = 0, \\ \Omega_2(R, C_1, C_2) - D_2 = 0, \\ G(R, C_1, C_2) = 0, \end{array} \right. \quad (\text{S3.6})$$

where $G(R, C_1, C_2) \equiv g(R, u_1(R, C_1, C_2), u_2(R, C_1, C_2), C_1, C_2)$. Evidently, Eq. S3.6 corresponds to three unparallel surfaces and hence share a common point. We verify this conclusion with numerical calculations shown in Figs. 1h and S7a-b, where the red dots represent the fixed points. These fixed points can be stable. Therefore, the two consumer species can steadily coexist.

S3.1.1 Analytical solutions of species abundances at steady state

At steady state, since $\dot{x}_i = \dot{y}_i = \dot{C}_i = 0$ ($i = 1, 2$), then,

$$\begin{cases} x_i = \alpha_i C_i, \\ C_i^{(F)} = K_i \alpha_i C_i / R^{(F)}, \\ y_i = \beta_i (K_i \alpha_i C_i)^2 [R^{(F)}]^{-2}, \end{cases} \quad (\text{S3.7})$$

Meanwhile $C_i = C_i^{(F)} + x_i + 2y_i$, then, as long as $C_i, R > 0$ ($i=1,2$), we have

$$C_i = \frac{(1-\alpha_i)[R^{(F)}]^2 - K_i \alpha_i R^{(F)}}{2\beta_i (K_i \alpha_i)^2}. \quad (\text{S3.8})$$

If the population abundance of resource species is much more than that of the consumers (i.e., $R \gg C_1 + C_2$), then $R \gg x_1 + x_2$ and $R^{(F)} \approx R$, thus,

$$C_i \approx \frac{(1-\alpha_i)R^2 - K_i \alpha_i R}{2\beta_i (K_i \alpha_i)^2}. \quad (\text{S3.9})$$

We further assume that the population dynamics of the resources follow the same construction rule as that of the MacArthur's consumer-resource model:

$$g(R, x_1, x_2, C_1, C_2) = \begin{cases} R_0 R (1 - R/K_0) - (k_1 x_1 + k_2 x_2), & \text{for biotic resources.} \\ R_a (1 - R/K_0) - (k_1 x_1 + k_2 x_2), & \text{for abiotic resources.} \end{cases} \quad (\text{S3.10})$$

Since $\dot{R} = 0$, then, for biotic resources,

$$R = \frac{k_1/(2\beta_1 K_1) + k_2/(2\beta_2 K_2) + R_0}{\frac{k_1(1-\alpha_1)}{2\beta_1 \alpha_1 (K_1)^2} + \frac{k_2(1-\alpha_2)}{2\beta_2 \alpha_2 (K_2)^2} + \frac{R_0}{K_0}}. \quad (\text{S3.11})$$

While for abiotic resources,

$$R = \frac{-\kappa_1 + \sqrt{\kappa_1^2 + 4\kappa_2 R_a}}{2\kappa_2}, \quad (\text{S3.12})$$

where $\kappa_1 = \frac{R_a}{K_0} - \frac{k_1}{2\beta_1 K_1} - \frac{k_2}{2\beta_2 K_2}$ and $\kappa_2 = \frac{k_1(1-\alpha_1)}{2\beta_1 \alpha_1 (K_1)^2} + \frac{k_2(1-\alpha_2)}{2\beta_2 \alpha_2 (K_2)^2}$.

Eqs. S3.9, S3.11, S3.12 are the analytical solutions to the steady-state species abundances when $R \gg C_1 + C_2$. As shown in Figure 1e, the analytical solutions agree well with the numerical results (the exact solutions). To conduct a systematic comparison for different model parameters, we assign D_i ($i=1,2$) to be the only parameter of each different value between species C_1 and C_2 (with $D_1 > D_2$), and define

$\Delta \equiv (D_1 - D_2)/D_2$ as the competitive difference between the two consumer species.

The comparisons between the analytical solutions and the numerical results are shown in Fig. S7c-d. Clearly, they are close to each other, exhibiting very good consistency for all cases regardless of the life form of the resources.

Furthermore, we test that if it is achievable to predict the species coexistence region of model parameters with the analytical solutions. As $D_i (i=1,2)$ is the only parameter of each different value between the two-consumer species (with $D_1 > D_2$), the supremum (upper limit) of the competitive difference for species coexistence (defined as $\bar{\Delta}$) corresponds to the case when the steady-state solutions of the species abundances satisfy $R, C_2 > 0$ and $C_1 = 0^+$, where 0^+ stands for the infinitesimal positive number.

In the upper surface of the coexistence region, $\Delta = \bar{\Delta}$ and $C_1 = 0^+$. Then, using Eq. S3.11, and note that $R > 0$, we have

$$R = \frac{K_1 \alpha_1}{1 - \alpha_1}, \quad (\text{S3.13})$$

Meanwhile,

$$\alpha_1 = \alpha_2 (\Delta + 1) = \alpha_2 (\bar{\Delta} + 1), \quad (\text{S3.14})$$

For biotic resources, combining Eqs. S3.11, S3.13 and S3.14, we have

$$\bar{\Delta} = \frac{1 - (K/K_0 + 1)\alpha}{k/(2\beta KR_0) + (K/K_0 + 1)\alpha}, \quad (\text{S3.15})$$

where $K = K_i$, $k = k_i$, and $\beta = \beta_i (i=1,2)$. For abiotic resources, combining Eqs. S3.12, S3.13 and S3.14, we have

$$\bar{\Delta} = \frac{1}{\alpha_2 (K_1 \rho + 1)} - 1, \quad (\text{S3.16})$$

where $\rho = \frac{1}{2} \left(\frac{1}{K_0} - \frac{k_2}{2R_a \beta_2 K_2} \right) + \frac{1}{2} \sqrt{\left(\frac{1}{K_0} - \frac{k_2}{2R_a \beta_2 K_2} \right)^2 + 2 \frac{k_2 (1 - \alpha_2)}{R_a \beta_2 \alpha_2 (K_2)^2}}$.

With Eqs. S3.15 and S3.16, we can calculate the upper surface of the coexistence region predicted by analytical solutions when $R \gg C_1 + C_2$. The comparisons between analytical predictions and numerical results (exact solution) are shown in Fig. S7e-f, which overall exhibits very good consistency.

S3.1.2 Stability analysis and a Hopf bifurcation

We apply linear stability analysis to study the local stability of the fixed points. Specifically, for a given fixed point E (e.g., $E(x_1, x_2, y_1, y_2, C_1, C_2, R)$), if all the eigenvalues (defined as λ_i , $i = 1, \dots, 7$) of the Jacobian matrix at point E are negative in the real parts, then, E is locally stable. In contrast, if there exist one or multiple eigenvalues with a nonnegative real part, then the fixed point E is unstable.

In our analysis, when the separation rate d' ($d' = d'_1 = d'_2$) of the interference-pair increases in the vicinity of the critical value d'_c , the population dynamics of the consumers and resources transits from a stable fixed point into a stable limit cycle (Fig. S6e-f, see also Fig. S6c-d). In particular, the amplitude of the oscillation gradually increases with the bifurcation parameter d' , and quantitatively, the amplitude is proportional to $\sqrt{d' - d'_c}$ (Figure S6e). This clearly demonstrates a supercritical Hopf bifurcation.

To further investigate if there exists a non-zero measure parameter space for species coexistence, we set D_i ($i = 1, 2$) to be the only parameter of each different value between species C_1 and C_2 , and then $\Delta = (D_1 - D_2)/D_2$ reflects the complete difference between the two consumer species. As shown in Fig. 2g-h, the region below the blue surface and above the red surface corresponds to stable coexistence, while that below the red surface and above $\Delta = 0$ corresponds to unstable fixed points, which may end in a limit cycle or C_1 extinction. An exemplified transection is shown in Fig. 2i, which corresponds to the $\Delta = 1$ plane in Fig. 2h. Above all, there exists a non-zero measure parameter region to promote species coexistence regardless the life form of the resources.

S3.2 M consumers species competing for N resources species

Here we consider the scenario involving chasing pair and intraspecific interference for the generic case with M types of consumers and N types of resources (see FigS9a-b). Then, the population dynamics of the consumers and resources can be described as follows:

$$\begin{cases} \dot{x}_{il} = a_{il}C_i^{(F)}R_l^{(F)} - (d_{il} + k_{il})x_{il}, \\ \dot{y}_i = a'_{ii}[C_i^{(F)}]^2 - d'_{ii}y_i, \\ \dot{C}_i = \sum_{l=1}^N w_{il}k_{il}x_{il} - D_iC_i, \\ \dot{R}_l = g_l(\{R_l\}, \{x_i\}, \{C_i\}), \quad i = 1, \dots, M, \quad l = 1, \dots, N. \end{cases} \quad (\text{S3.17})$$

Note that Eq. S3.17 is identical with Eqs. 1-2, and we use the same variables and parameters as that in the main text. Then, the population of the consumers and resources

are $C_i = C_i^{(F)} + \sum_{l=1}^N x_{il} + 2y_i$ and $R_l = R_l^{(F)} + \sum_{i=1}^M x_{il}$. For convenience, we define

$$K_{il} \equiv (d_{il} + k_{il})/a_{il}, \quad \alpha_{il} \equiv D_i/(w_{il}k_{il}), \quad \text{and} \quad \beta_i \equiv a'_{ii}/d'_{ii} \quad (i = 1, \dots, M, \quad l = 1, \dots, N).$$

S3.2.1 Analytical solutions of species abundances at steady state

At steady state, from $\dot{x}_i = 0$, $\dot{y}_i = 0$, and $\dot{C}_i = 0$, we have .

$$\begin{cases} x_{il} = C_i^{(F)}R_l^{(F)}/K_{il}, \\ y_i = \beta_i[C_i^{(F)}]^2, \\ C_i = \sum_{l=1}^N x_{il}/\alpha_{il} = \sum_{l=1}^N C_i^{(F)}R_l^{(F)}/(K_{il}\alpha_{il}). \end{cases} \quad (\text{S3.18})$$

Meanwhile, $C_i = C_i^{(F)} + \sum_{l=1}^N x_{il} + 2y_i$, and note that $C_i^{(F)} > 0$, thus

$$C_i^{(F)} = \frac{1}{2\beta_i} \left[-1 + \sum_{l=1}^N \left(\frac{1}{\alpha_{il}} - 1 \right) \frac{R_l^{(F)}}{K_{il}} \right]. \quad (\text{S3.19})$$

Combined with Eq. S3.19, and then

$$C_i = \sum_{l=1}^N \frac{R_l^{(F)}}{2\beta_i\alpha_{il}K_{il}} \left[-1 + \sum_{l'=1}^N \left(\frac{1}{\alpha_{il'}} - 1 \right) \frac{R_{l'}^{(F)}}{K_{il'}} \right]. \quad (\text{S3.20})$$

We further assume that the specific function of $g_l(\{R_l\}, \{x_i\}, \{C_i\})$ satisfy Eq. 4, i.e.,

$$g_l(\{R_l\}, \{x_i\}, \{C_i\}) = \begin{cases} R_0^{(l)}R_l \left(1 - R_l/K_0^{(l)} \right) - \sum_{i=1}^M k_{il}x_{il}, \text{ for biotic resources.} \\ R_a^{(l)} \left(1 - R_l/K_0^{(l)} \right) - \sum_{i=1}^M k_{il}x_{il}, \text{ for abiotic resources.} \end{cases} \quad (\text{S3.21})$$

For biotic resource, by combining Eqs. S3.19, S3.19 and S3.20, we have

$$R_0^{(l)} R_l \left(1 - \frac{R_l}{K_0^{(l)}} \right) = \sum_{i=1}^M \frac{k_i}{2\beta_i K_{il}} \left[-1 + \sum_{l'=1}^N \left(\frac{1}{\alpha_{il'}} - 1 \right) \frac{R_{l'}^{(F)}}{K_{il'}} \right] R_l^{(F)}. \quad (\text{S3.22})$$

If the population abundance of each resource species is much more than the total population of all consumers (i.e., $R_l \gg \sum_{i=1}^M C_i$, $l=1, \dots, N$), then $R_l \gg \sum_{i=1}^M x_{il}$ and

$R_l^{(F)} \approx R_l$. Since $R_l > 0$ ($l=1, \dots, N$), then

$$\sum_{l'=1}^N \left[\delta_{l,l'} \frac{R_0^{(l)}}{K_0^{(l)}} + \sum_{i=1}^M \frac{k_{il}}{2\beta_i K_{il} K_{il'}} \left(\frac{1}{\alpha_{il'}} - 1 \right) \right] R_{l'} = R_0^{(l)} + \sum_{i=1}^M \frac{k_{il}}{2\beta_i K_{il}}, \quad (\text{S3.23})$$

with $\delta_{l,l'} = \begin{cases} 0, & l \neq l'. \\ 1, & l = l'. \end{cases}$ To present Eq. S3.23 in a matrix form, we define matrix

$\mathbf{A} \equiv [A_{sq}] \in \mathbb{R}^{N \times N}$ (\mathbb{R} stands for the real number field), with

$$A_{sq} = \delta_{s,q} \frac{R_0^{(s)}}{K_0^{(s)}} + \sum_{i=1}^M \frac{k_{is}}{2\beta_i K_{is} K_{iq}} \left(\frac{1}{\alpha_{iq}} - 1 \right), \quad s, q = 1, \dots, N, \quad (\text{S3.24a})$$

and two arrays

$$\begin{cases} \mathbf{B} \equiv (R_0^{(1)} + \sum_{i=1}^M \frac{k_{i1}}{2\beta_i K_{i1}}, \dots, R_0^{(N)} + \sum_{i=1}^M \frac{k_{iN}}{2\beta_i K_{iN}})^T, \\ \mathbf{R} \equiv (R_1, \dots, R_N)^T, \end{cases} \quad (\text{S3.24b})$$

where ‘‘T’’ represents the transpose. Then, Eq. S3.23 can be written as

$$\mathbf{A} \cdot \mathbf{R} = \mathbf{B}. \quad (\text{S3.24c})$$

We can solve for \mathbf{R} :

$$\mathbf{R} = \frac{\text{adj}(\mathbf{A})}{\det(\mathbf{A})} \cdot \mathbf{B}, \quad (\text{S3.24d})$$

where the $\text{adj}(\mathbf{A})$ and $\det(\mathbf{A})$ denote the adjugate matrix and determinant of \mathbf{A} , respectively. Next, we define $\mathbf{C} \equiv (C_1, \dots, C_M)$. Note that $R_l \approx R_l^{(F)}$, combined with Eq. 3.20, we have,

$$\begin{cases} \mathbf{C} \equiv (C_1, \dots, C_M), \\ C_i = \sum_{l=1}^N \frac{R_l}{2\beta_i \alpha_{il} K_{il}} \left[-1 + \sum_{l'=1}^N \left(\frac{1}{\alpha_{il'}} - 1 \right) \frac{R_{l'}}{K_{il'}} \right], \quad i = 1, \dots, M. \end{cases} \quad (\text{S3.24e})$$

Then, for biotic resources, Eqs. S3.24a-S3.24e are the analytical solutions to the steady-

state species abundances when $R_l \gg \sum_{i=1}^M C_i$ ($l=1, \dots, N$). On the other hand, for

abiotic resource, by combining Eqs. S3.18, S3.19 and S3.21, we have

$$R_0^{(l)} \left(1 - \frac{R_l}{K_0^{(l)}} \right) = \sum_{i=1}^M \frac{1}{2\beta_i} \frac{k_i}{K_{il}} \left[-1 + \sum_{l'=1}^N \left(\frac{1}{\alpha_{il'}} - 1 \right) \frac{R_{l'}^{(F)}}{K_{il'}} \right] R_l^{(F)}. \quad (\text{S3.25})$$

If $R_l \gg \sum_{i=1}^M C_i$ ($l=1, \dots, N$), then $R_l \gg \sum_{i=1}^M x_{il}$ and $R_l^{(F)} \approx R_l$. Thus,

$$\left(\frac{R_0^{(l)}}{K_0^{(l)}} - \sum_{i=1}^M \frac{1}{2\beta_i} \frac{k_i}{K_{il}} + \sum_{l'=1}^N \sum_{i=1}^M \frac{1}{2\beta_i} \frac{k_i}{K_{il}} \left(\frac{1}{\alpha_{il'}} - 1 \right) \frac{R_{l'}}{K_{il'}} \right) R_l = R_0^{(l)}. \quad (\text{S3.26})$$

with $l=1, \dots, N$. Eq. S3.26 is a set of second-order ordinary differential equations (ODEs), which is clearly solvable.

Actually, when $N=1$, $M \geq 1$, and $R_l \gg \sum_{i=1}^M C_i$ ($l=1$), we can explicitly present the

analytical solution to the steady-state species abundances. To simplify the notations, we omit the “ l ” in the sub-/super-scripts since $N=1$. Then, for biotic resources,

$$\begin{cases} R = \frac{R_0 + \sum_{i=1}^M k_i / (2\beta_i K_i)}{\sum_{i=1}^M \frac{k_i (1 - \alpha_i)}{2\beta_i \alpha_i (K_i)^2} + \frac{R_0}{K_0}}, \\ C_i = \frac{1}{2\beta_i \alpha_i K_i} \left[\left(\frac{1}{\alpha_i} - 1 \right) \frac{R}{K_i} - 1 \right] R, \quad i = 1, \dots, M. \end{cases} \quad (\text{S3.27})$$

For abiotic resources,

$$\begin{cases} R = \frac{-\gamma_1 + \sqrt{\gamma_1^2 + 4\gamma_2 R_a}}{2\gamma_2}, \\ C_i = \frac{1}{2\beta_i \alpha_i K_i} \left[\left(\frac{1}{\alpha_i} - 1 \right) \frac{R}{K_i} - 1 \right] R, \quad i = 1, \dots, M, \end{cases} \quad (\text{S3.28})$$

where $\gamma_1 \equiv \frac{R_a}{K_0} - \sum_{i=1}^M \frac{k_i}{2\beta_i K_i}$ and $\gamma_2 \equiv \sum_{i=1}^M \frac{k_i (1 - \alpha_i)}{2\beta_i \alpha_i (K_i)^2}$. Thus, Eqs. S3.24a-S3.24e are

the analytical solutions to the steady-state species abundances when $R \gg \sum_{i=1}^M C_i$.

Numerically, consistent with the analytical predictions, a handful of resource species (N) can support an unexpected wide range of consumers species ($M \gg N$) to coexist at steady state (Figs. 3 and S9-S14). In the simulations, $D_i (i=1, \dots, M)$ is the only parameter of each different value among the consumer species, and thus each consumer species owns a unique competitiveness. The comparisons between the analytical predictions and the ODEs simulation results (exact solution) are shown in Figs. 3a-b and S9c-d, which clearly shows a very good consistency. In particular, with stochastic simulation algorithm (SSA), we have further identified that the facilitated biodiversity is resistant to stochasticity (see Figs. 3 and S10-S14).

S4 Scenario involving chasing pair and interspecific interference

Here we consider the scenario involving chasing pair and interspecific interference in the case of $M=2$ and $N=1$ (Fig. S16a-b), with everything follow that depicted in S2.3. Then, $C_i \equiv C_i^{(F)} + x_i + z$, $R \equiv R^{(F)} + x_1 + x_2$, and the population dynamics follows (identical with Eq. S2.24):

$$\begin{cases} \dot{x}_i = a_i R^{(F)} C_i^{(F)} - (d_i + k_i) x_i, & i=1,2, \\ \dot{z} = a'_{12} C_1^{(F)} C_2^{(F)} - d'_{12} z, \\ \dot{C}_i = w_i k_i x_i - D_i C_i, \\ \dot{R} = g(R, x_1, x_2, C_1, C_2). \end{cases} \quad (\text{S4.1})$$

Here the functional form of $g(R, x_1, x_2, C_1, C_2)$ is unspecified. For convenience, we define $K_i \equiv (d_i + k_i)/a_i$, $\alpha_i \equiv D_i/(w_i k_i)$ ($i=1,2$), and $\gamma = a'_{12}/d'_{12}$. At steady state, from $\dot{x}_i = 0$ ($i=1,2$) and $\dot{z} = 0$, we have

$$\begin{cases} x_i = R^{(F)} C_i^{(F)} / K_i, & i=1,2. \\ z = \gamma C_1^{(F)} C_2^{(F)}. \end{cases} \quad (\text{S4.2})$$

Note that $C_i \equiv C_i^{(F)} + x_i + z$ and $R \equiv R^{(F)} + x_1 + x_2$, then,

$$\begin{cases} C_1 = C_1^{(F)} + R^{(F)} C_1^{(F)} / K_1 + \gamma C_1^{(F)} C_2^{(F)}, \\ C_2 = C_2^{(F)} + R^{(F)} C_2^{(F)} / K_2 + \gamma C_1^{(F)} C_2^{(F)}, \\ R = R^{(F)} \left(1 + C_1^{(F)} / K_1 + C_2^{(F)} / K_2 \right). \end{cases} \quad (\text{S4.3})$$

For this moment, we regard C_1 , C_2 and R as parameters rather than variables, then in Eq. S4.3, there are three equations and three variables ($C_1^{(F)}$, $C_2^{(F)}$ and $R^{(F)}$).

Clearly, following similar analysis as that in Sec.3.1, we can present $C_1^{(F)}$, $C_2^{(F)}$ and $R^{(F)}$ with C_1 , C_2 and R , e.g., $C_1^{(F)} = \Phi'(C_1, C_2, R)$. Combined with Eqs. S4.2, we can express x_i and z using C_1 , C_2 and R . Specifically, for x_i , we have

$$x_i = u'_i(R, C_1, C_2), i = 1, 2. \quad (\text{S4.4})$$

If all species can coexist, by defining $\Omega'_i(R, C_1, C_2) \equiv \frac{w_i k_i}{C_i} u'_i(R, C_1, C_2)$, then, the

steady-state equations of $\dot{C}_i = 0$ ($i = 1, 2$) and $\dot{R} = 0$ are:

$$\begin{cases} \Omega'_1(R, C_1, C_2) - D_1 = 0, \\ \Omega'_2(R, C_1, C_2) - D_2 = 0, \\ G'(R, C_1, C_2) = 0. \end{cases} \quad (\text{S4.5})$$

where $G'(R, C_1, C_2) \equiv g(R, u'_1(R, C_1, C_2), u'_2(R, C_1, C_2), C_1, C_2)$. Evidently, Eq. S4.5 corresponds to three unparallel surfaces and hence share a common point. We verify this conclusion with numerical calculations shown in Figs. 1g and S17a-b, where the black dots represent the fixed points. Nevertheless, these fixed points are all unstable, and thus the consumer species still cannot coexist at steady state (Fig. 1d).

S4.1 Analytical results of the fixed-point solutions

Here we investigate the unstable fixed points where all species coexist ($R, C_1, C_2 > 0$).

From $\dot{x}_i = 0$ ($i = 1, 2$), $\dot{z} = 0$, $\dot{C}_i = 0$, and note that $C_i \equiv C_i^{(F)} + x_i + z$, we have

$$\begin{cases} C_i = K_i \alpha_i (R^{(F)})^{-1} C_i + \alpha_i C_i + z, \quad i = 1, 2. \\ z = \gamma K_1 \alpha_1 K_2 \alpha_2 (R^{(F)})^{-2} C_1 C_2. \end{cases} \quad (\text{S4.6})$$

Since $C_i > 0$, then

$$\begin{cases} C_1 = \frac{(1 - \alpha_2) (R^{(F)})^2 - K_2 \alpha_2 R^{(F)}}{\gamma K_1 \alpha_1 K_2 \alpha_2}, \\ C_2 = \frac{(1 - \alpha_1) (R^{(F)})^2 - K_1 \alpha_1 R^{(F)}}{\gamma K_1 \alpha_1 K_2 \alpha_2}. \end{cases} \quad (\text{S4.7})$$

If $R \gg C_1 + C_2$, then $R \gg x_1 + x_2$ and $R^{(F)} \approx R$, we have

$$\begin{cases} C_1 = \frac{(1-\alpha_2)R^2 - K_2\alpha_2 R}{\gamma K_1\alpha_1 K_2\alpha_2}, \\ C_2 = \frac{(1-\alpha_1)R^2 - K_1\alpha_1 R}{\gamma K_1\alpha_1 K_2\alpha_2}. \end{cases} \quad (\text{S4.8})$$

We further assume that the population dynamics of the resources follows Eq. S3.10.

For biotic resources, at the fixed points, $\dot{R} = 0$, then

$$R_0 R \left(1 - \frac{R}{K_0}\right) = k_1\alpha_1 C_1 + k_2\alpha_2 C_2. \quad (\text{S4.9})$$

Substituting Eq. S4.8 into Eq. S4.9, and note that $R > 0$, then we have

$$R = \frac{R_0 + \frac{k_1}{\gamma K_1} + \frac{k_2}{\gamma K_2}}{\frac{k_1\alpha_1 + k_2\alpha_2}{\gamma K_1\alpha_1 K_2\alpha_2} - \frac{k_1 + k_2}{\gamma K_1 K_2} + \frac{R_0}{K_0}}. \quad (\text{S4.10})$$

For abiotic resources, at the fixed points, $\dot{R} = 0$, then

$$R_a \left(1 - \frac{R}{K_0}\right) = k_1\alpha_1 C_1 + k_2\alpha_2 C_2. \quad (\text{S4.11})$$

Combined with Eq. S4.8, we have

$$R = \frac{-\kappa_1 + \sqrt{(\kappa_1)^2 + 4\kappa_2 R_a}}{2\kappa_2}, \quad (\text{S4.12})$$

where $\kappa_1 = \frac{R_a}{K_0} - \frac{k_1}{\gamma K_1} - \frac{k_2}{\gamma K_2}$ and $\kappa_2 = \frac{k_1(1-\alpha_2)}{\gamma K_1 K_2\alpha_2} + \frac{k_2(1-\alpha_1)}{\gamma K_1 K_2\alpha_1}$.

Eqs. S4.8, S4.10 and S4.12 are the analytical results of the fixed-point solutions when $R \gg C_1 + C_2$. As shown in Fig. S17c-d, the analytical predictions agree well with the numerical results (exact solutions).

S4.2 Stability analysis of the coexistence behavior

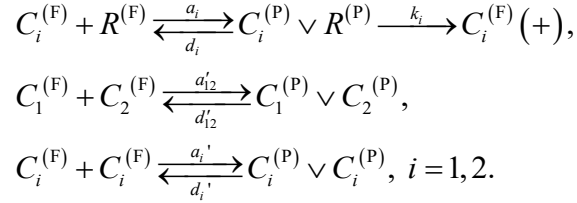
In the scenario involving chasing pair and interspecific interference, all fixed points are unstable (shown in Fig. S17e-f). For abiotic resources, the two-consumer species cannot enduringly coexist (Figs. 1d and S16c). For biotic resources, in the deterministic framework, both consumer species may oscillating coexist (Fig. S16e, g) or quasi-periodic oscillating coexist (Fig. S16f, h, see also Fig. S16 i and j for the Lyapunov exponents and Poincare map). However, within this scenario, for either life form of the resource, the two-consumer species fail to coexist along with stochasticity (Fig. 2a, see

also Fig. S16l and its ODEs simulation counterpart Fig. S16k).

S5 Scenario involving chasing-pairs and both intra- and inter-specific interference

5.1 Analytical solutions of species abundances at steady state

Here we consider the scenario involving chasing-pairs and both intra- and inter-specific interference in the simple case of $M = 2$ and $N = 1$ (Fig. S18a, b, combining that depicted in Sec. S3.1 and S4):



Then, $C_i \equiv C_i^{(F)} + x_i + 2y_i + z$ and $R \equiv R^{(F)} + x_1 + x_2$, and the population dynamics of the consumers and resources can be described as follows:

$$\begin{cases} \dot{x}_i = a_i R^{(F)} C_i^{(F)} - (d_i + k_i) x_i, \\ \dot{z} = a'_{12} C_1^{(F)} C_2^{(F)} - d'_{12} z, \\ \dot{y}_i = a'_i [C_i^{(F)}]^2 - d'_i y_i, \\ \dot{C}_i = w_i k_i x_i - D_i C_i, \\ \dot{R} = g(R, x_1, x_2, C_1, C_2), \quad i = 1, 2. \end{cases} \quad (\text{S5.1})$$

where the functional form of $g(R, x_1, x_2, C_1, C_2)$ follows Eq. S3.10. For convenience, we define $K_i \equiv (d_i + k_i)/a_i$, $\alpha_i \equiv D_i/(w_i k_i)$, $\beta_i \equiv a'_i/d'_i$ and $\gamma = a'_{12}/d'_{12}$ ($i = 1, 2$).

At steady state, from $\dot{x}_i = 0$, $\dot{y}_i = 0$, $\dot{z} = 0$, and $\dot{C}_i = 0$ ($i = 1, 2$), we have

$$\begin{cases} x_i = \alpha_i C_i, \\ C_i^{(F)} = K_i \alpha_i (R^{(F)})^{-1} C_i, \\ y_i = \beta_i (K_i \alpha_i)^2 (R^{(F)})^{-2} (C_i)^2, \\ z = \gamma K_1 \alpha_1 K_2 \alpha_2 (R^{(F)})^{-2} C_1 C_2. \end{cases} \quad (\text{S5.2})$$

Combined with $C_i \equiv C_i^{(F)} + x_i + 2y_i + z$, and note that $C_i > 0$ ($i = 1, 2$), then,

$$\begin{cases} (1 - \alpha_1)(R^{(F)})^2 - K_1\alpha_1R^{(F)} = 2\beta_1(K_1\alpha_1)^2 C_1 + \gamma K_1\alpha_1 K_2\alpha_2 C_2, \\ (1 - \alpha_2)(R^{(F)})^2 - K_2\alpha_2R^{(F)} = 2\beta_2(K_2\alpha_2)^2 C_2 + \gamma K_1\alpha_1 K_2\alpha_2 C_1. \end{cases} \quad (\text{S5.3})$$

If $R \gg C_1 + C_2$, then $R \gg x_1 + x_2$ and we can apply the approximation $R^{(F)} \approx R$.

Combined with Eq. S5.3, and then

$$\begin{cases} C_1 = R \frac{(2\beta_2 K_2 \alpha_2 (1 - \alpha_1) - \gamma K_1 \alpha_1 (1 - \alpha_2)) R + (\gamma - 2\beta_2) K_1 K_2 \alpha_1 \alpha_2}{K_1^2 K_2 \alpha_1^2 \alpha_2 (4\beta_1 \beta_2 - \gamma^2)}, \\ C_2 = R \frac{(2\beta_1 K_1 \alpha_1 (1 - \alpha_2) - \gamma K_2 \alpha_2 (1 - \alpha_1)) R + (\gamma - 2\beta_1) K_1 K_2 \alpha_1 \alpha_2}{K_1 K_2^2 \alpha_1 \alpha_2^2 (4\beta_1 \beta_2 - \gamma^2)}. \end{cases} \quad (\text{S5.4})$$

For biotic resources, with $\dot{R} = 0$, and note that $R > 0$, then we have

$$R = \frac{\frac{k_1(\gamma - 2\beta_2)}{K_1(4\beta_1\beta_2 - \gamma^2)} + \frac{k_2(\gamma - 2\beta_1)}{K_2(4\beta_1\beta_2 - \gamma^2)} - R_0}{\frac{k_1 2\beta_2(\alpha_1 - 1)}{K_1^2 \alpha_1(4\beta_1\beta_2 - \gamma^2)} + \frac{k_2 2\beta_1(\alpha_2 - 1)}{K_2^2 \alpha_2(4\beta_1\beta_2 - \gamma^2)} - \frac{k_1 \gamma(\alpha_2 - 1)}{K_1 K_2 \alpha_2(4\beta_1\beta_2 - \gamma^2)} - \frac{k_2 \gamma(\alpha_1 - 1)}{K_1 K_2 \alpha_1(4\beta_1\beta_2 - \gamma^2)} - \frac{R_0}{K_0}} \quad (\text{S5.5})$$

While for abiotic resources,

$$R = \frac{-\kappa'_2 + \sqrt{(\kappa'_2)^2 - 4\kappa'_1 R_a}}{2\kappa'_1}, \quad (\text{S5.6})$$

where $\kappa'_1 = \frac{\gamma(\alpha_1 - 1)k_2}{K_1 K_2 \alpha_1(4\beta_1\beta_2 - \gamma^2)} + \frac{\gamma(\alpha_2 - 1)k_1}{K_1 K_2 \alpha_2(4\beta_1\beta_2 - \gamma^2)} - \frac{2\beta(\alpha_1 - 1)k_1}{K_1^2 \alpha_1(4\beta_1\beta_2 - \gamma^2)} - \frac{2\beta_1(\alpha_2 - 1)k_2}{K_2^2 \alpha_2(4\beta_1\beta_2 - \gamma^2)}$,

and $\kappa'_2 = \frac{(\gamma - 2\beta_2)k_1}{K_1(4\beta_1\beta_2 - \gamma^2)} + \frac{(\gamma - 2\beta_1)k_2}{K_2(4\beta_1\beta_2 - \gamma^2)} + \frac{R_a}{K_0}$. Eqs. S5.4-S5.6 are the analytical

solutions to the steady-state species abundances when $R \gg C_1 + C_2$. As shown in Fig.

S19, the analytical predictions agree well with the numerical results (exact solutions).

S5.2 Stability analysis of the coexisting state

In the scenario involving chasing pair and both intra- and inter-specific interference, the behavior of species coexistence is very similar to that without interspecific interference. In the deterministic framework, the two-consumer species can coexist either at constant population densities or with time series dynamics such as oscillations (Fig. S18f-h). The fixed points can be globally attracting or there is a stable limit cycle (Fig. S18c-e and i-k). Clearly, there is a non-zero measure of parameter set where both

consumer species can steadily coexist with only one type of resource species (Fig. S18 i-k). In particular, just as the scenario involving chasing pair and intraspecific interference, the facilitated coexistence state can be maintained along with stochasticity (Fig. S20).

Effectively, the influence of interspecific interference is negligible when the separation rate d'_{12} is tremendously large, and vice versa for the intraspecific interference, if the separation rate $d'_i (i=1,2)$ is enormous.

S6 Methods

6.1 Derivation of the encounter rates with mean-field approximations

In the model scenario depicted in Fig. 1a, freely consumer and resource individuals move randomly in space, and we can regard the movements as Brownian motions. Specifically, at moment t , a consumer individual of species C_i ($i=1, \dots, M$) moves at speed v_{C_i} and with velocity $\mathbf{v}_{C_i}(t)$, while a resource individual of species R_l ($l=1, \dots, N$) moves at speed v_{R_l} and with velocity $\mathbf{v}_{R_l}(t)$. Here v_{C_i} and v_{R_l} are two time invariants, while the directions of $\mathbf{v}_{C_i}(t)$ and $\mathbf{v}_{R_l}(t)$ change constantly. At moment t , the relative velocity is $\mathbf{u}_{C_i-R_l}(t) \equiv \mathbf{v}_{R_l}(t) - \mathbf{v}_{C_i}(t)$. We denote the relative speed denoted as $u_{C_i-R_l}(t)$ and use $\theta(t)$ to represent the angle between $\mathbf{v}_{C_i}(t)$ and $\mathbf{v}_{R_l}(t)$. Evidently, $(u_{C_i-R_l}(t))^2 = v_{C_i}^2 + v_{R_l}^2 - 2v_{C_i} \cdot v_{R_l} \cdot \cos \theta(t)$. Since the system is homogenous, then, $\overline{\cos \theta} = 0$ (the overline means time average), and the average relative speed is $\overline{u_{C_i-R_l}} = \sqrt{v_{C_i}^2 + v_{R_l}^2}$. Similarly, the average relative speed between two consumer individuals (of species C_i and C_j , respectively, with $i, j=1, \dots, M$) is $\overline{u_{C_i-C_j}} = \sqrt{v_{C_i}^2 + v_{C_j}^2}$. Clearly, $\overline{u_{C_i-C_i}} = \sqrt{2}v_{C_i}$.

Next, we apply the mean-field approximations to calculate encounter rates a_{il} (among

individuals of species C_i and R_l) and a'_{ij} (among individuals of species C_i and C_j), which in essence is the same method in statistical physics applied to calculate the mean free path of gas particles. For convenience, we denote the concentrations of consumer species C_i and resource species R_l as n_{C_i} and n_{R_l} . Then, $n_{C_i} = C_i/L^2$ and $n_{R_l} = R_l/L^2$. Likewise, we can obtain the concentration of the freely wandering part of both species: $n_{C_i^{(F)}} = C_i^{(F)}/L^2$ and $n_{R_l^{(F)}} = R_l^{(F)}/L^2$.

In the well-mixed system, consider that all individuals of resource species R_l stand still, while a consumer individual (of species C_i) moves randomly at speed $u_{C_i-R_l}(t)$ (Fig. S21). For a given time interval Δt (corresponds to a macroscopic short, while microscopic long interval in statistical physics), the number of encounters between the given consumer individual and freely individuals from resource species R_l can be approximated by $2r_{il}^{(C)}n_{R_l^{(F)}}\overline{u_{C_i-R_l}}\Delta t$ ($r_{il}^{(C)}$ represents the radius to form a chasing pair, see Fig.1a). Then, for all freely individuals of species C_i , the total number of encounters with $R_l^{(F)}$ in interval Δt is $\frac{2r_{il}^{(C)}\overline{u_{C_i-R_l}}C_i^{(F)}R_l^{(F)}}{L^2}\Delta t$. Meanwhile, in the ODEs representation, this corresponds to $a_iR_l^{(F)}C_i^{(F)}\Delta t$. Comparing both terms above, evidently, for chasing pair, we have $a_{il} = 2r_{il}^{(C)}L^{-2}\overline{u_{C_i-R_l}} = 2r_{il}^{(C)}L^{-2}\sqrt{v_{C_i}^2 + v_{R_l}^2}$. Likewise, for interspecific interference, we have $a'_{ij} = 2r_{ij}^{(I)}L^{-2}\overline{u_{C_i-C_j}} = 2r_{ij}^{(I)}L^{-2}\sqrt{v_{C_i}^2 + v_{C_j}^2}$, while for intraspecific interference, we have $a'_{ii} = 2\sqrt{2}r_{ij}^{(I)}v_{C_i}L^{-2}$.

6.2 Stochastic simulations and Individual-based modeling

To consider the impact of stochasticity on species coexistence, we apply stochastic simulation algorithm (SSA) [50] and individual-based modeling (IBM) [51-52] to simulate the stochastic process. For the SSA, we follow the Gillespie's standard algorithm and the simulation procedures.

For the IBM, we consider a 2D system of squared landscape in a length of L with

periodic boundary conditions, and only for the case of $M = 2$ and $N = 1$. Consumer C_i ($i = 1, 2$) individuals move at speed v_{C_i} , while resource R individuals move at speed v_R . In our simulations, the unit length is $\Delta l = 1$, and all the populations move probabilistically. For instance, when Δt is very small ($v_{C_i} \Delta t \ll 1$), a C_i individual moves a unit length with probability $v_{C_i} \Delta t$. Specifically, we simulate the time evolution of the model system following the procedures below.

Initialization. The initial point of each individual is chosen randomly from a uniform distribution in the squared landscape. For convenience, we only consider the points with both integers in the x and y coordinates.

Moving. The destination of a movement is chosen randomly among four directions (x -positive, x -negative, y -positive, y -negative) following a uniform distribution. Then consumer C_i individuals move Δl with probability $v_{C_i} \Delta t$, while resource individuals move Δl with probability $v_R \Delta t$.

Forming pairs. When a consumer C_i individual and a resource individual get close in space within a distance of $r_i^{(C)}$, the two individuals form a chasing-pair. Likewise, when two consumer individuals C_i and C_j stand within a distance of $r_{ij}^{(I)}$, they form a chasing-pair.

Dissociating pairs. In the simulations, we update the system with small time step Δt so that $d_i \Delta t, k_i \Delta t \ll 1$. Then, a random number $\tilde{\zeta}$ is chosen from a uniform distribution between 0 and 1. If $\tilde{\zeta}$ is smaller than the $d_i \Delta t$ ($i = 1, 2$), then, the pair dissociates into the two separated individuals. One individual occupies the same position as the previous pair, while the other individual gets just out of the encounter radius in a random angle that is uniformly distributed. In the consumption process, if $\tilde{\zeta}$ is greater than $d_i \Delta t$ yet smaller than $(d_i + k_i) \Delta t$ ($i = 1, 2$), then the biomass of the resource flows into the consumer populations (updated according to the birth procedure), while the consumer individual occupies the same position as the previous pair and then updated following the moving procedure. Finally, if $\tilde{\zeta}$ is greater than

$(d_i + k_i)\Delta t$ ($i=1, 2$), the pair maintain its current status.

Birth and death. In each time step of the updates, the birth and death of each species accumulates, and we count them using a positive number with decimals. The integer part of this number will be updated in this run if it is no less than 1. A newborn is updated following the initialization procedure. The death process is also chosen randomly from the living species.

Supplemental Figures

Chasing pair

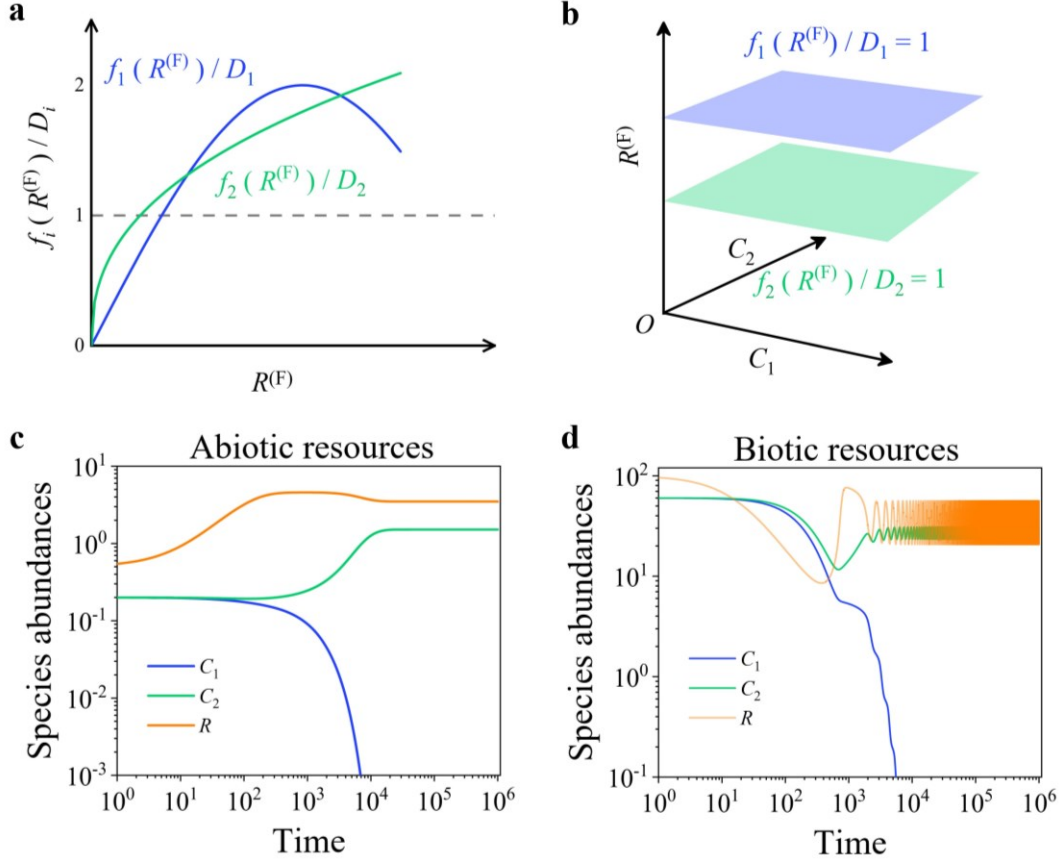


Figure S1 | Chasing-pair scenario is under the constraint of competitive exclusion.

(a) If all consumer species coexist at steady state, $f_i(R^{(F)})/D_i = 1$ ($i=1, 2$), where

$f_i(R^{(F)}) \equiv R^{(F)}/(R^{(F)} + K_i) = D_i$, with $K_i = (d_i + k_i)/a_i$. This means that the three

lines $f_i(R^{(F)})/D_i, i=1,2$ and $y=1$ share a common point, which is generally

impossible except for special parameter settings. (b) The blue plane is parallel to the green one, and hence they do not have a common point. (c-d) Time courses of the

species abundances in the scenario involving only chasing pair. The two consumer species cannot enduringly coexist. In (c): $a_1 = a_2 = 0.1$, $k_1 = k_2 = 0.1$, $w_1 = w_2 = 0.1$,

$d_1 = d_2 = 0.5$, $D_1 = 0.002$, $D_2 = 0.001$, $K_0 = 5$, $R_a = 0.05$. In (d): $a_1 = a_2 = 0.1$,

$w_1 = w_2 = 0.1$, $k_1 = k_2 = 0.05$, $d_1 = d_2 = 0.2$, $K_0 = 100$, $D_1 = 0.005$, $D_2 = 0.004$, $R_0 = 0.05$.

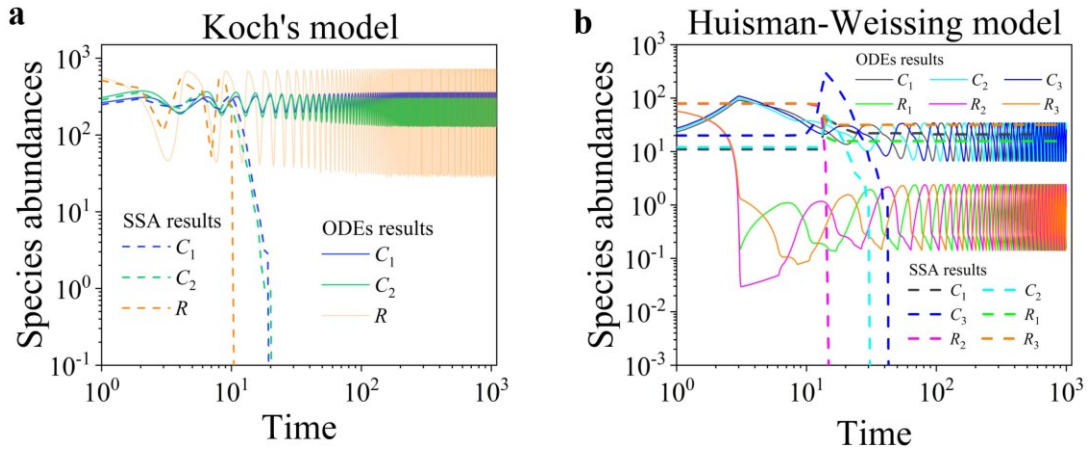


Figure S2 | Stochasticity jeopardizes species coexistence. (a-b) We simulate Koch's model [19] and Huisman-Weissing model [20] using stochastic simulation algorithm (SSA) with identical parameters as their deterministic model. Nevertheless, the two deterministic cases of oscillating coexistence fail as stochasticity is introduced. See Ref. [19] and [20] for the simulation parameters.

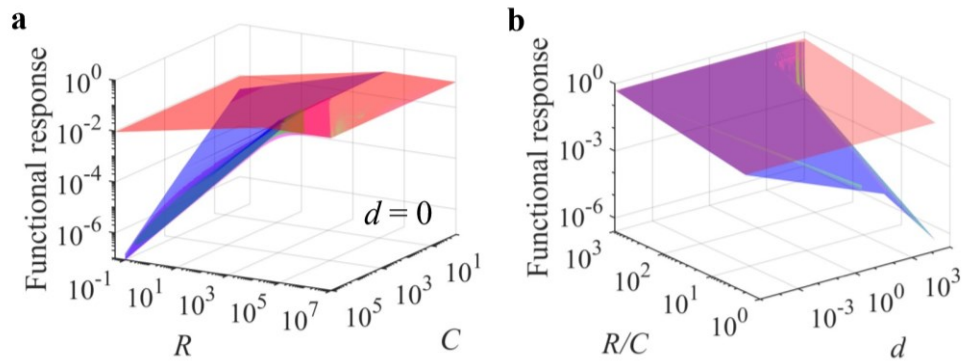


Figure S3 | Functional response in the scenario involving only chasing pair. (a-b) The red surface corresponds to the B-D model (calculated with Eq.2.9), while the green surface represents the exact solutions to our mechanistic model (using Eq. S2.6), and the magenta (using Eq. S2.7) and blue (using Eq. S2.8) surfaces represent the approximate solutions to our model. In (a-b): $k = 0.1$, $a = 0.25$. In (a): $d = 0$. In (c): $k = 0.5$, $a = 0.025$.

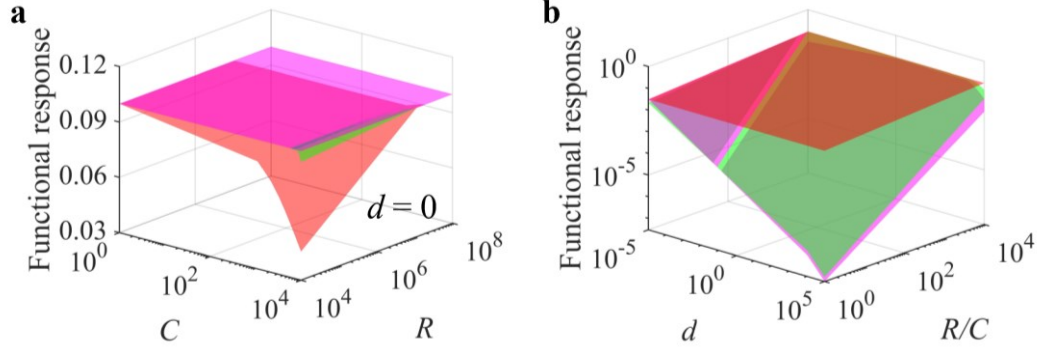


Figure S4 | Functional response in the scenario involving chasing pair and intraspecific interference. (a-b) The red surface corresponds to the B-D model (calculated with Eq.2.23), while the green surface represents the exact solutions to our mechanistic model (using Eq. S2.16), and the blue surface (with Eq. S2.18) and the magenta surface (with Eq. S2.20) represent the quasi-rigorous and the approximate solutions to our model, respectively. In (a-b): $a = 0.1$, $k = 0.1$, $d' = 0.1, a' = 0.12$.

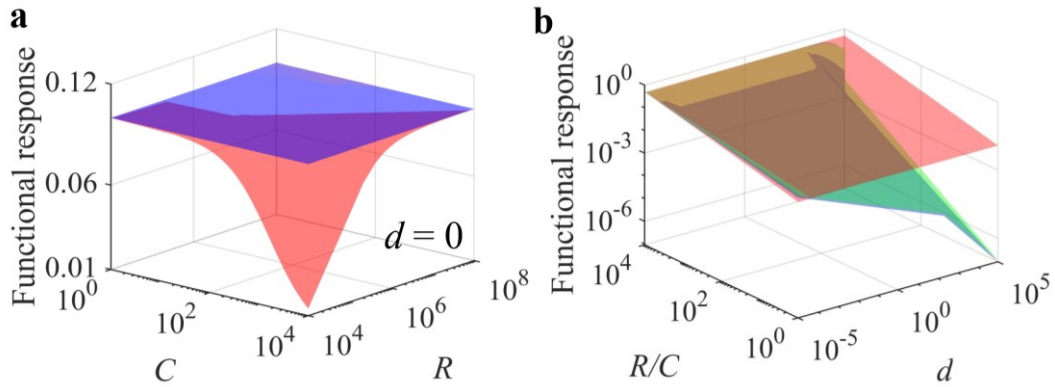


Figure S5 | Functional response in the scenario involving chasing pair and interspecific interference. (a-b) The red surface corresponds to the B-D model (calculated with Eq.2.30), while the green surface represents the quasi-rigorous solutions to our mechanistic model (using Eq. S2.26), and the blue surface (using Eq. S2.28) represents the approximate solutions to our model. In (a-c): $a_1 = a_2 = 0.1$, $k_1 = k_2 = 0.1$, $a'_{12} = 0.6, d'_{12} = 0.1$.

Chasing pair & Intraspecific interference

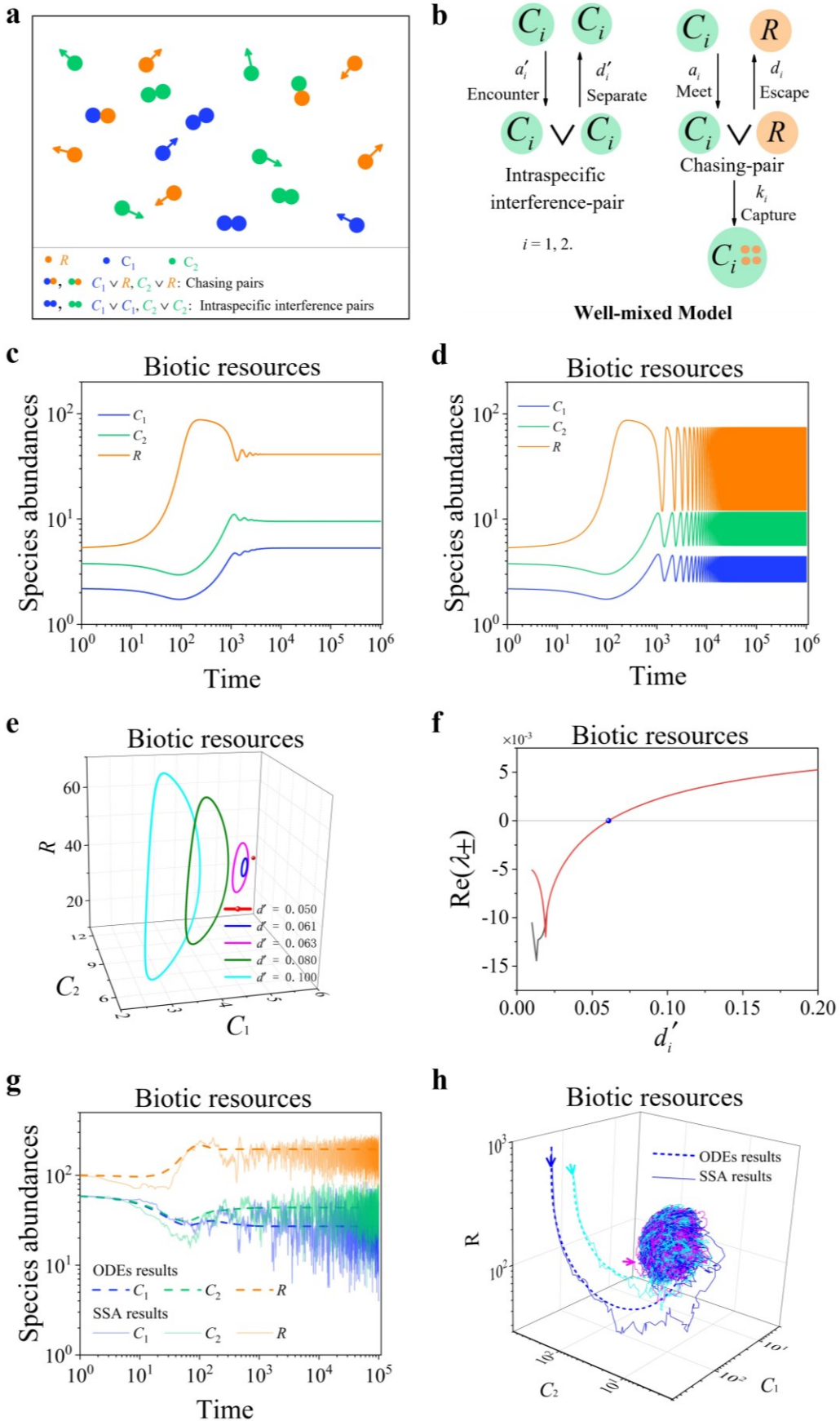


Figure S6 | Numerical results in the scenario involving chasing pair and intraspecific interference. (a-b) Model scenario in the case of $M=2$ and $N=1$. (c-d) The time series dynamics exhibit two types of coexisting behavior. The two-consumer species may coexist either at steady state or with oscillating behavior. (e) The phase diagram of Hopf bifurcation when varying parameter d' ($d' \equiv d'_1 = d'_2$). (f) The Hopf bifurcation curve when varying parameter d' . (g) The two-consumer species can enduringly coexist along with stochasticity (h) The stochastic coexistence state is stable and globally attractive (see (g) for the time courses). In (c-f): $a_1 = a_2 = 0.1$, $a'_1 = a'_2 = 0.125$, $d_1 = d_2 = 0.1$, $k_1 = k_2 = 0.1$, $w_1 = w_2 = 0.1$, $K_0 = 100$, $D_1 = 0.0085$, $D_2 = 0.008$, $R_0 = 0.05$. In (c): $d'_1 = d'_2 = 0.05$. In (d): $d'_1 = d'_2 = 0.1$. In (g-h): $a_1 = a_2 = 0.06$, $a'_1 = a'_2 = 0.075$, $d_1 = d_2 = 2$, $d'_1 = d'_2 = 2$, $k_1 = k_2 = 0.22$, $w_1 = w_2 = 0.32$, $K_0 = 350$, $D_1 = 0.052$, $D_2 = 0.05$, $R_0 = 0.13$.

Chasing pair & Intraspecific interference

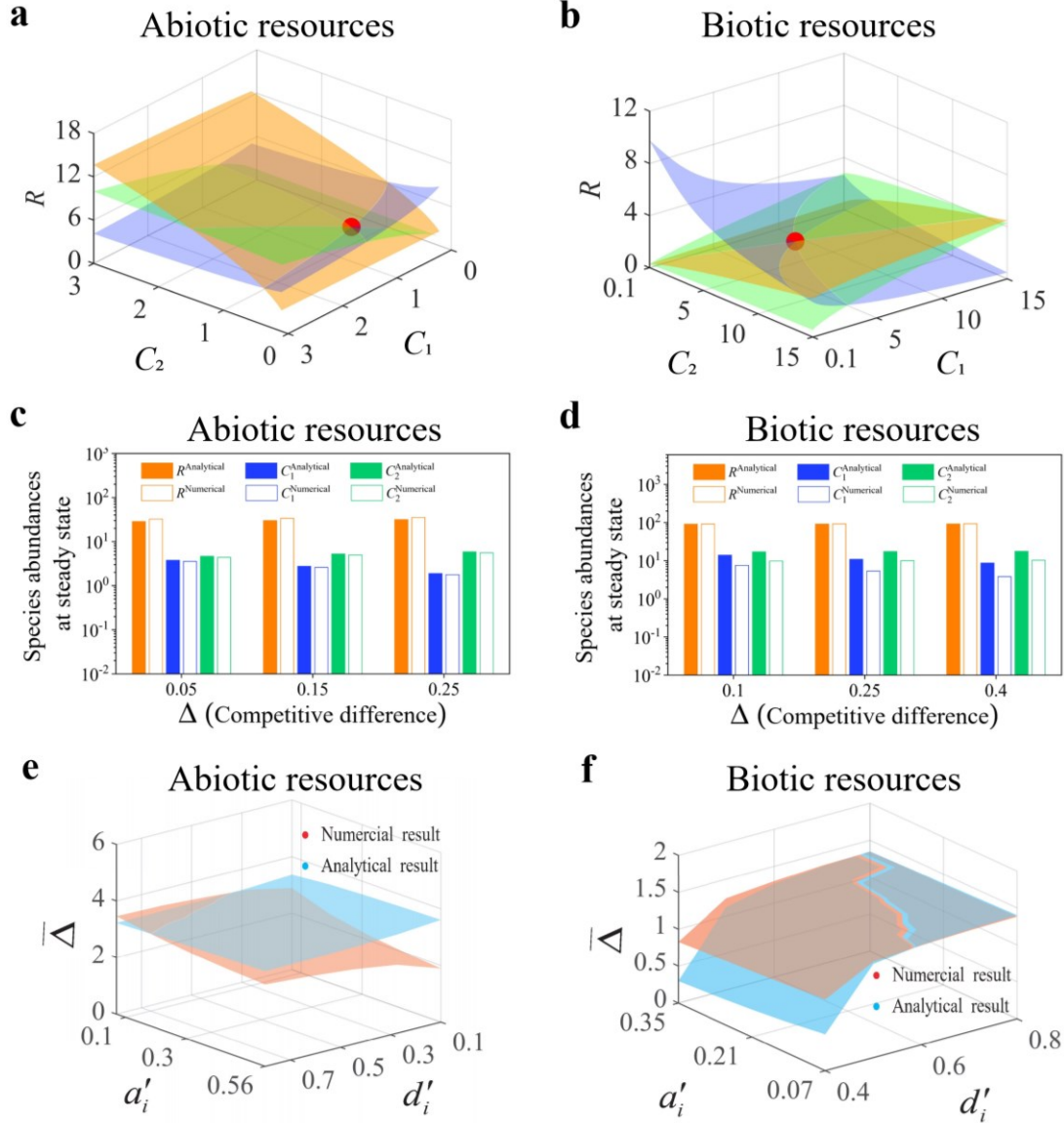


Figure S7 | Fixed point solutions in the case of $M = 2$ and $N = 1$ involving intraspecific interference. $D_i (i = 1, 2)$ is the only parameter of each different value between the consumer species, and $\Delta = (D_1 - D_2)/D_2$ represents the competitive differences between them. (a-b) Positive solutions to the steady-state equations: $\dot{R}_1 = 0$ (orange surface), $\dot{C}_1 = 0$ (blue surface), $\dot{C}_2 = 0$ (green surface). The intersection point marked by red dots are stable fixed points. (a-b) were calculated with Eqs. S3.1 and S3.10. (c-d) Comparisons between numerical results and analytical solutions of the steady-state species abundances in this system. Color bars are analytical solutions while hollow bars are numerical results. The numerical results (labeled with superscript ‘Numerical’) were calculated from Eqs. S3.1 and S3.10, while the analytical solutions (labeled with superscript ‘Analytical’) were calculated

from Eqs. S3.9, S3.11 and S3.12. (e-f) Comparison between the numerical results and analytical solutions of the coexistence region. Here $\bar{\Delta}$ represents the maximum tolerated Δ for species coexistence. The red and cyan surfaces represent the analytical solutions (calculated with Eqs. S3.15, S3.16) and numerical results (calculated with Eqs. S3.1, S3.10), respectively. In (a-b) $a_1 = a_2 = 0.5$, $a'_1 = a'_2 = 0.625$, $d_1 = d_2 = 0.5$, $d'_1 = d'_2 = 0.5$, $k_1 = k_2 = 0.4$, $D_2 = 0.02$, $w_1 = w_2 = 0.5$, $K_0 = 10$. In (a): $D_1 = 1.2D_2$, $R_a = 0.1$. In (b): $D_1 = 1.05D_2$, $R_0 = 0.3$. In (c): $a_1 = a_2 = 0.1$, $a'_1 = a'_2 = 0.12$, $k_1 = k_2 = 0.12$, $w_1 = w_2 = 0.3$, $D_2 = 0.02$, $K_0 = 100$, $R_a = 0.8$, $d_1 = d_2 = 0.5$, $d'_1 = d'_2 = 0.05$. In (d): $a_1 = a_2 = 0.05$, $a'_1 = a'_2 = 0.06$, $k_1 = k_2 = 0.12$, $w_1 = w_2 = 0.2$, $D_2 = 0.008$, $K_0 = 100$, $R_0 = 0.1$, $d_1 = d_2 = 0.8$, $d'_1 = d'_2 = 0.01$. In (e): $a_1 = a_2 = 0.5$, $k_1 = k_2 = 0.2$, $w_1 = w_2 = 0.2$, $D_2 = 0.008$, $K_0 = 60$, $R_a = 0.8$, $d_1 = d_2 = 0.8$. In (f): $a_1 = a_2 = 0.5$, $k_1 = k_2 = 0.1$, $w_1 = w_2 = 0.2$, $D_2 = 0.008$, $K_0 = 100$, $R_0 = 0.2$, $d_1 = d_2 = 0.8$.

Chasing pair & Intraspecific interference Abiotic resources

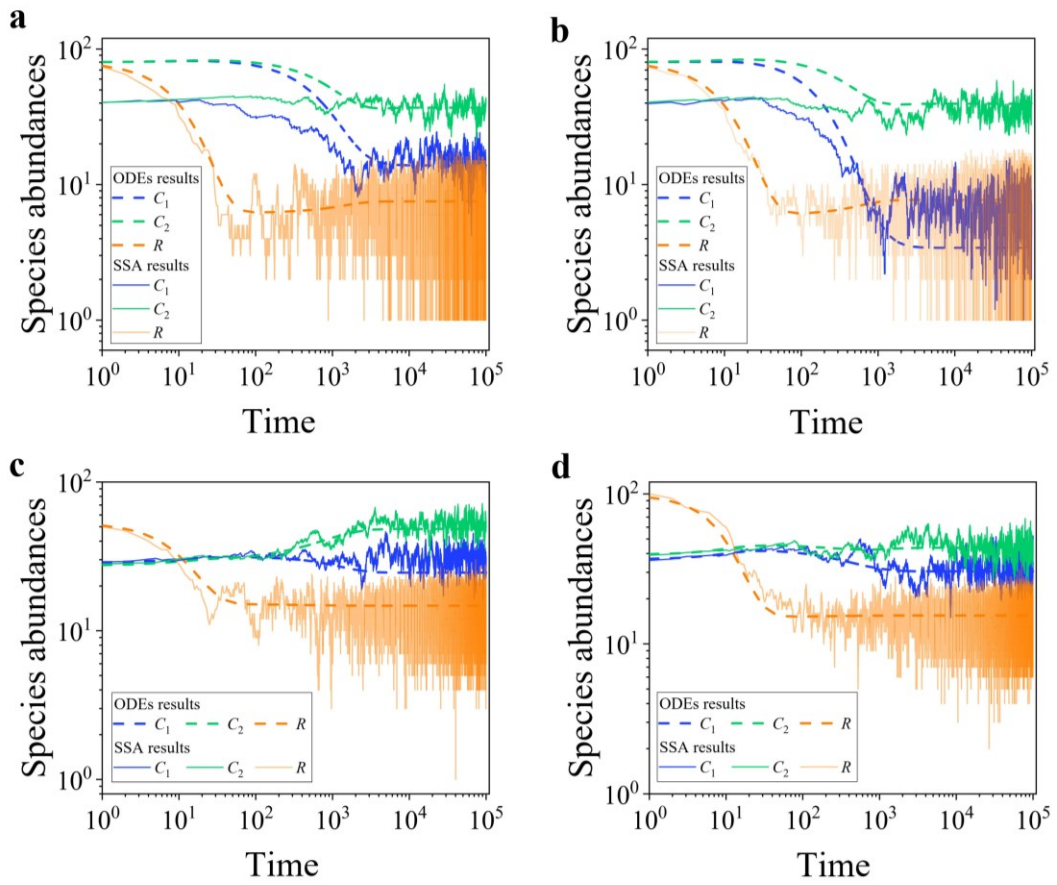


Figure S8 | Time series which corresponds to Fig. 4 in the long-term behavior. The simulation details are the same as Fig. 4.

Chasing pair & Intraspecific interference

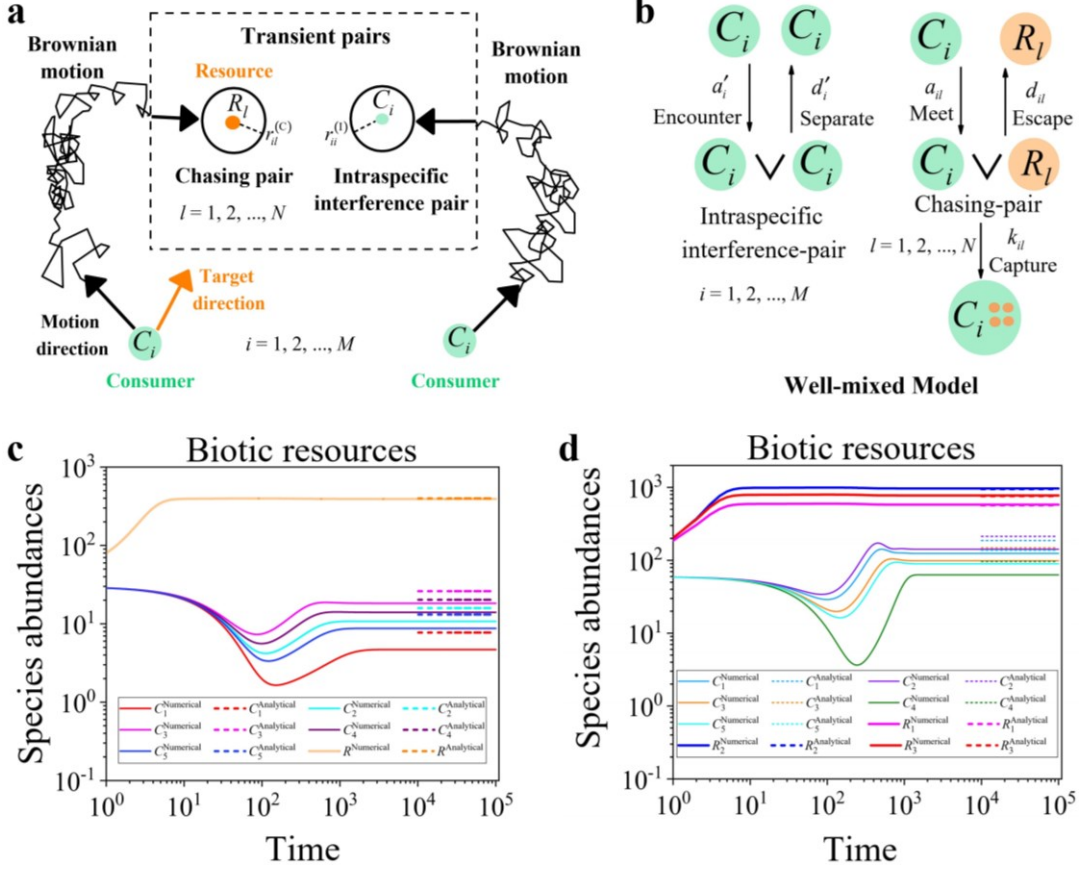


Figure S9 | With intraspecific interference, a single biotic resource species ($N = 1$) can support 5 consumers species ($M = 5$) to coexist at steady state. (a-b) is a simplified version of Fig. 1(a-b), where the interspecific interference is omitted. (c-d) Time courses of the species abundances simulated with ODEs. Here, $D_i (i = 1, \dots, M)$ is the only parameter of each different value among the consumer species, and thus each consumer species owns a unique competitiveness. The dotted lines in (c-d) are the analytical solutions at steady state (calculated from Eqs. S3.23-S3.28). In (c): $a_i = 0.04$, $a'_i = 0.056$, $d_i = 0.6$, $d'_i = 0.04$, $w_i = 0.45$, $k_i = 0.15$, $i = 1, \dots, 5$, $D_1 = 0.0619$, $D_2 = 0.0595$, $D_3 = 0.057$, $D_4 = 0.0584$, $D_5 = 0.0603$, $K_0 = 400$, $R_a = 0.9$. In (d): $a_{il} = 0.05$, $a'_i = 0.07$, $d_{il} = 0.98$, $d'_i = 0.018$, $w_{il} = 0.45$, $k_{il} = 0.16$, $i = 1, \dots, 5$, $l = 1, 2, 3$, $K_0^{(1)} = 600$, $K_0^{(2)} = 1000$, $K_0^{(3)} = 800$, $R_0^{(1)} = R_0^{(2)} = 0.9$, $R_0^{(3)} = 0.95$, $D_1 = 0.062$, $D_2 = 0.0615$, $D_3 = 0.0639$, $D_4 = 0.066$, $D_5 = 0.0644$.

Abiotic resources

$$M = 20, N = 1$$

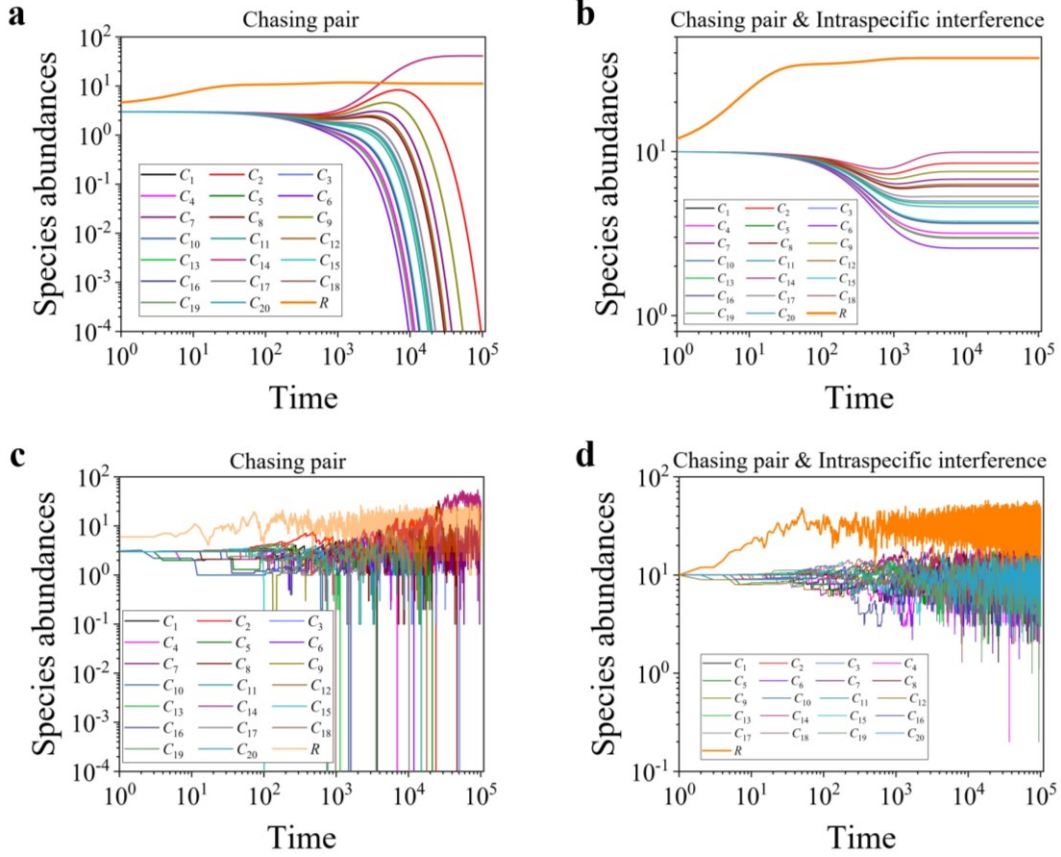


Figure S10 | With intraspecific interference, one type of abiotic resource species ($N = 1$) can support a wide range of consumer species ($M = 20$) to enduringly coexist regardless of stochasticity. Here, $D_i (i = 1, \dots, M)$ is the only parameter of each

different value among the consumer species, so each consumer species owns a unique competitiveness. (a-b) Time series of the consumer and resource species simulated with ODEs. (c-d) Time series of the consumer and resource species simulated with SSA (with the same parameters as that in (a-b)). (a, c) With only chasing-pair, consumer species cannot coexist. (b, d) With chasing-pair and intraspecific interference, all consumer species can enduringly coexist regardless of stochasticity.

In (a-d): $a_i = 0.1$, $d_i = 0.5$, $w_i = 0.1$, $k_i = 0.1$, $D_i = 0.002 + 0.002 \times p_i$, $p_i \in [0, 1]$,

$i = 1, \dots, 20$, $K_0 = 1000$, $R_a = 2.95$. In (a, c): $a'_i = 0$, $d'_i = 0$. In (b, d): $a'_i = 0.125$, $d'_i = 0.1$.

Biotic resources

$M = 20, N = 1$

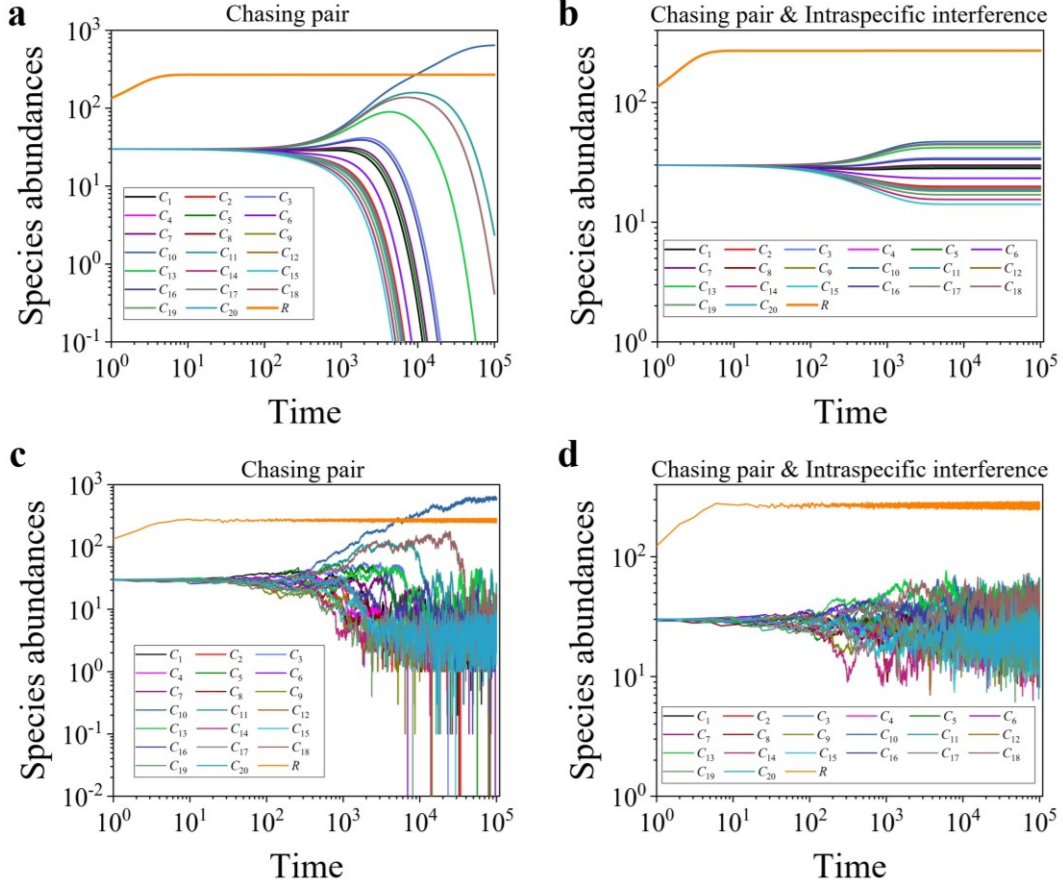


Figure S11 | With intraspecific interference, one type of biotic resource species ($N = 1$) can support a wide range of consumers species ($M = 20$) to enduringly coexist regardless of stochasticity. Here, $D_i (i = 1, \dots, M)$ is the only parameter of each

different value among the consumer species, so each consumer species owns a unique competitiveness.

(a-b) Time series of the consumer and resource species simulated with ODEs. (c-d) Time series of the consumer and resource species simulated with SSA (same parameters as that in (a-b)).

(a, c) With only chasing-pair, consumer species cannot coexist. (b, d) With chasing-pair and intraspecific interference, all

consumer species can coexist regardless of stochasticity. In (a-d): $a_i = 0.1, d_i = 0.3$,

$R_0 = 0.95$, $w_i = 0.1$, $k_i = 0.1$, $D_i = 0.004 + 0.002 \times p_i$, $p_i \in [0, 1]$, $i = 1, \dots, 20$,

$K_0 = 300$. In (a, c): $a'_i = 0, d'_i = 0$. In (b, d): $a'_i = 0.125, d'_i = 0.3$.

Chasing pair & Intraspecific interference

$$M = 100, N = 1$$

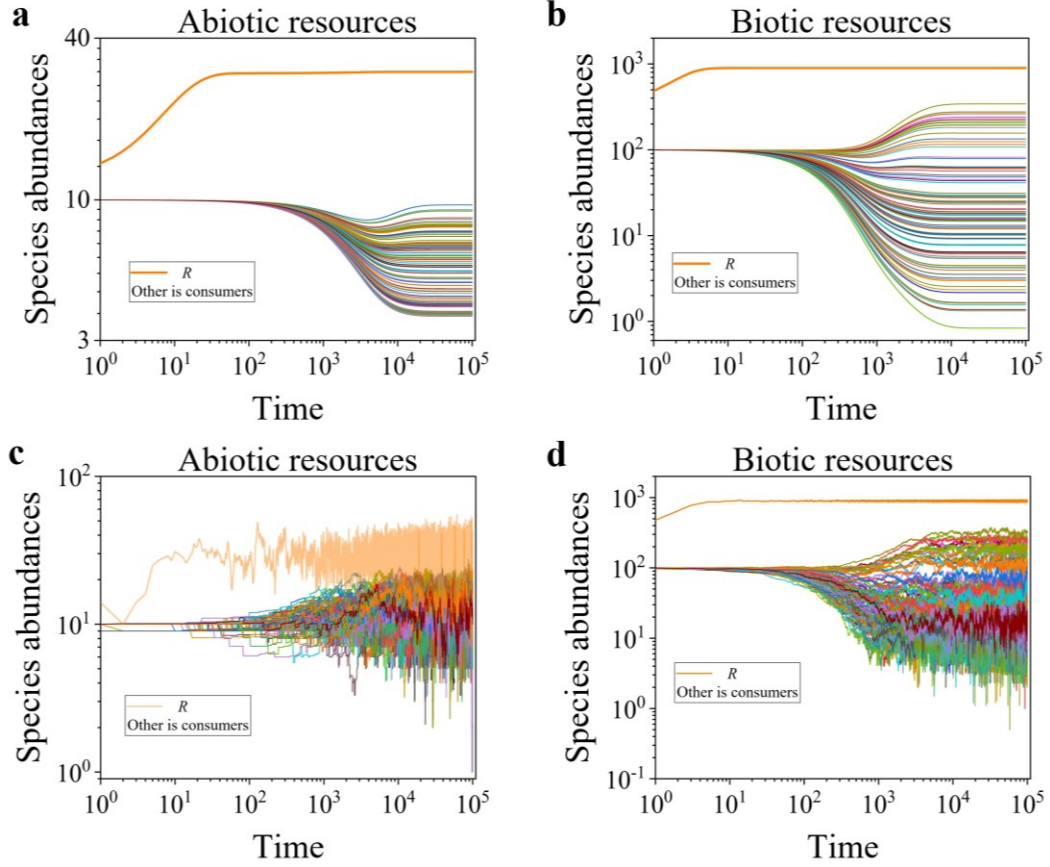


Figure S12 | In the scenario involving chasing-pair and intraspecific interference, one type of resource species ($N = 1$) can support an unexpected wide range of consumers species ($M = 100$) to enduringly coexist regardless of stochasticity. Here, $D_i (i = 1, \dots, M)$ is the only parameter of each different value among the consumer species, so each consumer species owns a unique competitiveness. (a-b) Time series of ODEs simulations. (c-d) Time series of SSA simulations, which share the same parameter set as that in (a-b). In (a, c): $a_i = 0.1$, $a'_i = 0.125$, $d_i = 0.5$, $d'_i = 0.1$, $w_i = 0.1$, $k_i = 0.1$, $R_a = 2.95$, $K_0 = 1000$, $D_i = 0.0004 + 0.0002 \times p_i$, $p_i \in [0, 1]$, $i = 1, \dots, 100$. In (b, d): $a_i = 0.1$, $a'_i = 0.125$, $d_i = 0.3$, $d'_i = 0.3$, $R_0 = 0.95$, $w_i = 0.1$, $k_i = 0.1$, $K_0 = 1000$, $D_i = 0.001 + 0.005 \times p_i$, $p_i \in [0, 1]$, $i = 1, \dots, 100$.

Chasing pair & Intraspecific interference

$$M = 18, N = 3$$

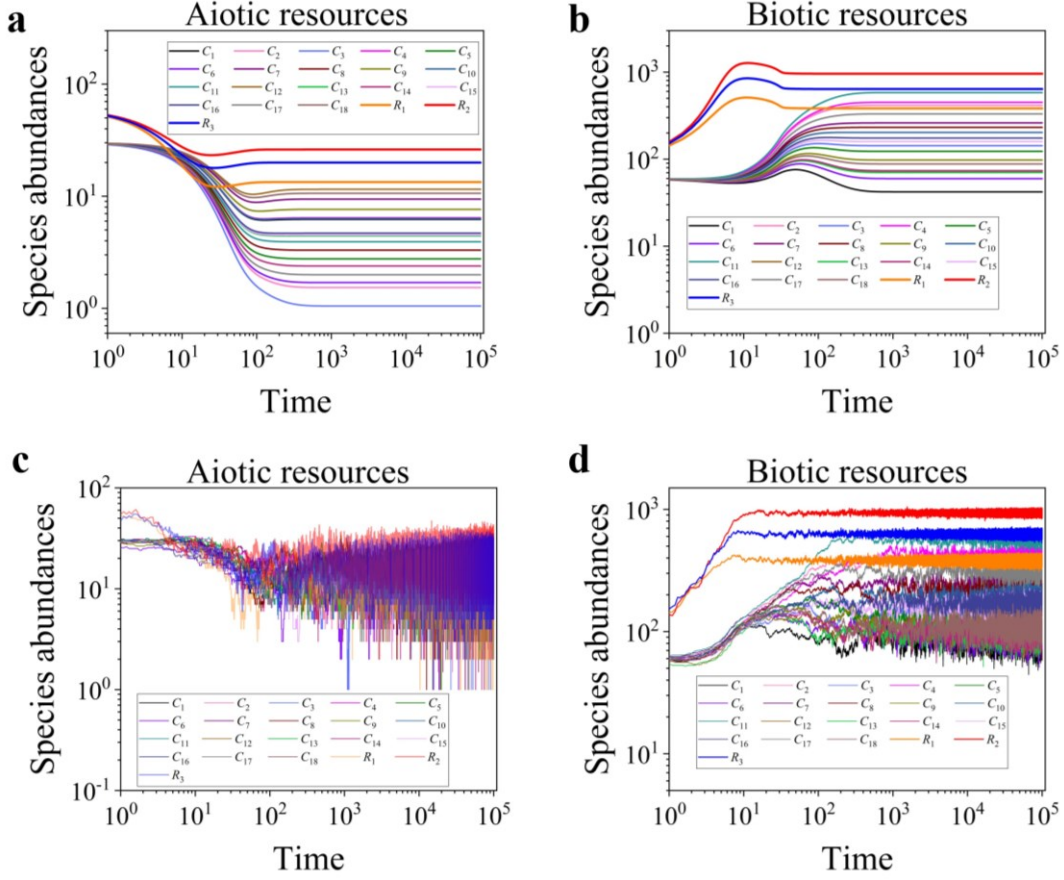


Figure S13 | In the scenario involving chasing-pair and intraspecific interference, a handful of resource species ($N = 3$) can support a wide range of consumers species ($M = 18$) to enduringly coexist regardless of stochasticity. Here, D_i ($i = 1, \dots, M$) is the only parameter of each different value among the consumer species, so each consumer species owns a unique competitiveness. (a-b) Time series of ODEs simulations. (c-d) Time series of SSA simulations, which share the same parameter set as that in (a-b). In (a, c): $a_{il} = 0.2$, $a'_i = 0.25$, $d_{il} = 0.5$, $d'_i = 0.1$, $w_{il} = 0.5$, $k_{il} = 0.2$, $K_0^{(1)} = 5000$, $K_0^{(2)} = 1000$, $K_0^{(3)} = 3000$, $D_i = 0.04 + 0.03 \times p_i$, $p_i \in [0, 1]$, $i = 1, \dots, 18$, $l = 1, 2, 3$, $R_a^{(1)} = 2$, $R_a^{(2)} = 4$, $R_a^{(3)} = 3$. In (b, d): $a_{il} = 0.2$, $a'_i = 0.25$, $d_{il} = 0.4$, $d'_i = 0.2$, $w_{il} = 0.3$, $k_{il} = 0.3$, $R_0^{(l)} = 0.8$, $K_0^{(1)} = 600$, $K_0^{(2)} = 1500$, $K_0^{(3)} = 1000$, $D_i = 0.03 + 0.03 \times p_i$, $p_i \in [0, 1]$, $i = 1, \dots, 18$, $l = 1, 2, 3$.

Chasing pair & Intraspecific interference

$M = 98, N = 3$

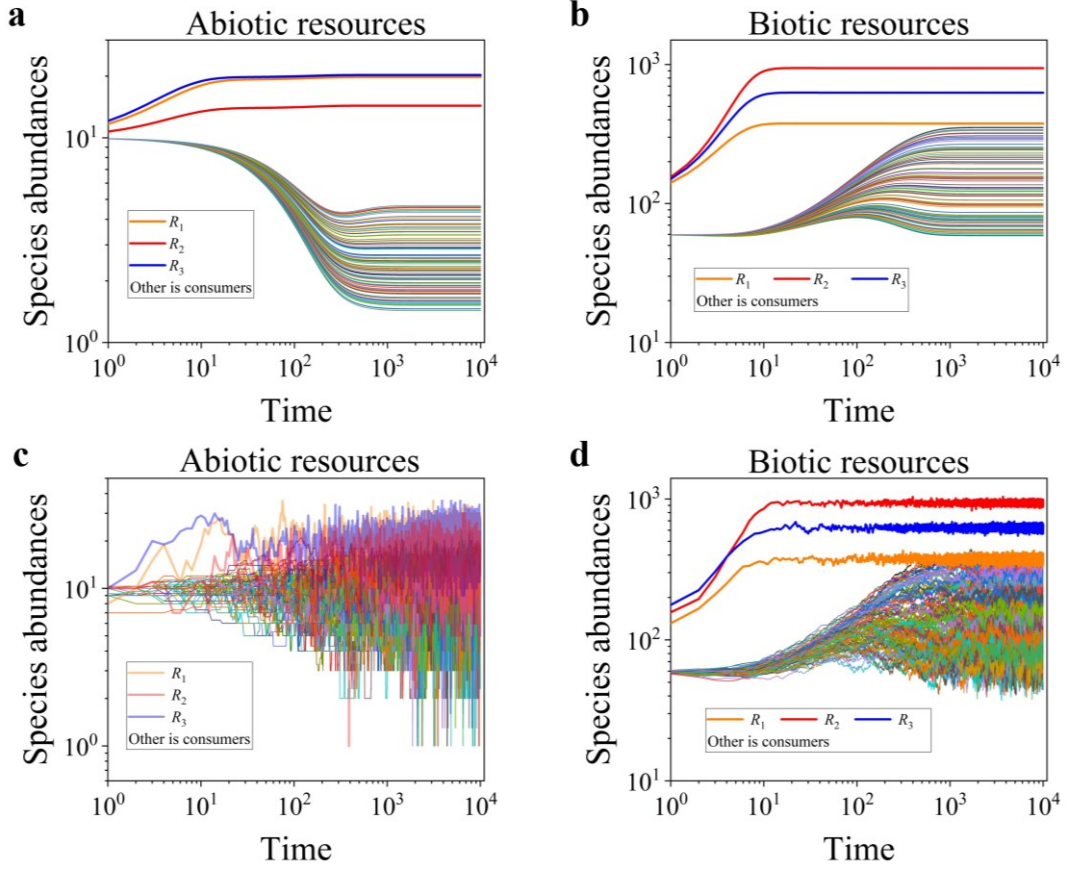


Figure S14 | In the scenario involving chasing-pair and intraspecific interference, a handful of resource species ($N = 3$) can support an unexpected wide range of consumers species ($M = 98$) to enduringly coexist regardless of stochasticity. Here, $D_i (i = 1, \dots, M)$ is the only parameter of each different value among the consumer species, so each consumer species owns a unique competitiveness. (a-b) Time series of ODEs simulations. (c-d) Time series of SSA simulations, which share the same parameter set as that in (a-b). In (a, c): $a_{il} = 0.1$, $a'_l = 0.125$, $d_{il} = 0.2$, $d'_l = 0.1$, $w_{il} = 0.3$, $k_{il} = 0.3$, $K_0^{(1)} = 500$, $K_0^{(2)} = 100$, $K_0^{(3)} = 300$, $D_i = 0.01 + 0.005 \times p_i$, $p_i \in [0, 1]$, $i = 1, \dots, 98$, $l = 1, 2, 3$, $R_a^{(1)} = 3.9$, $R_a^{(2)} = 4.8$, $R_a^{(3)} = 2.85$. In (b, d): $a_{il} = 0.2$, $a'_l = 0.25$, $d_{il} = 0.2$, $d'_l = 0.1$, $w_{il} = 0.3$, $k_{il} = 0.3$, $K_{01} = 600$, $K_{03} = 1500$, $K_{02} = 1000$, $R_0^{(l)} = 0.8$, $D_i = 0.008 + 0.01 \times p_i$, $p_i \in [0, 1]$, $i = 1, \dots, 98$, $l = 1, 2, 3$.

Chasing pair & Intraspecific interference

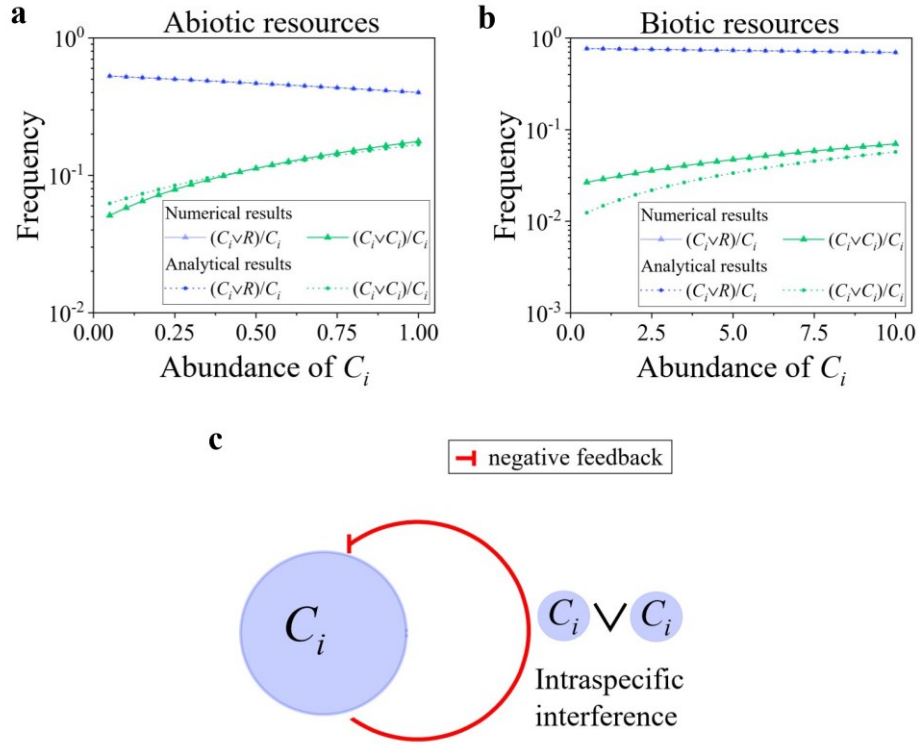


Figure S15 | Intraspecific interference results in a negative feedback and thus promotes biodiversity. (a-b) As the population density of consumer species C_i increases, a larger fraction of species C_i are involved in an intraspecific interference pair which temporarily absent from hunting. Meanwhile, the fraction of species C_i within a chasing pair decrease. (c) The formation of intraspecific interference virtually leads to a negative feedback and thus promotes biodiversity. In (a): $a_i = 0.2$, $a'_i = 0.25$, $w_i = 0.5$, $k_i = 0.15$, $d_i = 0.3$, $d'_i = 0.05$, $R_a = 0.35$, $K_0 = 3000$, $D_i = 0.03 + i \times 5 \times 10^{-4}$, $i = 1, \dots, 20$. In (b): $a_i = 0.008$, $a'_i = 0.0112$, $w_i = 0.45$, $k_i = 0.15$, $d_i = 0.6$, $d'_i = 0.04$, $R_0 = 0.8$, $K_0 = 400$, $D_i = 0.047 + i \times 2.5 \times 10^{-4}$, $i = 1, \dots, 20$.

Chasing pair & Interspecific interference

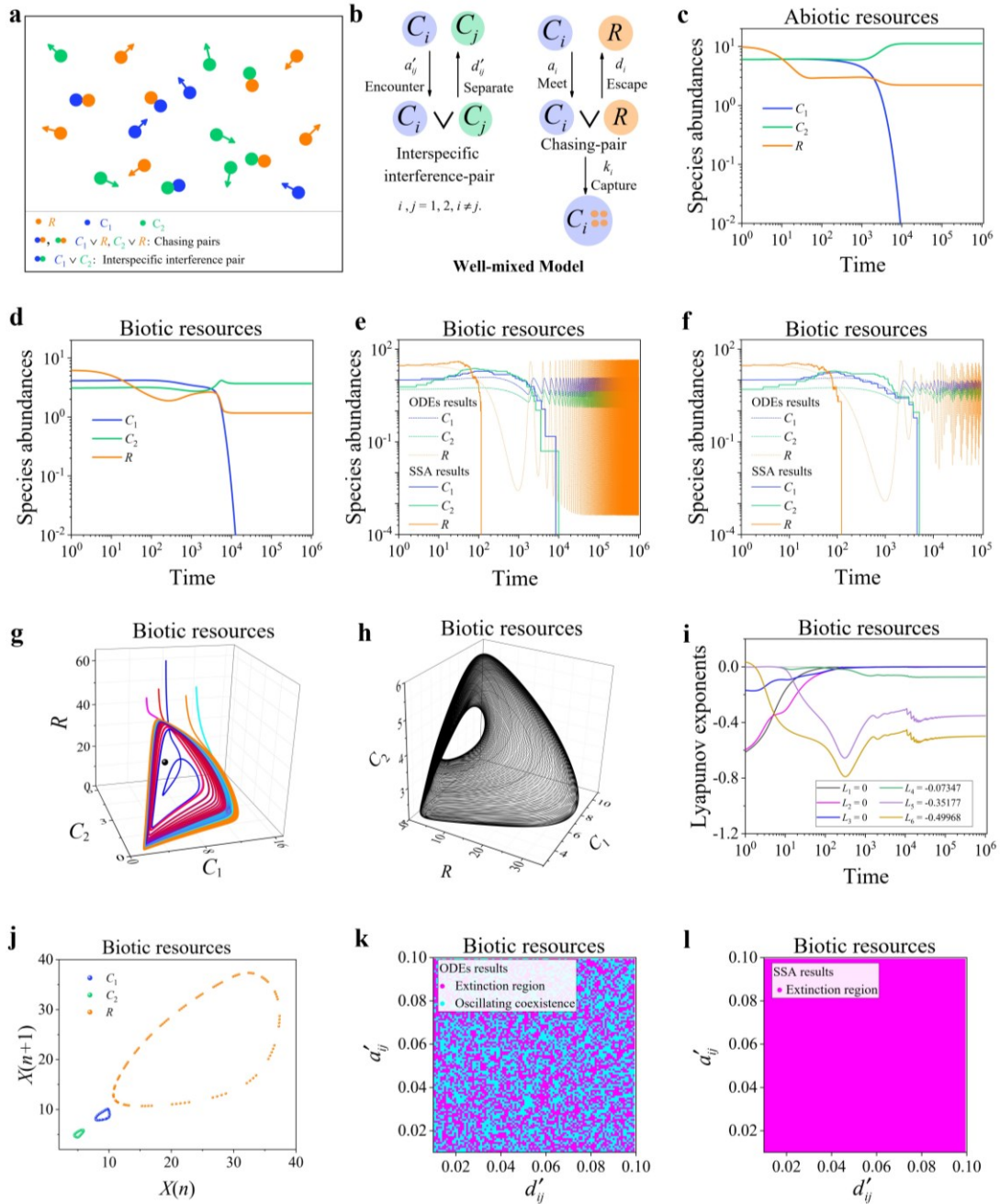


Figure S16 | Interspecific interference may facilitate oscillating coexistence without stochasticity. (a-b) Model scenario involving chasing-pairs and interspecific interference in the case of $M=2$ and $N=1$. (c-d) The simulate results of species abundances for abiotic or biotic resources. The two-consumer species cannot coexist at steady state. (e-f) In the ODEs simulations, both consumer species may coexist with time series dynamics. However, in the SSA simulations where we apply the same set of parameters, the two-consumer species do not coexist. (g-h) In a 3D phase space, the ODEs simulation in (e-f) corresponds to a limit cycle or a quasi-periodic torus. (i-j) The Lyapunov exponent analysis in (i) and Poincaré map in (j) further suggest that the dynamics in (f) and (h) is a quasi-periodic oscillation. In (i),

L_1, L_2, \dots, L_6 represents the Lyapunov exponents. Then, in the Lyapunov spectrum, three exponents are zeros while the rest are all negative, which clearly suggest a 3-D torus. In (j) The loops in the Poincare map indicate a quasi-periodic oscillation. (k) In the ODEs simulations, the cyan region represents oscillating coexistence while the magenta region represents species extinction. (l) In the SSA simulation results, which share the parameter region as that in (k), there is no area for species coexistence. In (c-j): $a_1 = a_2 = 0.05$, $d_1 = d_2 = 0.1$, $k_1 = k_2 = 0.1$, $w_1 = w_2 = 0.05$, $D_1 = 0.0009$, $D_2 = 0.0007$. In (c): $K_0 = 10$, $a'_{12} = 0.02$, $R_a = 0.2$, $d'_{12} = 0.02$. In (d): $K_0 = 10$, $a'_{12} = 0.02$, $R_0 = 0.05$, $d'_{12} = 0.02$. In (e, g): $K_0 = 60$, $R_0 = 0.05$, $a'_{12} = 0.06$, $d'_{12} = 0.02$. In (f, h, e, j): $K_0 = 60$, $R_0 = 0.05$, $a'_{12} = 0.02$, $d'_{12} = 0.02$; In (i): $K_0 = 60$, $R_0 = 0.05$. In (k-l): $a_1 = a_2 = 0.15$, $d_1 = d_2 = 0.1$, $k_1 = k_2 = 0.2$, $w_1 = w_2 = 0.1$, $D_1 = 0.0009$, $D_2 = 0.0007$, $K_0 = 60$, $R_0 = 0.15$.

Chasing pair & Interspecific interference

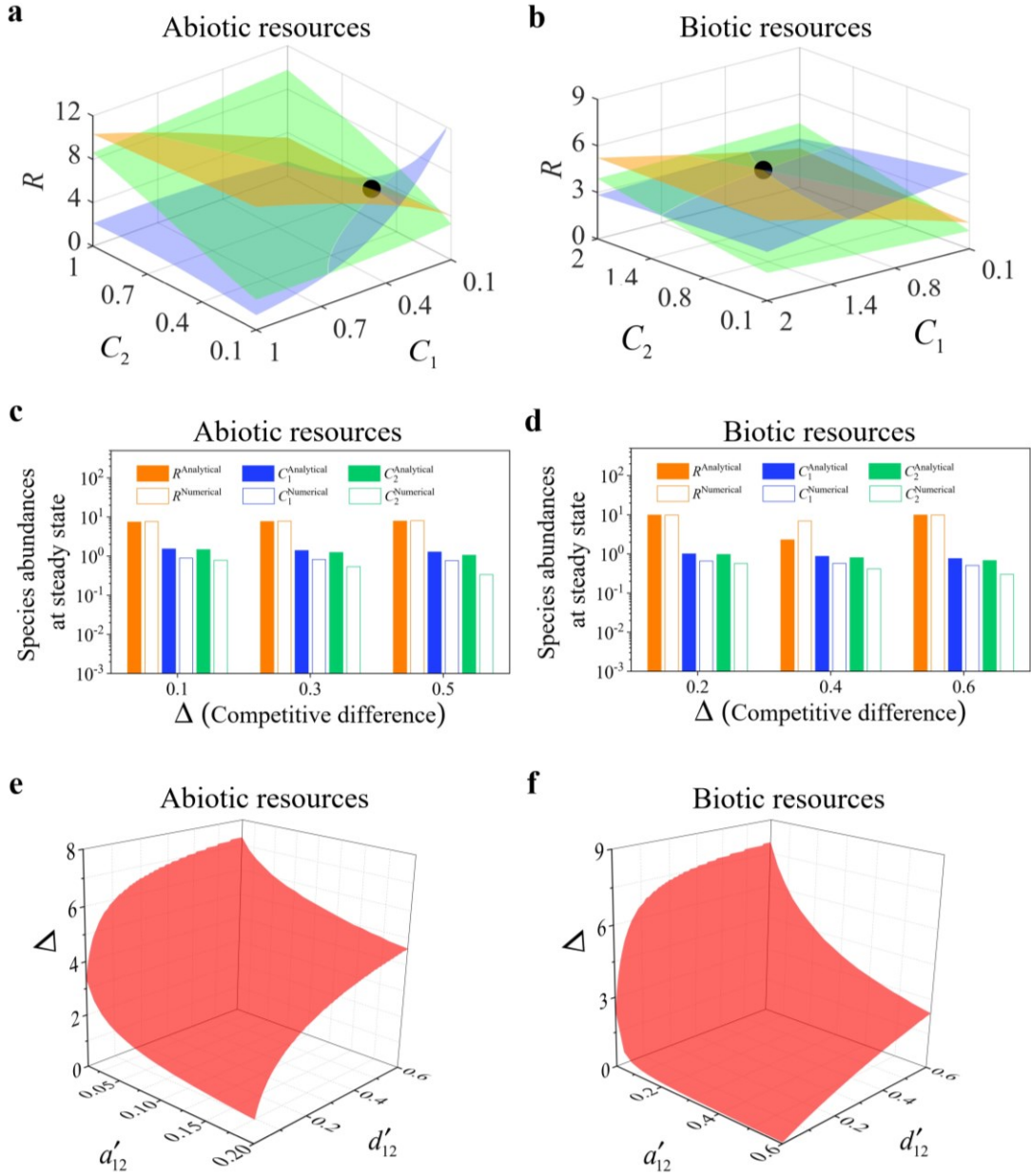


Figure S17 | Fixed point solutions in the case of $M = 2$ and $N = 1$ involving chasing pair and interspecific interference. $D_i (i=1,2)$ is the only parameter of each different value between the consumer species, and $\Delta = (D_1 - D_2)/D_2$ represents the competitive differences between them. (a-b) Positive solutions to the steady-state equations: $\dot{R}_i = 0$ (orange surface), $\dot{C}_1 = 0$ (blue surface), $\dot{C}_2 = 0$ (green surface). The intersection point marked by black dots are unstable fixed points. (a-b) were calculated using Eqs. S4.1, S3.10. (c-d) Comparisons between numerical results and analytical solutions of the steady-state species abundances in this system. Color bars are analytical solutions while hollow bars are numerical results. The numerical

results (labeled with superscript ‘Numerical’) were calculated from Eqs. S3.1 and S3.10, while the analytical solutions (labeled with superscript ‘Analytical’) were calculated from Eqs. S4.10, S4.12. (e-f) In this scenario, there is no parameter space for steady coexistence. The region below the red surface and above $\Delta = 0$ represents unstable fixed points, which may end in a limit cycle (see Fig. S16e, g), a torus (see Fig. S16f, h), or C_1 extinction (see Fig. S16c-d, $D_1 > D_2$). In (a): $a_1 = a_2 = 0.05$, $k_1 = k_2 = 0.02$, $d_1 = d_2 = 0.05$, $K_0 = 20$, $a'_{12} = 0.3$, $d'_{12} = 0.01$, $w_1 = w_2 = 0.08$, $D_1 = 0.001$, $D_2 = 0.0009$, $R_a = 0.01$. In (b): $a_1 = a_2 = 0.05$, $k_1 = k_2 = 0.02$, $d_1 = d_2 = 0.05$, $K_0 = 5$, $a'_{12} = 0.3$, $d'_{12} = 0.1$, $w_1 = w_2 = 0.08$, $D_1 = 0.001$, $D_2 = 0.0008$, $R_0 = 0.02$. In (c): $a_1 = a_2 = 0.04$, $k_1 = k_2 = 0.1$, $K_0 = 10$, $d_1 = d_2 = 0.2$, $w_1 = w_2 = 0.3$, $D_2 = 0.008$, $R_a = 0.2$, $K_0 = 100$, $a'_{12} = 0.6$, $d'_{12} = 0.1$. In (d): $a_1 = a_2 = 0.05$, $k_1 = k_2 = 0.1$, $K_0 = 10$, $d_1 = d_2 = 0.2$, $w_1 = w_2 = 0.2$, $D_2 = 0.005$, $R_0 = 0.2$, $a'_{12} = 0.6$, $d'_{12} = 0.02$. In (e-f): $a_1 = a_2 = 0.05$, $k_1 = k_2 = 0.1$, $d_1 = d_2 = 0.1$, $K_0 = 100$, $w_1 = w_2 = 0.05$, $D_2 = 0.0005$. In (f): $R_a = 0.5$; In (f): $R_0 = 0.05$.

Chasing pair & Interspecific and intraspecific interference

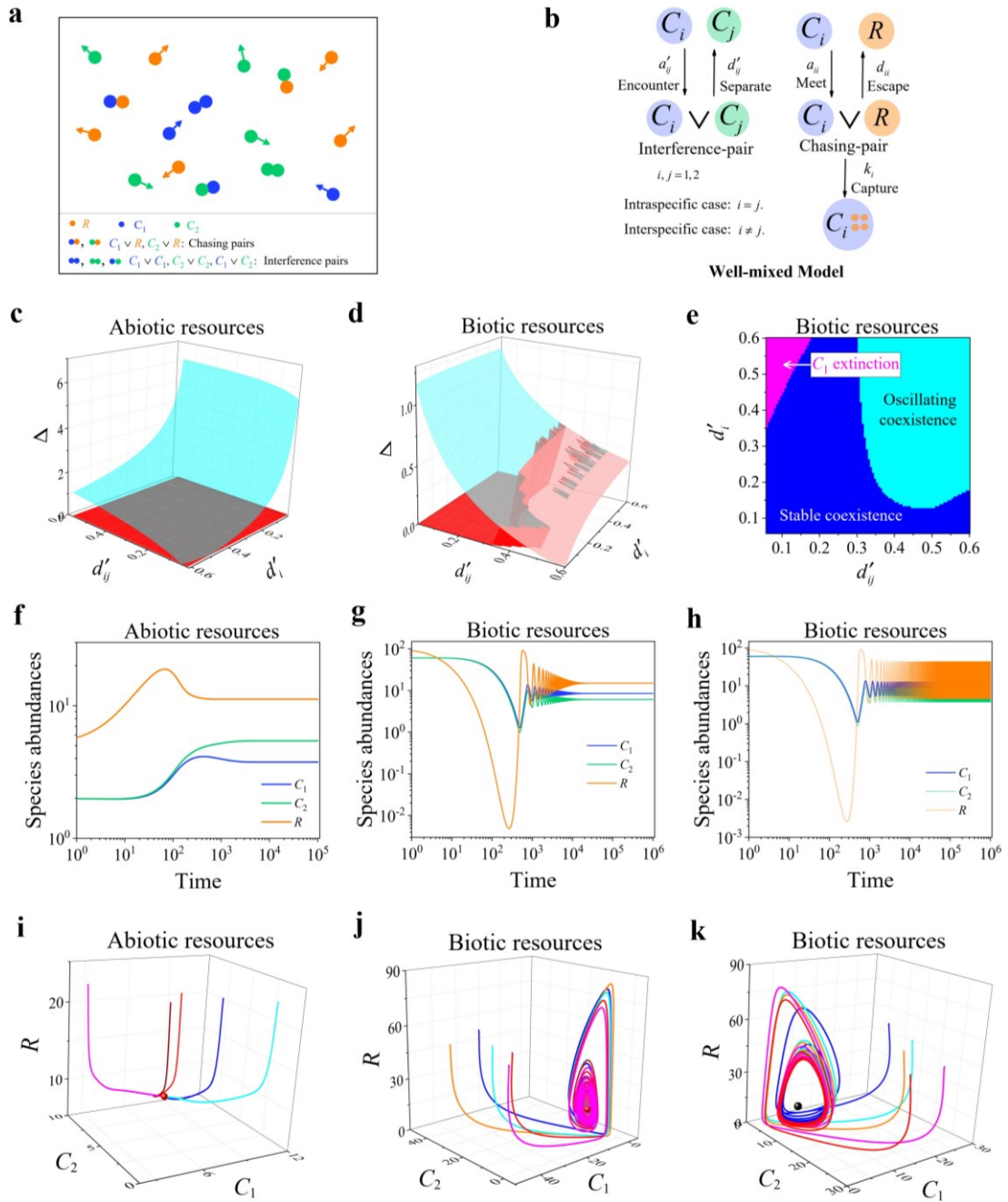


Figure S18 | Numerical results in the scenario involving chasing pair and both intra- and inter-specific interference. The species coexistence behavior is similar to that without interspecific interference. (a-b) Model scenario in the case of $M=2$ and $N=1$.

(c-e) 3D Phase diagram of species coexistence region. $D_i (i=1,2)$ is the only parameter of each different value between the consumer species, and then $\Delta = (D_1 - D_2)/D_2$ measures the competitive difference between the two species.

The parameter region below the blue surface yet above the red surface represents species stable coexistence, while that below the red surface and above $\Delta=0$ represents

unstable fixed points. (e) The transection corresponding to the plane $\Delta = 0.2$ in (d). The blue, cyan and magenta region represent stable coexistence, oscillating coexistence and C_1 extinction, respectively. (f-h) Time series of the species coexistence either at constant population densities (f-g) or with oscillations. (i-j) The coexistence state is globally stable attractors. (k) The coexistence state is globally unstable, and all trajectories attract to a stable limit cycle. In (c): $a_1 = a_2 = 0.1$, $a'_1 = a'_2 = 0.12$, $k_1 = k_2 = 0.1$, $w_1 = w_2 = 0.1$, $D_2 = 0.001$, $K_0 = 100$, $R_a = 0.3$, $d_1 = d_2 = 0.3$, $a'_{12} = 0.05$. In (f, i): $a_1 = a_2 = 0.1$, $a'_1 = a'_2 = 0.12$, $k_1 = k_2 = 0.2$, $w_1 = w_2 = 0.1$, $D_1 = 0.0009$, $D_2 = 0.0085$, $K_0 = 100$, $R_a = 0.9$, $d_1 = d_2 = 0.2$, $d'_1 = d'_2 = 0.3$, $a'_{12} = 0.05$, $d'_{12} = 0.2$. In (d-e, g-h, i-k): $a_1 = a_2 = 0.1$, $a'_1 = a'_2 = 0.14$, $k_1 = k_2 = 0.2$, $w_1 = w_2 = 0.05$, $D_1 = 0.0009$, $D_2 = 0.0085$, $K_0 = 100$, $R_0 = 0.1$, $d_1 = d_2 = 0.2$, $d'_1 = d'_2 = 0.3$, $a'_{12} = 0.05$. In (e): $\Delta = 0.2$; In (g, j): $d'_{12} = 0.2$; In (h, k): $d'_{12} = 0.4$.

Chasing pair & Interspecific and intraspecific interference

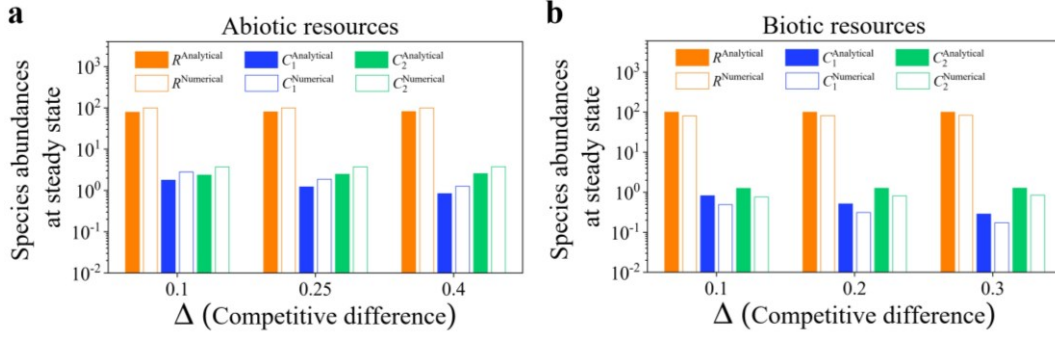


Figure S19 | Comparisons between numerical results and analytical solutions of the steady-state species abundances in the scenario involving chasing pair and both intra- and inter-specific interference. $D_i (i=1,2)$ is the only parameter of each different

value between the consumer species, and $\Delta = (D_1 - D_2)/D_2$ measures the

competitive differences between the two species. Color bars are analytical solutions while hollow bars are numerical results. The numerical results (labeled with superscript 'Numerical') were calculated from Eqs. S5.1, S3.10, while the analytical solutions (labeled with superscript 'Analytical') were calculated from Eqs. S5.4-

S5.6. In (a): $a_1 = a_2 = 0.05$, $a'_1 = a'_2 = 0.06$, $k_1 = k_2 = 0.1$, $w_1 = w_2 = 0.2$, $D_2 = 0.008$,

$K_0 = 100$, $R_a = 0.8$, $d_1 = d_2 = 0.5$, $d'_1 = d'_2 = 0.06$, $a'_{12} = 0.2$, $d'_{12} = 0.2$. In (b): $a_1 =$

$a_2 = 0.05$, $a'_1 = a'_2 = 0.06$, $k_1 = k_2 = 0.05$, $w_1 = w_2 = 0.2$, $D_2 = 0.006$, $K_0 = 100$, $R_0 =$

0.2 , $d_1 = d_2 = 0.5$, $d'_1 = d'_2 = 0.002$, $a'_{12} = 0.2$, $d'_{12} = 0.2$.

Chasing pair & Interspecific and intraspecific interference

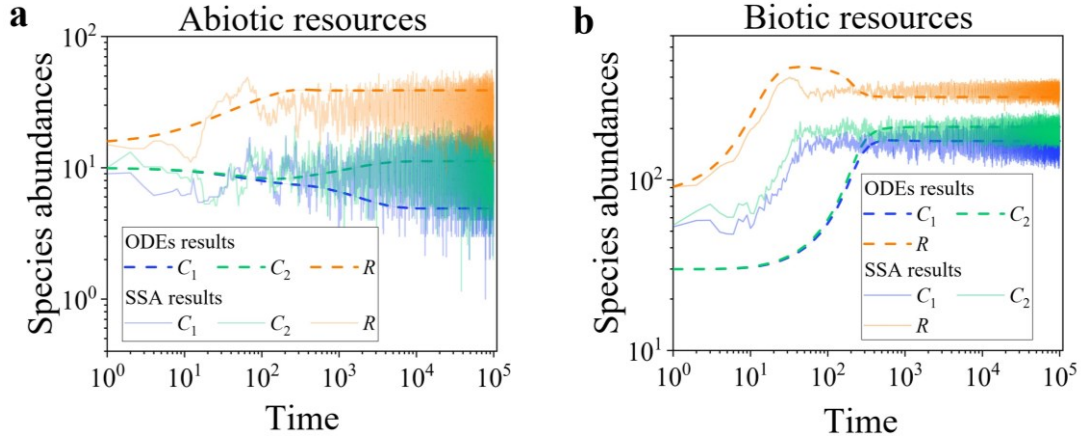


Figure S20 | Outcomes of two types consumers species competing for single resource species involving chasing pair and intra- and inter-specific interference. (a-b) Both consumer species can coexist with either lifeform of the resources regardless of stochasticity. In (a): $a_1 = a_2 = 0.1$, $a'_1 = a'_2 = 0.11$, $k_1 = k_2 = 0.1$, $w_1 = w_2 = 0.15$, $D_1 = 0.0125$, $D_2 = 0.012$, $K_0 = 300$, $R_a = 0.8$, $d_1 = d_2 = 0.3$, $d'_1 = d'_2 = 0.5$, $a'_{12} = 0.01$, $d'_{12} = 0.8$. In (b): $a_1 = a_2 = 0.1$, $a'_1 = a'_2 = 0.11$, $k_1 = k_2 = 0.1$, $w_1 = w_2 = 0.15$, $D_1 = 0.013$, $D_2 = 0.0125$, $K_0 = 500$, $R_0 = 0.2$, $d_1 = d_2 = 0.3$, $d'_1 = d'_2 = 0.5$, $a'_{12} = 0.05$, $d'_{12} = 0.4$.

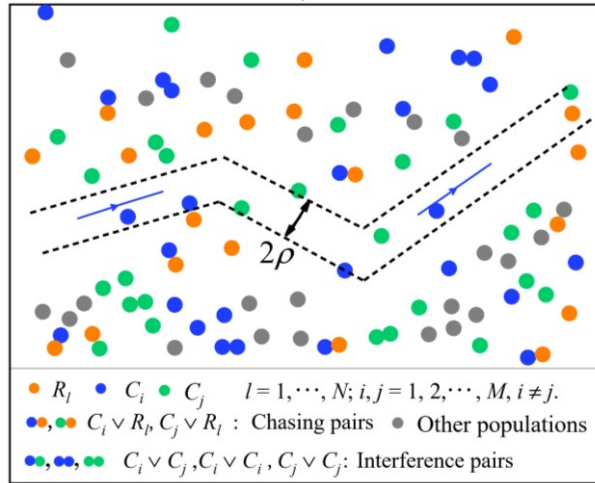


Figure S21 | Estimation of the pairwise encounter rate with mean-field approximations. To calculate the average collisions frequency, supposing that all the populations stand still except for one individual (e.g., a consumer from species C_i).

Over a short time interval Δt , this consumer moves from the middle left to the upper right of the depicted region (a very small part of the whole system) following the center of the two parallel dashed lines. Meanwhile it encounters many individuals from, e.g., resource species R_l . Then we can estimate the collisions frequency and thus the encounter rate a_{il} by counting the number of R_l individuals within the area between the two dashed lines. ρ stands for the radius of encounter.

Supplemental Tables

Table S1: Simulation details of the main text Figures.

| In Figure 1 |
|---|
| In 1c, f: $a_1 = a_2 = 0.1, k_1 = k_2 = 0.1, w_1 = w_2 = 0.1, d_1 = d_2 = 0.5, D_1 = 0.002, D_2 = 0.001, K_0 = 5, R_a = 0.05.$ |
| In 1d, g: $a_1 = a_2 = 0.05, k_1 = k_2 = 0.02, w_1 = w_2 = 0.08, d_1 = d_2 = 0.5, b = 0.3, e = 0.01, D_1 = 0.001, D_2 = 0.0009, K_0 = 20, R_a = 0.01.$ |
| In 1e, h: $a_1 = a_2 = 0.5, a'_1 = a'_2 = 0.625, k_1 = k_2 = 0.4, w_1 = w_2 = 0.2, d_1 = d_2 = 0.5, D_1 = 0.022, D_2 = 0.02, K_0 = 10, d'_1 = d'_2 = 0.5, R_a = 0.1.$ |
| In Figure 2 |
| In 2a-b: $a_1 = a_2 = 0.05, D_1 = 0.0009, D_2 = 0.0007, d_1 = d_2 = 0.1, b = 0.02, e = 0.02, k_1 = k_2 = 0.1, w_1 = w_2 = 0.05, K_0 = 60, R_0 = 0.05.$ |
| In 2c: $a_1 = a_2 = 0.05, D_1 = 0.0009, D_2 = 0.0007, d_1 = d_2 = 0.1, k_1 = k_2 = 0.2, w_1 = w_2 = 0.1, K_0 = 60, R_0 = 0.15.$ |
| In 2d: $a_1 = a_2 = 0.1, a'_1 = a'_2 = 0.125, d_1 = d_2 = 0.1, d'_1 = d'_2 = 0.05, k_1 = k_2 = 0.1, w_1 = w_2 = 0.1, K_0 = 100, D_1 = 0.0035, D_2 = 0.0038, R_a = 0.3.$ |
| In 2e-f: $a_1 = a_2 = 0.1, a'_1 = a'_2 = 0.125, d_1 = d_2 = 0.1, k_1 = k_2 = 0.1, w_1 = w_2 = 0.1, K_0 = 100, D_1 = 0.0085, D_2 = 0.008, R_0 = 0.05.$ |
| In e: $d'_1 = d'_2 = 0.05.$ In (f): $d'_1 = d'_2 = 0.1.$ |
| In 2g: $a_1 = a_2 = 0.1, a'_1 = a'_2 = 0.125, d_1 = d_2 = 0.1, k_1 = k_2 = 0.1, w_1 = w_2 = 0.1, K_0 = 100, D_2 = 0.001, \Delta = (D_1 - D_2)/D_2, R_a = 0.1.$ |
| In 2h-i: $a_1 = a_2 = 0.1, a'_1 = a'_2 = 0.125, d_1 = d_2 = 0.1, k_1 = k_2 = 0.1, w_1 = w_2 = 0.1, K_0 = 100, D_2 = 0.001, \Delta = (D_1 - D_2)/D_2, R_0 = 0.05.$ |
| In 2i: $\Delta = 1.$ |
| In 2j, m: $a_1 = a_2 = 0.02, a'_1 = a'_2 = 0.025, D_1 = 0.0112, D_2 = 0.01, d_1 = d_2 = 0.7, d'_1 = d'_2 = 0.7, k_1 = k_2 = 0.05, w_1 = w_2 = 0.4, K_0 = 2000, R_a = 5.5.$ |
| In 2k-l: $a_1 = a_2 = 0.06, a'_1 = a'_2 = 0.075, d_1 = d_2 = 2, d'_1 = d'_2 = 2, k_1 = k_2 = 0.22, w_1 = w_2 = 0.32, K_0 = 5000, D_1 = 0.052, D_2 = 0.05, R_0 = 0.13.$ |

In 2m-o: $L = 120, r = 5, v_C = v_R = 1, l = 50, a_1 = a_2 = 0.0039l, a'_1 = a'_2 = 0.0039l, k_1 = k_2 = 0.1, w_1 = w_2 = 0.3, d'_1 = d'_2 = 0.3, D_1 = 0.0155, D_2 = 0.015, R_0 = 0.5, d_1 = d_2 = 0.3, K_0 = 200.$

In Figure 3

In 3a: $a_i = 0.1, a'_i = 0.125, d_i = 0.3, d'_i = 0.05, w_i = 0.35, k_i = 0.5, i = 1, \dots, 5, R_a = 0.35, D_5 = 0.036, D_1 = 0.032, D_2 = 0.0335, D_3 = 0.0345, D_4 = 0.035, D_5 = 0.036.$

In 3b: $a_{il} = 0.05, a'_i = 0.07, d_{il} = 0.98, d'_i = 0.018, w_{il} = 0.45, k_{il} = 0.16, i = 1, \dots, 5, K_0^{(1)} = 600, K_0^{(2)} = 1000, K_0^{(3)} = 800, R_0^{(1)} = R_0^{(2)} = 0.9, R_0^{(2)} = 0.95, D_1 = 0.062, D_2 = 0.0615, D_3 = 0.0639, D_4 = 0.066, D_5 = 0.0644.$

In 3c, e: $a_i = 0.1, a'_i = 0.125, d_i = 0.5, d'_i = 0.1, w_i = 0.1, k_i = 0.1, D_i = 0.002 + 0.002 \times p_i, p_i \in [0, 1], i = 1, \dots, 20, R_a = 2.95, K_0 = 1000.$

In 3d, f: $a_{il} = 0.2, a'_i = 0.25, d_{il} = 0.4, d'_i = 0.2, w_{il} = 0.2, k_{il} = 0.3, R_0^{(1)} = 0.8, D_i = 0.03 + 0.03 \times p_i, p_i \in [0, 1], i = 1, \dots, 18, l = 1, 2, 3, K_0^{(1)} = 600, K_0^{(2)} = 1500, K_0^{(3)} = 1000.$

In Figure 4

In 4a-d: $a_1 = a_2 = 0.1, a'_1 = a'_2 = 0.125.$

In 4a: $k_1 = k_2 = 0.1, w_1 = w_2 = 0.2, D_1 = 0.0015, D_2 = 0.001, R_a = 0.5, d_1 = d_2 = 0.4, d'_1 = d'_2 = 0.289, K_0 = 200.$

In 4b: $k_1 = k_2 = 0.5, w_1 = w_2 = 0.5, R_a = 0.5, d_1 = d_2 = 0.289, d'_1 = d'_2 = 0.233, D_1 = 0.005, D_2 = 0.002, K_0 = 200.$

In 4c: $k_1 = k_2 = 0.1, w_1 = w_2 = 0.18, D_1 = 0.0027, D_2 = 0.002, R_a = 1.2, d_1 = d_2 = 0.2, d'_1 = d'_2 = 0.005, K_0 = 60.$

In 4d: $k_1 = k_2 = 0.1, w_1 = w_2 = 0.2, D_1 = 0.0035, D_2 = 0.003, R_a = 1.6, d_1 = d_2 = 0.1, d'_1 = d'_2 = 0.1, K_0 = 60.$